NMR Spectroscopy of Multi-domain Proteins: Immunoglobulin-like Domains of Human Filamin A

OUTI KOSKELA

Laboratory of Organic Chemistry, Department of Chemistry,
Faculty of Science, University of Helsinki, Finland

ACADEMIC DISSERTATION

To be presented, with the permission of the Faculty of Science,
University of Helsinki, for public examination in
the Auditorium A129, Chemicum, A.I. Virtasen aukio 1,
on the 18th of December 2009, at 12 o'clock noon.

Helsinki 2009

Supervisor

Professor Ilkka Kilpeläinen
Laboratory of Organic Chemistry, Department of Chemistry
University of Helsinki
Finland

Reviewers

Professor Johanna Ivaska
Medical Biotechnology, VTT Technical Research Centre of Finland
Turku Centre for Biotechnology, University of Turku and Åbo Akademi University
Department of Biochemistry and Food Chemistry, University of Turku
Finland

Professor Arto Annila
Department of Physics, Department of Biosciences and Institute of Biotechnology
University of Helsinki
Finland

Opponent

Professor Stephan Grzesiek
Division of Structural Biology
Biozentrum
University of Basel
Switzerland

ISBN 978-952-92-6623-4 (paperback)
ISBN 978-952-10-5929-2 (PDF)

Helsinki University Print
Helsinki 2009

ABSTRACT

Proteins are complex biomacromolecules playing fundamental roles in the physiological processes of all living organisms. They function as structural units, enzymes, transporters, process regulators, and signal transducers. Defects in protein functions often derive from genetic mutations altering the protein structure, and impairment of essential protein functions manifests itself as pathological conditions. Proteins operate through interactions, and all protein functions depend on protein structure. In order to understand biological mechanisms at the molecular level, one has to know the structures of the proteins involved.

This thesis covers structural and functional characterization of human filamins. Filamins are actin-binding and -bundling proteins that have numerous interaction partners. In addition to their actin-organizing functions, filamins are also known to have roles in cell adhesion and locomotion, and to participate in the logistics of cell membrane receptors, and in the coordination of intracellular signaling pathways. Filamin mutations in humans induce severe pathological conditions affecting the brain, bones, limbs, and cardiovascular system. Filamins are large modular proteins composed of an N-terminal actin-binding domain and 24 consecutive immunoglobulin-like domains (IgFLNs).

Nuclear magnetic resonance (NMR) spectroscopy is a versatile method of gaining insight into protein structure, dynamics and interactions. The latest advancements in this technique enable the efficient characterization of multi-domain proteins, which are challenging targets due to their large size and dynamic behavior. NMR spectroscopy was employed in this thesis to study the atomic structure and interaction mechanisms of C-terminal IgFLNs, which are known to house the majority of the filamin interaction sites.

The structures of IgFLN domains 17 (**I**) and 23 (**II**) were determined using NMR spectroscopy. NMR spectroscopy was also employed to characterize the interactions of domains 17 and 23 with glycoprotein Ibα and FilGAP, respectively. The structures of IgFLN domain pairs 16–17 and 18–19 (**III**, **IV**) both revealed novel domain–domain interaction modes of IgFLNs. The interaction of IgFLN domain 19 with integrin β7 and dopamine receptors was studied using NMR titrations. Domain packing of IgFLN domain sextet 16–21 was further characterized using residual dipolar couplings and NMR relaxation analysis (**V**). This thesis demonstrates the versatility and potential of NMR spectroscopy in structural and functional studies of multi-domain proteins.

ACKNOWLEDGEMENTS

This work was carried out in the Laboratory of Organic Chemistry, Department of Chemistry, University of Helsinki from 2004–2009. Here I want to acknowledge all those who have contributed to this work and helped me during these years. It has been a pleasure to work with these people.

I want to thank my supervisor, Professor Ilkka Kilpeläinen, for introducing me to the field of protein NMR spectroscopy and providing me with excellent surroundings to finish this thesis. I am grateful for my special position—I always had a chance to be myself and do my own thing. I also want to apologize for not always being the humblest student to supervise.

This thesis was reviewed by Professor Johanna Ivaska and Professor Arto Annila. I want to thank them for their careful inspection and constructive criticism on the manuscript. Besides being thorough they also gave their comments remarkably fast.

Professor Jari Ylänne is the one to whom I want to acknowledge for my research topic. Professor Ylänne and his research groups in University of Jyväskylä and University of Oulu have helped me a great deal during these years. Proficient technician Arja Mansikkaviita has contributed to this work by preparing most of my protein samples. I also want to acknowledge Salla Ruskamo and all who have helped me in the lab when I have been visiting Jyväskylä. I also want to acknowledge Dr. Olli Pentikäinen for collaboration.

Most of the NMR spectra presented in this thesis were recorded in the Finnish Biological NMR Center in the Institute of Biotechnology. Dr. Perttu Permi has made my work considerably easier by providing me with sufficient spectrometer time and excellent NMR data. I want to thank everyone in Viikki for sharing their lab space and especially Dr. Helena Tossavainen for helping me five years ago when I was taking my first steps in field of protein NMR.

Dr. Sami Heikkinen has also helped me a great deal on NMR-related problems by keeping up our spectrometers and setting up NMR experiments. Valtteri Mäkelä has maintained my computing facilities and successfully solved all my Linux problems.

During my PhD project I had the chance to supervise two talented Bachelor students Olga Kupiainen and Tatu Iivanainen. They both made an important contribution to the research articles included in this thesis and I am grateful to them for their help.

I have had the pleasure to work with two excellent research groups abroad. I want to thank Professor Iain Campbell and Dr. Pengju Jiang in the University of Oxford and Dr. Fumihiko Nakamura in Harvard Medical School, Boston, for fruitful collaboration. During this project I also had the opportunity to visit the SON Large Scale NMR Facility, Utrecht, and record some NMR data there. I am grateful for the help of Dr. Rainer Wechselberger and Dr. Tammo Diercks in setting up NMR experiments.

During my PhD studies I have been privileged to be a member of National Graduate School in Informational and Structural Biology, ISB. ISB has helped me

to make connections with talented Finnish people working in life sciences. I also want to thank ISB for travel grants. During my PhD studies I have also received financial support from The University of Helsinki Funds and Chancellor´s Travel Grants. I am very grateful for funding provided by Orion-Farmos Research Foundation to finish this thesis.

During these five years I have been surrounded by marvelous workmates. I want to thank you all for friendship and laughter both during and outside office hours. One of you deserves a special acknowledgement: I want to thank my long-time roommate Dr. Mari Granström for invaluable friendship and for sharing the endless passion for science. I have also had pleasure to share an office and feelings with Jari Kavakka, Johanna Majoinen and Paula Järvi.

I want to thank my Mom and Dad for always understanding my endless passion for studying.

I am deeply indebted to my beloved husband Harri for all the support during these years. He has contributed to this thesis in so many ways by teaching me NMR, setting up experiments, guiding me in data analysis and especially listening and understanding during the most difficult moments. Thank you Harri for being so endlessly patient and showing how easily everything goes if you *just do it*. Thank you for reminding me that there are also aspects in life other than obsessive studying.

Thanks to "Nulikka" for spurring and giving me time to finish this thesis.

Outi Koskela
16th of November 2009
Helsinki

CONTENTS

LIST OF ORIGINAL PUBLICATIONS

This thesis is based on the following original publications, referred to in the text by their Roman numerals.

(I) Nakamura F, Pudas R, **Heikkinen O**, Permi P, Kilpeläinen I, Munday AD, Hartwig JH, Stossel TP, Ylänne J (2006) The structure of the GPIb–filamin A complex. *Blood* **107**:1925–32.

(II) Nakamura F, **Heikkinen O**, Pentikäinen OT, Osborn TM, Kasza KE, Weitz DA, Kupiainen O, Permi P, Kilpeläinen I, Ylänne J, Hartwig JH, Stossel TP (2009) Molecular basis of filamin A–FilGAP interaction and its impairment in congenital disorders associated with filamin A mutations. *PLoS One* **4**:e4928.

(III) **Heikkinen O**, Permi P, Koskela H, Ylänne J, Kilpeläinen I (2009) ^{1}H, ^{13}C and ^{15}N resonance assignments of the human filamin A tandem immunoglobulin-like domains 16–17 and 18–19. *Biomolecular NMR Assignments* **3**:53–6.

(IV) **Heikkinen OK**, Ruskamo S, Konarev PV, Svergun DI, Iivanainen T, Heikkinen SM, Permi P, Koskela H, Kilpeläinen I, Ylänne J (2009) Atomic structures of two novel immunoglobulin-like domain-pairs in the actin cross-linking protein filamin. *The Journal of Biological Chemistry* **284**:25450–8.

(V) **Koskela O**, Permi P, Jiang P, Campbell ID, Ylänne J, Kilpeläinen I. Protein domain organization studies using residual dipolar couplings: Filamin A immunoglobulin-like domains 16–21. *Manuscript in preparation.*

Also some unpublished results are included.

OK (former OH) conducted the protein NMR studies presented in this thesis and wrote the related sections of the research articles.

The results of article (**I**) have been previously used in the PhD thesis of Regina Pudas in 2006 (University of Oulu).

ABBREVIATIONS

τ_c	Correlation time
τ_e	Timescale for internal bond vector motion
A_a	Axial component of alignment tensor
ABD	Actin-binding domain
ABP	Actin-binding protein
ABP-120	*Dictyostelium* filamin
ABS	Actin-binding sequence
AO [I/III]	Atelosteogenesis [I/III]
A_r	Rhombic component of alignment tensor
BMRB	Biological Magnetic Resonance Data Bank
BPNH	Bilateral periventricular nodular heterotopia
CATH	Protein Structure Classification database
CC	Coiled-coil (domain)
CH[1/2]	Calponin-homology domain [1/2]
CRINEPT	Polarization transfer by cross-correlated relaxation
$D_{[2/3]}$	Dopamine receptor type $_{[2/3]}$
Da	Dalton
DNA	Deoxyribonucleic acid
DNP	Dynamic nuclear polarization
DTT	Dithiothreitol
EDTA	Ethylenediaminetetraacetic acid
EM	Electron microscopy
ER	Endoplasmic reticulum
FilGAP	Filamin A-binding RhoGTPase-activating protein
FLN[a/b/c]	Filamin [A/B/C]
FMD	Frontometaphyseal dysplasia
GAP	GTPase-activating protein
GDP	Guanosine-5'-diphosphate
GEF	Guanine nucleotide exchange factor
GP	Glycoprotein
GPCR	G protein-coupled receptor
GPIbα	Glycoprotein Ibα
GPIb-IX-V	Glycoprotein Ib-IX-V complex
GRK2/3	G-protein receptor kinase 2/3
GST	Glutathione S-transferase
GTP	Guanosine-5'-triphosphate
H[1/2]	Hinge [1/2]
HSQC	Heteronuclear single quantum coherence
Ig	Immunoglobulin-like (domain/fold)

IgFLN([a/b/c])	Filamin-type immunoglobulin-like domain (of filamin[A/B/C])
K_d	Dissociation constant
MFM	Myofibrillar myopathy
MNS	Melnik-Needles syndrome
mRNA	Messenger RNA
MSG	Malate synthase G
MW	Molecular weight
NMR	Nuclear magnetic resonance
NOE	Nuclear Overhauser enhancement
NOESY	Nuclear Overhauser enhancement spectroscopy
OD_λ	Optical density at wavelength λ
OPD [1/2]	Otopalatodigital spectrum disorder [1/2]
PCS	Pseudocontact shift
PDB	Protein Data Bank
PH	Pleckstrin homology (domain)
PH/PNH/PVNH	Periventricular (nodular) heterotopia
PK[A/B/C]	Protein kinase[A/B/C]
PRE	Paramagnetic relaxation enhancement
R_1	Longitudinal relaxation rate
$R_{1\rho}$	Longitudinal relaxation rate in rotating reference frame
R_2	Transverse relaxation rate
RDC	Residual dipolar coupling
R_{ex}	Relaxation due to conformational exchange
RMSD	Root mean square deviation
RNA	Ribonucleic acid
S^2	Generalized order parameter
SANS	Small-angle neutron scattering
SAXS	Small-angle X-ray scattering
SCOP	Structural Classification of Proteins database
SCT	Spondylocarpotarsal syndrome
STD	Saturation transfer difference
T_1	Longitudinal relaxation time
T_2	Transverse relaxation time
TCE	Transferred cross-saturation experiment
TM	Transmembrane helix
trNOE	Exchange-transferred nuclear Overhauser enhancement
TROSY	Transverse relaxation optimized spectroscopy
VWF	von Willebrand factor
XMVD	X-linked myxomatous valvular dystrophy

“Almost all aspects of life are engineered at the molecular level, and without understanding molecules we can only have a very sketchy understanding of life itself.”

- Francis Crick 1916–2004 -

1. GENERAL INTRODUCTION

This thesis gives an overview of modern biomolecular nuclear magnetic resonance (NMR) spectroscopy and its potential in structural and functional studies of multi-domain proteins. The original publications included in this thesis deal with the structure and interactions of the immunoglobulin-like domains of human filamin A (IgFLNa). The experimental part of the thesis summarizes the results of the original research papers and also presents some unpublished results closely related to the topic.

As an introduction to the experimental part, the text begins with a broad literature review. The review is divided into three separate chapters: (i) multi-domain proteins; (ii) filamins; and (iii) NMR spectroscopy of multi-domain proteins. The first chapter introduces general aspects of protein structure and modularity of proteins. As filamin is the target protein of the experimental part of the study its structure, function and biological role are presented in detail in the second chapter. The third introductory chapter covers the latest advances in protein NMR spectroscopy. As multi-domain proteins are usually rather large molecular systems, specialized NMR methods are needed in their studies. The NMR techniques employed in studies of large protein systems will be thus covered in more detail.

The original research papers contain results obtained using a range of experimental techniques: biochemical and whole cell experiments, molecular modeling, small-angle X-ray scattering (SAXS), electron microscopy, X-ray crystallography and NMR spectroscopy. The experimental summary of this thesis focuses on the results derived by NMR spectroscopy, but some other results are also high-lighted.

2. MULTI-DOMAIN PROTEINS

All life, as we know it on earth, depends on proteins. Proteins are complex biomacromolecules playing fundamental roles in the physiological processes of all living organisms. They make most of the cellular machinery by serving as structural units, enzymes, transporters, regulators and signal transducers. Information on the protein assembly of an organism is coded in the DNA sequence. Nucleotide sequences of genes code for protein sequences. The genetic information is first transcribed into mRNA which is transported from nucleus to cytosol and then transcribed to protein sequences at the ribosomes. Via complicated folding pathways, protein sequences form delicate three-dimensional architectures that break up easily through denaturation. Proteins function through interactions—they can interact with other proteins, nucleic acids, carbohydrates, lipid membranes and small molecules, *e.g.*, neurotransmitters and drugs (Keskin *et al.* 2008). These interactions are specific and proteins recognize their binding partners with great fidelity. Protein interactions and function depends on their structure. The structure of a protein determines its function, and flaws in protein function also derive from its structure. Since protein structure is such an essential part of life, it is important to know and understand structures of proteins in great detail.

2.1. Protein Structure

Protein structure is often described using four levels of structural organization: primary, secondary, tertiary and quaternary structure (Fig. 1). *Primary structure* of a protein, *i.e.*, the amino acid sequence, determines the higher-order structure of the protein. *Secondary structure* is formed through and defined by hydrogen bond patterns of the protein backbone. The most common secondary structure elements are α helix and antiparallel β strand, but also other structures such as parallel β strands, 3_{10} helix, π helix and polyproline II helix are often found. Around 2/3 of the protein sequence is arranged into regular secondary structure elements; the remainder consists of loops, turns and coils. *Tertiary structure* is the spatial folding pattern of the entire polypeptide chain. The fold of a protein describes the number and the arrangement of the secondary structural elements in a protein. Tertiary structure is formed through non-covalent forces—ion/dipole interactions, hydrogen bonds, van der Waals forces, and the hydrophobic effect—which in principle tend to bury hydrophobic residues inside the structure while retaining hydrophilic ones at the surface. Covalent disulfide bridges also contribute to the formation of tertiary structure. Even if protein fold is determined by the protein sequence, folding is an extremely complex process and at the moment no efficient computational methods exist to determine the protein fold directly from the amino acid sequence. Some proteins are intrinsically disordered and attain the folded state only in complexes with their physiological targets (Wright and Dyson 2009). *Quaternary structure* is formed when several polypeptide chains (subunits) join together in order to make up a fully functional homo-oligomer. However, protein structure categorization is not quite as simple as this, since several intermediate levels of structural

organization exist (Caetano-Anollés *et al.* 2009). *Supersecondary structures* are recurrent patterns of secondary structure elements that are encountered in many structures. *Domains* are to some extent independent subunits of tertiary structure, having an isolated hydrophobic core, and they are an especially important level of organization when describing the structure of modular multi-domain proteins. There are also higher levels of structural organization to quaternary structure. Many proteins form multi-protein *complexes* where subunits carry out their functions cooperatively. Multi-enzyme complexes, *e.g.*, tryptophan synthase (Barends *et al.* 2008), are excellent examples of functional protein complexes co-localizing several processes of complicated biological pathways (Srere 1987). Many proteins go through post-translational modifications; *e.g.*, proteolytic processing, glycosylation and phosphorylation; which can alter their structure and function (Kyte 2007, p. 113–125). One has to also keep in mind that protein structure is not as solid as a rock but proteins are dynamic entities and internal motions are frequently involved in protein function (McCammon and Harvey 1988; Kern and Zuiderweg 2003; Tousignant and Pelletier 2004).

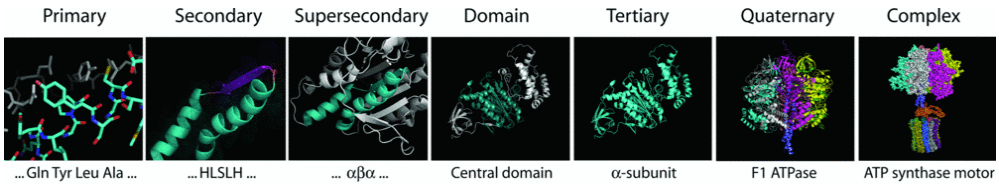

Fig. 1 The protein structure organization levels represented using F1 ATPase as an example. Reprinted with permission from (Caetano-Anollés *et al.* 2009). © 2009 the Biochemical Society.

2.1.1. Protein Domains: Immunoglobulin-like Domains

Protein domains, or modules, are generally regarded as rather independent structural components of proteins that can often be expressed as a single isolated unit (Han *et al.* 2007). However, protein domain can be understood and defined in several different ways: functional domains, sequence domains, evolutionary domains, structural domains or domains as independent folding units (Majumdar *et al.* 2009). It has been noted that the domain structure is more strongly conserved in evolution than protein sequence (Chothia and Lesk 1986) and sequentially rather distant polypeptides can have similar folds. This is obviously an indication of conservation of protein function which is determined by its structure. Some proteins have only one domain, whereas others can have dozens or even hundreds of domains, such as giant muscle protein titin (Labeit and Kolmerer 1995), which is the largest protein known so far. Protein domains serve for several different purposes: they can have structural, enzymatic and interactive roles. Some domains function as spacers between other domains, placing them in optimal spatial orientation for their function. Enzymatic domains perform catalytic reactions. Domains mediating interactions can bind other proteins, nucleic acids, lipids and membranes, carbohydrates and small ligands. Protein–protein interaction domains

are specified to recognize protein surfaces based on their shape and charge distribution. Enzymes can have separate domains for enzymatic activity; *i.e.*, binding and processing of the substrate; and binding of activity modulators. Transcription factors bind to their target genes using specific DNA sequence-recognizing and -binding domains. Some domains anchor proteins to membranes. Protein structure classification databases, *e.g.*, SCOP and CATH (Murzin *et al.* 1995; Orengo *et al.* 1997), catalog hundreds of different domains or fold superfamilies, but there is no purpose in repeating the list here. To give examples of protein domains, Table 1 presents an overview of frequently encountered domains participating in protein interactions.

Table 1 Overview of common protein domains having roles in protein interactions (adapted from Kyte 2007, p. 386). α, α helix; β, β strand; L, loop; RC, random coil; Ccyn, n cystine bridges.

Domain	Approximate length	Structure	Function
EF hand	40	$\alpha L \alpha$	Calcium binding
Immunoglobulin	100	β_7	Protein–protein interaction
Leucine-rich repeat	30	$(\beta\alpha)_n$	Protein–protein interaction
RNA recognition motif	80	$\beta\alpha\beta_2\alpha\beta$	RNA binding
EGF	50	$RC(Ccy_{3\text{-}4})$	Protein–protein interaction
Cohesin	140	β_9	Protein–protein interaction
Ankyrin	40	$(\beta_2\alpha_2)_n$	Protein–protein interaction
C2	120	β_8	Calcium and membrane binding
SH2	100	$\beta\alpha\beta_5\alpha\beta$	Protein binding through pTyr
SH3	60	β_5	Protein–protein interaction
Kringle	80	$RC(Ccy_3)$	Protein–protein interaction
SAND	80	$\beta_2\alpha\beta_2\alpha_2\beta\alpha$	DNA binding
Pleckstrin homology	100	$\beta_7\alpha$	Lipid/membrane binding
Fibronectin type I	50	β_5	Protein–protein interaction
Fibronectin type II	60	$\beta_3\alpha\beta$	Protein–protein interaction
Armadillo	50	α_3	Protein–protein interaction
Fibronectin type III	90	β_7	Protein–protein interaction
START	200	$\alpha\beta_3\alpha_2\beta_6\alpha$	Lipid binding
Hemopexin	200	Four-bladed β propeller	Protein–protein interaction

Immunoglobulin-like Domains

The immunoglobulin-like (Ig) domain, *i.e.*, a protein domain with an immunoglobulin-like fold, is one of the most widespread protein modules (Williams and Barclay 1988; Bork *et al.* 1994; Halaby and Mornon 1998; Barclay 2003; Gelfand *et al.* 2007). Ig domain was first observed in proteins of the immune system, from whence it got its name, but later Ig domains have been found in proteins with diverse functions. Ig domains are most often encountered in cell adhesion molecules (Aricescu and Jones 2007) and in structural proteins of the cytoskeleton, especially in sarcomeres (Pinotsis *et al.* 2009), but also in membrane receptors, *e.g.*, receptor tyrosine kinases (Wiesmann *et al.* 2000). Usually Ig domains serve structural and binding roles—no enzymatic activity has been observed for natural Ig domains. Ig domains are often part of multi-domain proteins, either as repeats of Ig domains or combined with other domain types.

Sequences of Ig domains are remarkably divergent and structures also vary considerably, but some similarities can still be found (Halaby *et al.* 1999). Ig

domain is composed of around 100 amino acid residues and it belongs to class of all-β proteins. Ig fold is a β sandwich of two β sheets. Conventional topology contains seven β strands but some forms have additional strands up to total of 10. β strands are named in alphabetical order starting from N-terminus. Traditionally, Ig folds are divided into four structural sets; V-, C1-, C2- and I-type Ig folds; according to their topologies (Fig. 2), but also other more detailed categories have been proposed (Bork *et al.* 1994; Halaby *et al.* 1999). In addition to the β sandwich fold there are other partly conserved features in the structures of Ig domains. Many Ig domains of extracellular proteins have a disulfide bridge between strands B and F and a tryptophan residue located at the strand C is an essential part of the hydrophobic core of many Ig domains (Chothia *et al.* 1998). Hemmingsen *et al.* have identified the so-called tyrosine corner as an important structural feature of several Ig domains (Hemmingsen *et al.* 1994).

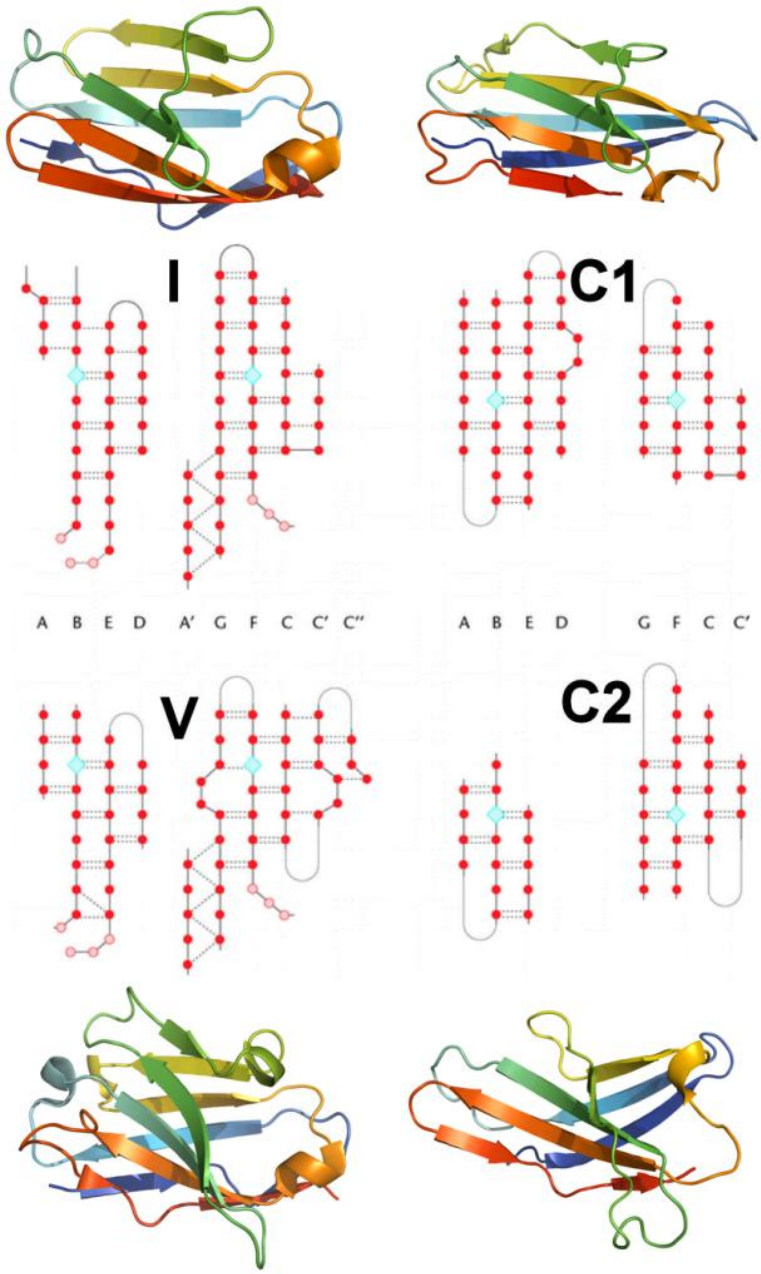

Fig. 2 The traditional topological classes (I, C1, V and C2) of Ig domains. Nomenclature of the β strands is shown with small capital letters. Closed circle, β sheet residue; open circle, loop residue having conserved conformation; dashed lines, hydrogen bonds; diamond, location of highly conserved cysteine residues. PDB codes of the example structures: I, 2YXM; C1, 1X7Q; V, 1UZ8; C2, 2D9Q. Reprinted and adapted with permission from (Gelfand *et al.* 2007). © 2007 John Wiley & Sons Ltd.

2.1.2. Protein Modularity

There are several examples of proteins that are made of only a single domain but around two-thirds of proteins contain multiple domains, *i.e.*, they are multi-domain or modular proteins. Structure, function and evolution of multi-domain proteins have been recently reviewed by Vogel *et al.* and Han *et al.* (Vogel *et al.* 2004a; Han *et al.* 2007). About 20% of proteins contain tandem domain repeats but more often multi-domain proteins are combinations of different types of domains. Architecture of multi-domain protein describes the domain content of the protein in N- to C-terminal order. Protein domains are traditionally seen as structurally and functionally independent units but this is not necessarily the case in multi-domain proteins. Domain structures might mold at the domain interfaces or the structure of a domain might be entirely different in different domain combinations. Sometimes it is difficult to clearly determine the domain boundaries without knowledge of the structure of the entire unit (Holland *et al.* 2006).

There are several databases, *e.g.*, SCOP and CATH, for protein fold classification (Hadley and Jones 1999). SCOP (structural classification of proteins) categorizes proteins according to class, fold, superfamily and family (Murzin *et al.* 1995) whereas CATH classifies structures of protein domains according to class, architecture, topology and homologous superfamily (Orengo *et al.* 1997). These classification schemes overlap but also have some differences. Many protein comparison tools rely on sequence alignment, *i.e.*, comparison of primary structure, but there are also tools *e.g.*, DALI (Holm and Sander 1998) for 3D structural alignment (Hasegawa and Holm 2009). The latest CATH release (CATH version 3.2) contains over 2000 homologous domain superfamilies (Cuff *et al.* 2009). After decades of protein sequence analysis and structure determination, it has become evident that variation in the level of protein folds is limited and it has been speculated that our knowledge of single-domain folds is almost complete (Levitt 2009).

In the case of modular proteins, the domain boundaries and folds are not always straightforward to predict and determine. Sippl has recently reviewed protein structures with unconventional domain constructions (Sippl 2009). Although SCOP database is a good collection of clear cut domains encountered in proteins and it also contains specific class for multi-domain proteins (Murzin *et al.* 1995), a specific domain definition database has been created for multi-domain proteins with complex inter-domain geometry (Majumdar *et al.* 2009). Relative to each other, modules can be rigid or flexible. During protein function structures of individual modules usually stay unchanged while protein as a whole can undergo large shape changes (Gerstein *et al.* 1994). In addition, the assumption that the domain is an autonomous folding unit can be misleading, as adjacent domains might affect each other's folding and even structure (Han *et al.* 2007). Folding of domains in multi-domain proteins can be different from isolated domains (Batey *et al.* 2005; Fitter 2009). Yet most of the folding studies have been conducted on small globular proteins containing a single domain. There are some excellent examples of experimental folding studies of multi-domain constructs; for example Hsu *et al.* have studied the folding of tandem Ig domain protein using NMR spectroscopy (Hsu *et al.* 2007).

Multi-functionality of proteins with multiple domains was recognized several decades ago (Kirschner and Bisswanger 1976). Domains of a modular protein can function cooperatively, *e.g.*, active sites of enzymes, can sometimes reside between domains or accessibility of the active site may be regulated by other domains. Multi-enzyme synthases are multi-domain enzymes functioning as molecular assembly lines that house several steps of biological pathways in the same polypeptide (Hawkins and Lamb 1995; Weissman and Müller 2008; Meier and Burkart 2009). Evolution of protein modularity has been recently reviewed (Han *et al.* 2007; Trifonov and Frenkel 2009) and it has been noted that new protein functions can evolve by combination of different domains (Bashton and Chothia 2007). Domain combination can, *e.g.*, modify substrate binding or regulate enzyme function, regulate DNA binding of transcription factors, generate multifunctional enzymes, change the structural contexts of the function or even gain entirely new catalytic activity.

To understand the function of a modular protein and the roles of the individual domains, one needs to know the three-dimensional structure of the entire system. Unfortunately, the majority of protein structures available to date in the PDB database are single domains in isolation. Structure determination of modular proteins is challenging due to their large size and dynamicity. Dynamicity poses a problem in protein crystallization for X-ray crystallographic structure analysis and large size complicates NMR spectroscopic structure determination. Sometimes, especially when there is a strong interaction between the domains, heterologous expression of the multi-domain protein might turn out to be difficult (Han *et al.* 2007). Modeling methods have been employed to predict the structures of multi-domain proteins using predetermined structures of the sub-domains, which are often easier to solve than the structure of the whole system (Wollacott *et al.* 2007). Vogel *et al.* have identified especially abundant supra-domains, *i.e.*, two- or three-domain combinations that occur frequently in modular proteins, whose structure determination should be given first priority (Vogel *et al.* 2004b).

2.2. Protein Structure Determination

The first step on the long road to solving the structure of a protein is determination of its sequence. Protein sequencing can be done in several ways. Entire genomic sequences of several organisms are readily available in public databases, and often the most straightforward way to protein sequence is through the sequence of the gene coding it; alternatively, if the DNA sequence is not yet available, through sequencing of the DNA or the mRNA coding the protein. Proteins can be also sequenced *de novo* (Findlay and Geisow 1989). Edman degradation (Edman 1950), *i.e.*, chemical sequencing of peptides and proteins, became available in the 1950s and the method was soon automated. Edman degradation is still used in some cases, but sequencing by mass spectrometry has largely replaced it (Standing 2003). Mass spectrometry also gives detailed information on post-translational modifications of the protein (Witze *et al.* 2007).

Even if the protein sequence determines the three-dimensional structure of a protein, at present, it is not feasible to predict the structure and function of a protein *de novo* from the sequence alone—at least not efficiently. Sadowski and

Jones have recently reviewed the attempts to reveal protein sequence–structure–function relationships (Sadowski and Jones 2009). It has been demonstrated that structures of small proteins can be modeled quite accurately directly from the sequence, but these are still rare examples. Homology modeling is frequently used to derive protein structures especially in drug discovery (Venselaar *et al.* 2009). This method, however, requires a predetermined structure of a closely related protein, which is not always available, and might produce deceptive results if a template is used that is too distant. There is, therefore, a need for efficient and accurate experimental methods to determine protein structures, especially now in the post-genomic era when the number of structure determination targets is expanding.

Two experimental methods are available to study the detailed atomic structure of proteins: X-ray crystallography and NMR spectroscopy. X-ray crystallography has been employed to determine the structures of biomacromolecules for over five decades (Drenth 2007) and the majority of structures in the PDB database are crystal structures. Bottleneck of X-ray crystallographic structure determination is protein crystallization which, even if it has been largely automated, can be rather laborious or, in some cases, turn out to be practically impossible (Chayen and Saridakis 2008). Crystal structures have been criticized for not representing the protein structure in the natural monomeric solution environment. Still, crystallography is usually the most effective method of protein structure determination in terms of time and money. NMR spectroscopy enables protein structure determination both in solution and in solid state (Cavanagh *et al.* 2007). The first NMR structure of a protein was solved 25 years ago (Williamson *et al.* 1985). NMR spectroscopic protein structure determination is rather time consuming, but NMR spectroscopy is a versatile tool which can be used also in studies of protein dynamics and interactions (see Chapter 4 for further details on protein NMR spectroscopy).

Traditional protein structure determination projects have largely focused on rather small isolated protein domains. This is due to ease in crystallization and the good NMR properties of these rigid structures. Keeping in mind that two-thirds of proteins contain more than one domain and domains often affect each other, structures of larger systems should also be studied. In principle, protein size does not set up any limits for X-ray crystallography, but multi-domain systems are often somewhat dynamic and thus difficult to crystallize. Size matters in NMR spectroscopy and thus large modular structures have not been routinely tackled with this method. There are also other methods of gaining low resolution structural information on biomacromolecules. In the case of modular proteins, even low resolution structural data may be very informative. Electron microscopy provides a structural view of biomacromolecules which is close to atomic resolution (Jonic and Vénien-Bryan 2009) and it is often used jointly with X-ray crystallography. Small-angle X-ray and neutron scattering (SAXS and SANS, respectively) are also frequently used in structural studies of macromolecular assemblies and modular proteins (Petoukhov and Svergun 2007). These methods provide information on the dimensions and shape of the molecules in solution state, and the data analysis is often accompanied by detailed atomic structures from X-ray and NMR studies.

3. FILAMINS

Filamins are actin-binding, -cross-linking and -bundling proteins (van der Flier and Sonnenberg 2001b). Filamin, or actin-binding protein as it was called at that time, was identified in 1975 as high-molecular weight actin-binding protein of rabbit lung macrophages (Hartwig and Stossel 1975) and chicken gizzard (Wang *et al.* 1975). Within a couple of years, filamin was purified and characterized in more detail (Shizuta *et al.* 1976; Wang 1977; Wang and Singer 1977; Wallach *et al.* 1978b). Filamins were the first family of actin-binding proteins found outside muscle cells. Soon after their discovery, filamins were also identified in many other organs and tissues such as skeletal and smooth muscle (Bechtel 1979; Koteliansky *et al.* 1981b; Small *et al.* 1986) and heart (Koteliansky *et al.* 1981a; Koteliansky *et al.* 1986). In addition to vertebrate filamins, filamin-related proteins were later found in several other organisms, *e.g.*, in *Dictyostelium discoideum*, *Drosophila melanogaster*, *Entamoeba histolytica* and *Caenorhabditis elegans*. This review will be confined to human filamins, but some examples of studies made on other vertebrates and structural studies of *Dictyostelium* filamins will be included.

Three filamin isoforms have been identified in humans: filamin A (FLNa), filamin B (FLNb) and filamin C (FLNc). Alphabetical naming is the most common but sometimes, especially in the past, other naming systems have also been used (Table 2) (van der Flier and Sonnenberg 2001b). FLNa isoform was the first one found, and early literature does not clearly differentiate between the isoforms. FLNb and FLNc were identified as different isoforms about two decades later (Maestrini *et al.* 1993; Takafuta *et al.* 1998; Xu *et al.* 1998). Kesner *et al.* have recently studied the phylogeny and molecular evolution of filamin isoforms using sequence alignment (Kesner *et al.* 2009b). The three isoforms have emerged through gene duplication and FLNc has diverged least from the common ancestor.

Table 2 Nomenclature of filamin isoforms

Filamin isoform	Other names
Filamin A (FLNa)	α-filamin, actin-binding protein, ABP-280, FLN1
Filamin B (FLNb)	β-filamin, ABP-278, ABP-276, FLN3
Filamin C (FLNc)	γ-filamin, ABPL, FLN2

FLNa and FLNb are the most ubiquitously expressed isoforms present in most tissues and organs, while expression of FLNc is mainly restricted to striated and cardiac muscle (Thompson *et al.* 2000). Chiang *et al.* have studied the expression of filamin isoform genes in mouse embryos and expression of *FLNa* and *FLNb* seems to be especially active in organs with a high proportion of epithelial and smooth muscle cells, whereas expression of *FLNc* is largely localized into striated and cardiac muscles during development (Chiang *et al.* 2000). Filamins, especially FLNa and FLNb, seem to have somewhat overlapping tissue and cell distribution. Different isoforms presumably have partially complementary roles and they can compensate for each other (Feng and Walsh 2004; Baldassarre *et al.* 2009). In cells, filamins are mostly located at peripheral cytoplasm and FLNc is located at

the Z-discs of myofibrils (Maestrini *et al.* 1993). Normally intracellular filamins have also been detected at the cell surface of several human cell lines (Bachmann *et al.* 2006) and recently, even a secreted variant of FLNa was observed in the plasma of cancer patients (Alper *et al.* 2009).

Filamin genes are located in different chromosomes: *FLNa* gene is mapped to chromosome Xq28 (Maestrini *et al.* 1993; Fox *et al.* 1998), *FLNb* to 3p14.3 (Bröcker *et al.* 1999) and *FLNc* to 7q32–35 (Gariboldi *et al.* 1994). It should be noted that inheritance of *FLNa* is X-linked. Filamin genes were sequenced in the 1990s (Xie *et al.* 1998) which enabled closer comparison of the different isoforms. Protein sequence alignment shows that filamins share about 70% homology and are presumed to be structurally very similar (van der Flier and Sonnenberg 2001b).

3.1. Physiological Implications

Filamins function in close collaboration with the cytoskeleton. The cytoskeleton is a dynamic intracellular protein network that is responsible for cell shape, cell adhesion, phagocytosis, locomotion, cell division, and for a range of other fundamental cellular processes (Khurana 2006). Three types of protein filaments—microfilaments, intermediate filaments and microtubules—form the mechanical constructions of cytoskeleton. Microfilaments, also known as actin filaments and thin filaments in muscle cells, are formed through polymerization of actin monomers and are about 8 nm in diameter. Intermediate filaments have an average diameter of 10 nm and are composed of ~70 filamentous proteins, *e.g.*, keratin, vimentin, desmin, neurofilaments and nuclear lamin (Szeverenyi *et al.* 2008). Microtubules are hollow tubes with diameter of 25 nm formed through polymerization of heterodimers of α- and β-tubulin. Actin filaments and microtubules are polar structures polymerizing at the plus-end and depolymerizing at the minus-end. Cytoskeleton is constantly reorganized and modified in structure. Actin filaments, together with intermediate filaments and microtubules, form the physical support structures of the cytoskeleton but they are accessorized with a wide repertoire of other cytoskeletal proteins. Many of these proteins belong to a protein class called actin-binding proteins (ABPs), which, as the name implies, are able to bind actin. ABPs control polymerization and depolymerisation of the actin filaments; they organize actin filaments into bundles and networks by cross-linking several filaments together; they link the filaments to proteins of the cell membrane and other cellular components; and they even participate in cellular signaling cascades (Dos Remedios and Thomas 2001; Dos Remedios *et al.* 2003; Winder 2003; Winder and Ayscough 2005; Uribe and Jay 2009).

Filamins also belong to the group of cytoskeletal actin-binding proteins. Filamins bind actin and bundle it into orthogonal networks or thick ropes depending on the relative protein concentrations (Hartwig *et al.* 1980; Niederman *et al.* 1983). Filamins contribute to cell morphology and movement and they are essential for mammalian development. Cultured cells lacking filamin have unstable surfaces exhibiting so-called blebbing, are incapable of locomotion and have impaired mechanical resistance (Cunningham *et al.* 1992; Flanagan *et al.* 2001). Recent results have shown that filamins play a role in initiation of cell migration and loss of filamin does not, as such, alter cell speed (Baldassarre *et al.* 2009). Filamin gene

knockout models have shed light on the roles and physiological importance of different filamin isoforms. *FLNa* knockout mice have severe cardiac structural defects leading to embryonic lethality (Feng *et al.* 2006; Hart *et al.* 2006). *FLNb* is required in mice for skeletal and microvascular development (Lu *et al.* 2007; Zheng *et al.* 2007; Zhou *et al.* 2007b) and *FLNc* is necessary for normal myogenesis (Dalkilic *et al.* 2006)

Filamin mutations in humans cause a variety of developmental malformations affecting mainly the brain, bone, limbs and the cardiovascular system (Feng and Walsh 2004; Zhou *et al.* 2007a). Even small deletions and point mutations in filamins lead to diverse congenital anomalies (Robertson 2004; Robertson 2005). Table 3 recapitulates human diseases shown to be associated with filamin mutations. Null mutations of *FLNa* lead to defects in neuronal migration, vascular function, and connective tissue integrity (Fox *et al.* 1998; Parrini *et al.* 2006). Missense mutations in *FLNa* are linked to skeletal abnormalities and they are suggested to be gain-of-function mutations (Robertson *et al.* 2003; Robertson 2007). It should be noted that as *FLNa* gene is located at the X chromosome, mutations blocking the expression of functional FLNa often lead to embryonic death in males. *FLNb* mutations disrupt bone morphogenesis (Krakow *et al.* 2004). Mutations in *FLNc* are manifested as myofibrillar myopathies (Shatunov *et al.* 2009). In light of the different filamin-associated diseased, filamins seem to have rather complicated roles in mammalian physiology and they are essential for normal human development.

Table 3 Filamin mutation-associated human disorders.

	Disorder	Description	Mutated domains	References
FLNa	Periventricular heterotopias (PH, PVNH, PNH, BPNH)	Neuronal migration disorder: brain malformation, late-onset epilepsy. Other symptoms: gut dysmotility, congenital cardiovascular abnormalities, defects in connective tissue integrity. Mainly affecting women	Several truncated and frame-shifted versions. Deletions: 11, 15, 23, 24 Insertions: 22, 24 Substitutions: ABD, 4, H2, 23, 24	Fox *et al.* 1998; Sheen *et al.* 2001; Guerrini *et al.* 2004; Zenker *et al.* 2004; Gérard-Blanluet *et al.* 2006; Hehr *et al.* 2006; Parrini *et al.* 2006; Tsuneda *et al.* 2008; Sole *et al.* 2009
	West syndrome	Infantile epilepsy accompanied by PH and developmental regression	Substitutions: 2	Masruha *et al.* 2006
	Ehler's–Danlos syndrome	Connective tissue fragility, joint hypermobility and development of aortic dilatation accompanied by PH.	Truncations Substitutions: ABD (CH1)	Sheen *et al.* 2005; Gomez-Garre *et al.* 2006
	Otopalatodigital spectrum disorders 1 & 2 (OPD1 & OPD2)	OPD1 Conduction deafness, cleft palate, facial malformations, generalized bone dysplasia. Mostly affects males. OPD2 Like OPD1 but more severe + microcephaly and mental retardation. Affects both females and males	OPD1 Substitutions: ABD (CH2) OPD2 Deletions: 14 Substitutions: ABD (CH2), 3, 14–15	Robertson *et al.* 2003; Hidalgo-Bravo *et al.* 2005
	Frontometaphyseal dysplasia (FMD)	Morphogenetic defects of bone, overgrowth of frontal facial bones. Deafness, digital anomalies, osteodysplasia. Affects more males than females.	Substitutions: ABD (CH2), 9–10, 14–16, 22–23	Robertson *et al.* 2003; Zenker *et al.* 2004; Stefanova *et al.* 2005; Robertson *et al.* 2006; Zenker *et al.* 2006
	Melnik–Needles syndrome (MNS)	Malformed skull and craniofacial structures; irregular constrictions in the ribs; deformed clavicles, scapula and pelvis; curved long bones. Mostly affects females.	Substitutions: 10	Robertson *et al.* 2003
	FG syndrome	Congenital hypotonia, delayed development of speech, macrocephaly, anal anomalies or severe constipation, dysmorphic facial features.	Substitutions: 11	Unger *et al.* 2007
	X-linked myxomatous valvular dystrophy (XMVD)	Cardiac valvular dystrophy	Deletion: 5–7 Substitutions: 1, 4–5	Kyndt *et al.* 2007

Table 3 *(continued)*

	Disorder	Description	Mutated domains	References
FLNb	Spondylocarpotarsal syndrome (SCT)	Short-trunk dwarfism of postnatal onset, unsegmented thoracic vertebrae, carpal bone fusions	Truncations	Krakow *et al.* 2004; Farrington-Rock *et al.* 2008
	Larsen syndrome	Multiple joint dislocations, craniofacial abnormalities, accessory carpal bones	Substitutions: ABD, 2, 13–15, 17	Krakow *et al.* 2004; Zhang *et al.* 2006; Bicknell *et al.* 2007; Dobbs *et al.* 2008
	Atelosteogenesis I and III (AOI and AOIII)	Skeletal dysplasia with vertebral abnormalities, disharmonious skeletal muscles and poorly modeled long bones and joint dislocations	Substitutions & short inframe deletions: ABD (CH2), 6, 14–15	Krakow *et al.* 2004; Farrington-Rock *et al.* 2006
	Boomerang dysplasia	Perinatal lethal osteochondrodysplasia; absence or underossification of the limb bones and vertebrae	Substitutions: ABD (CH2)	Bicknell *et al.* 2005
FLNc	Myofibrillar myopathies (MFMs)	Neuromuscular disorder, Focal myofibrillar destruction and abnormal accumulation of several proteins within skeletal muscle fibres	Short inframe deletion: 7 Truncation: 24	Vorgerd *et al.* 2005; Kley *et al.* 2007; Löwe *et al.* 2007; Shatunov *et al.* 2009

3.2. Structure of Filamins

Filamins are large homodimeric multi-domain proteins. Molecular weights of FLNa, FLNb and FLNc are 280 kDa, 278 kDa and 290 kDa, respectively. When FLNa sequence was first analyzed in detail (Gorlin *et al.* 1990), it was noted that the structure contained an N-terminal actin-binding domain (ABD) and 24 tandem immunoglobulin-like domains (IgFLNs), also called Ig repeats (Fig. 3). Filamins form non-covalent tail-to-tail homodimers through the 24th IgFLN domain (Hartwig and Stossel 1981; Pudas *et al.* 2006). ABD resembles α-actinin and spectrin ABDs with two calponin homology (CH) domains CH1 and CH2. IgFLNs 1–15 and 16–24 form the rod domains 1 and 2, respectively. Linkers between the Ig domains are short and proline rich except for the two flexible hinges, hinge 1 (H1) and hinge 2 (H2), that interrupt the series of Ig repeats. H1 is located between domains 15–16 and H2 between domains 23–24 and they are 27 and 35 residues in length, respectively. Hinges are sequentially less conserved than other regions: they show only 45% homology while there is 70% overall sequence homology between FLN isoforms (van der Flier and Sonnenberg 2001b). Electron microscopic images of FLNs show V-shaped flexible chains with an overall monomer length of ~80 nm (Hartwig *et al.* 1980; Hartwig and Stossel 1981).

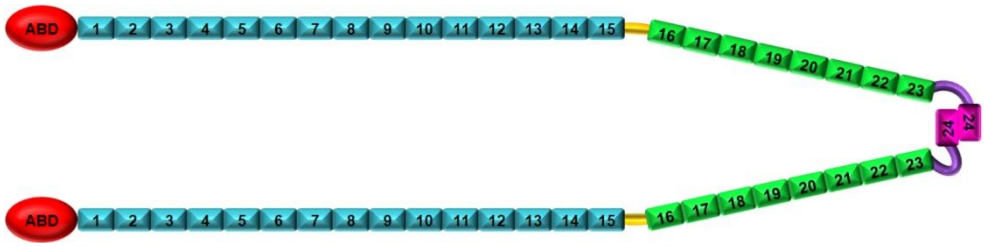

Fig. 3 Schematic representation of filamin structure. Red ellipse, actin-binding domain (ABD); rectangle, filamin-type Ig domain (IgFLN); cyan, rod domain 1; green, rod domain 2; yellow, hinge 1 (H1); purple, hinge 2 (H2); pink, dimerization domain.

Filamins are known to be selectively proteolyzed by several proteases and some filamin functions are presumably regulated through proteolysis. Filamin proteolysis was first studied by Davies *et al.* (Davies *et al.* 1978). The hinge regions are susceptible to proteolysis by calpain (Guyon *et al.* 2003; Raynaud *et al.* 2006). Elevated calpain 2 activity and increased levels of FLNa16–24 fragment have been detected in patients with Marfan syndrome; a heritable disorder of connective tissue affecting principally skeletal, ocular, and cardiovascular systems (Pilop *et al.* 2009). C-terminal fragment of FLNa (IgFLNa16–24) is known to translocate to nucleus and interact there with androgen receptor (Loy *et al.* 2003). Granzyme B and caspase cleavage of FLN is detected in apoptotic cells (Browne *et al.* 2000). Protein activity can also be regulated by targeting proteins for proteasomal degradation. ASB2 has been shown to target FLNa and FLNb for proteasomal degradation in leukemia cells (Heuze *et al.* 2008). Filamin function can be regulated by alternative splicing and several splicing variants of filamins have been identified (Maestrini *et al.* 1993; Patrosso *et al.* 1994; Xie *et al.* 1998; van der Flier *et al.* 2002). Filamins are also likely to be regulated by phosphorylation. Filamin phosphorylation was studied soon after protein identification by Wallach and coworkers (Wallach *et al.* 1978a). Filamin is known to be phosphorylated by several kinases (see Table 5) and Ser2152 of FLNa is one of the frequently encountered target residues. Phosphorylation seems to inhibit filamin proteolysis by calpain (Chen and Stracher 1989). Calcineurin has been shown to dephosphorylate the C-terminal region of filamin (García *et al.* 2006) and FLNa seems to associate with protein tyrosine phosphatase PTP-PEST (Playford *et al.* 2006). Apart from proteolysis and phosphorylation not much is known about filamin post-translational modifications and how these contribute to FLN structure and function. Recently FLNa has been detected to undergo serotonylation by transglutaminase in arterial vascular smooth muscle (Watts *et al.* 2009).

3.2.1. Actin-binding Domain

ABDs of FLNs are closely related to the ABDs of spectrin, α-actinin, dystrophin, utrophin, plectin and fimbrin (Gorlin *et al.* 1990; Clark *et al.* 2009; Sawyer *et al.* 2009). FLN ABDs are 240–270 residues in length and contain two calponin homology (CH) domains, CH1 and CH2. The CH domains of FLN isoforms share

87% sequence identity and they are presumed to be very similar regarding structure and actin-binding properties. FLNa and FLNc have a 20–30 residue N-terminal tail not present in FLNb.

The first structure of FLN ABDs was the structure of FLNb ABD. Crystal structures of FLNb ABD (PDB accession code 2WA5) and its W148R (PDB: 2WA6) and M202V (PDB: 2WA7) mutants were solved by Sawyer *et al.* (Sawyer *et al.* 2009). The structure shows two CH domains with same overall fold tightly bound together in closed conformation (Fig. 4). Both CH domains contain helices A, C, D and E. There are additional short one-turn helices B and D' in CH1 and CH2, respectively. The flexible loop connecting the CH domains is closely located with the C-terminus of the ABD and it is possible that it could interact with the first Ig repeat. Substitution M202V is associated with atelosteogenesis I and III while W148R is seen only in atelosteogenesis I (Krakow *et al.* 2004; Farrington-Rock *et al.* 2006). The substitution mutants W148R and M202V closely retain the fold of the native structure but lower the thermal stability of the domain. W148 is located at helix A' of CH2 and it points to the interior of CH2. M202 is located at CH2 helix E' and it resides in a rather hydrophobic environment. FLNb ABD mutations W148R and M202V evoke increased F-actin binding affinities, which could explain the gain-of-function phenotype of atelosteogenesis I and III.

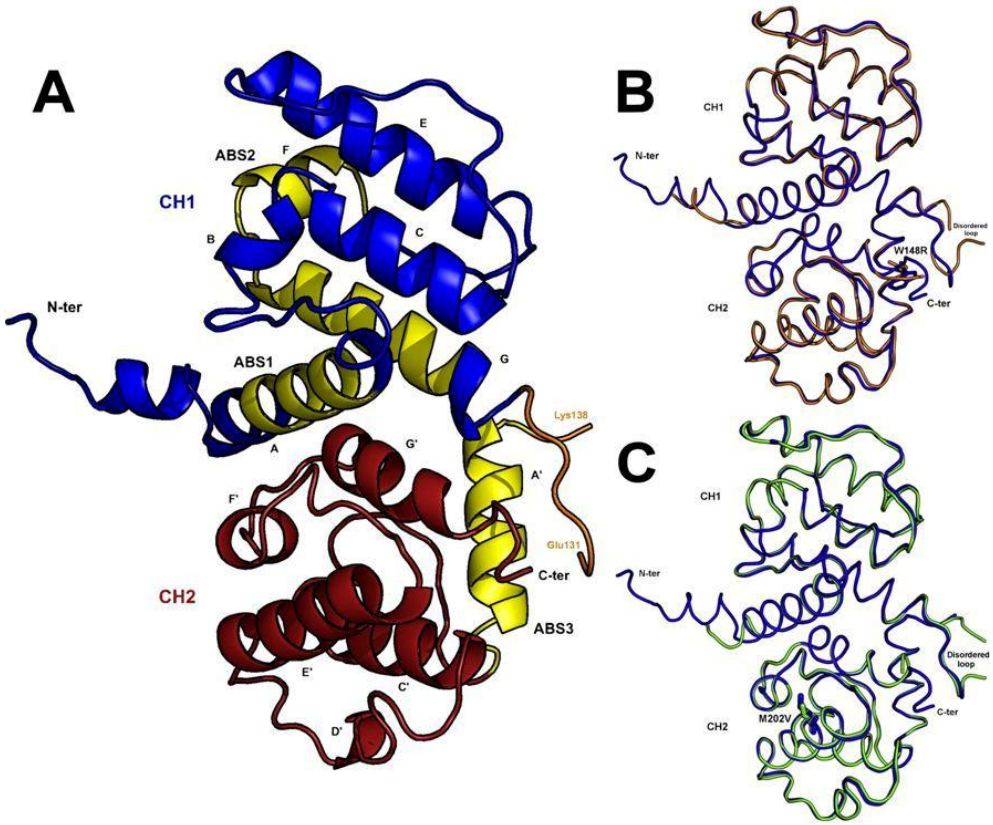

Fig. 4 The structure of FLNb ABD (Sawyer *et al.* 2009). (**A**) Native FLNb ABD. CH1 and CH2 domains are colored in blue and red, respectively, and the helices are marked with their letter codes. Yellow areas correspond to the known actin-binding sequences (ABS). Panels (**B**) and (**C**) show the superpositions of the native FLNb ABD structure (blue) and the structures of W148R (orange) and M202V (green) mutants, respectively. Mutated residue is indicated with stick representation. Superpositions show that the structures of the mutated forms closely match with the native structure. Reprinted with permission from (Sawyer *et al.* 2009). © 2009 Elsevier.

The structure of FLNa ABD has recently been solved by two independent research groups (Clark *et al.* 2009; Ruskamo and Ylänne 2009). FLNa and FLNb ABDs are structurally very similar (Fig. 5). N-terminal tail of FLNa ABD not present in FLNb is not observed in the electron density map and is thus presumably disordered. Clark *et al.* have also determined the structure of FLNa ABD with E254K mutation (Clark *et al.* 2009). This mutation, which is manifested in humans as otopalatodigital syndrome type 2 (OPD2), is located at the CH2 domain of FLNa ABD (Robertson *et al.* 2003). Like the FLNb ABD mutants studied by Sawyer *et al.*, FLNa ABD E254K mutant closely retains the fold of wild-type domain (Fig. 5) but the structure has reduced stability. The phenotype of OPD2 is thought to arise

from a gain-of-function mechanism and consistency with this, E254K mutation was shown to enhance the actin-binding affinity of FLNa ABD.

Fig. 5 The structure of FLNa ABD. Structures of wild-type FLNa ABD (blue) and its E254K mutant (cyan) (Clark *et al.* 2009) and the structure of FLNb ABD (magenta) (Sawyer *et al.* 2009) were superimposed to visualize their structural differences. The mutated residue of FLNa ABD (E254) forming a salt bridge with K169 and the structurally equivalent residues of FLNb ABD are represented with stick models. Compared to the perspective shown in Fig. 4, the structures have been rotated 180° along the vertical axis. The overall fold of FLNa and FLNb ABDs is almost identical. FLNa ABD E254K mutant closely retains the structure of the native domain. PDB accession codes: FLNa ABD, 3HOP; FLNa ABD E254K, 3HOC; FLNb ABD, 2WA5.

3.2.2. Rod Domain: Immunoglobulin-like Domains

Filamins contain two elongated rod domains which are composed of 24 consecutive immunoglobulin-like domains. The seven β sheet fold of the rod repeats (Fig. 6) was first suggested by Gorlin *et al.* based on sequence comparisons (Gorlin *et al.* 1990). FLN Ig repeats have an average length of ~96 residues. It was also pointed out that the C-terminal repeat is responsible for filamin dimerization. The first

structural evidence to support the immunoglobulin-like fold of the FLN rod repeats was obtained from structure determination of highly homologous *Dictyostelium* filamin (ABP-120) rod domain segment 4 (Fucini *et al.* 1997). This structure was determined by solution state NMR spectroscopy and it was the first example of Ig fold found in ABP. The structure was closest to the topological subtype C1 of the immunoglobulin superfamily (Fig. 2) which was previously seen only in cell-surface proteins. The sequence of ABP-120 rod repeat 4 does not show close homology to any other proteins with Ig fold. As IgFLN sequence resembles the sequence of ABP-120 repeats it was suggested that IgFLN repeats also potentially have the same fold.

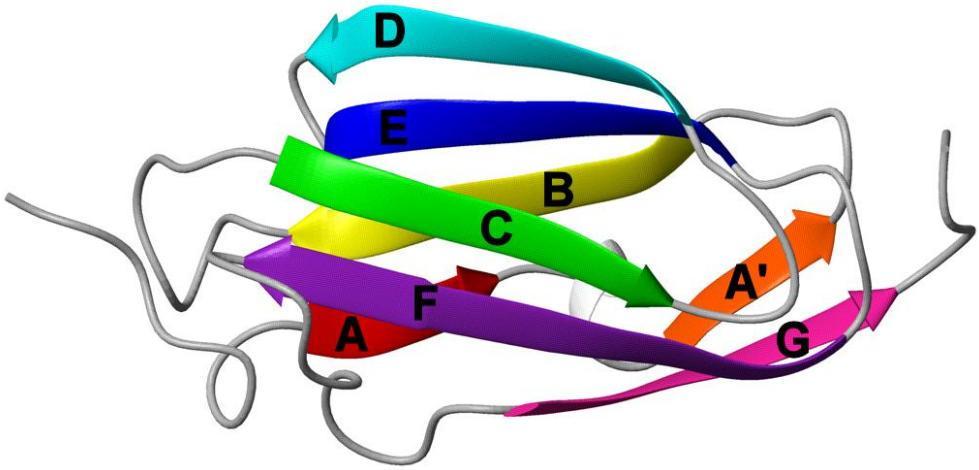

Fig. 6 General structure and topology of filamin-type Ig domains presented using IgFLNa23 (PDB code: 2K3T) as an example. Letter codes used for the β strands are indicated.

To date there are several structures of human IgFLNs in the PDB database (see Table 4). Most of them are isolated single-domain structures. IgFLN fold belongs to the E-set superfamily of the immunoglobulin-like folds (Murzin *et al.* 1995) resembling the I-topology of immunoglobulin superfamily (Fig. 2). The majority of the structures are solved using NMR spectroscopy as part of the structural genomics initiative and they have not been published as part of any research article. At the moment there are no structures of IgFLNs 1–8 in the PDB database. For some domains there are structures available for several isoforms. Structural comparison shows that the highly homologous isoforms are also structurally very similar (see Fig. 26 for an example). Complex structures of IgFLNa17 and 21 with their binding partners reveal general interaction mechanism of IgFLNs (see Chapter 3.3.2).

Table 4 Presently available filamin domain structures in the PDB database.

FLN isoform: domain	Description	PDB code	Reference (if available)
A: ABD	X-ray: Native protein, reduced and E254K mutant	3HOC, 3HOP, 3HOR	Clark *et al.* 2009
A: ABD	X-ray	2WFN	Ruskamo and Ylänne 2009
B: ABD	X-ray: Native protein, W148R and M202V mutants	2WA5, 2WA6, 2WA7	Sawyer *et al.* 2009
B: ABD	X-ray	3FER	
B: 9	NMR	2DI9	
B: 10	NMR	2DIA	
B: 11	NMR	2DIB	
B: 12	NMR	2DIC	
B: 13	NMR	2DJ4	
B:14	NMR	2E9J	
C: 14	NMR	2D7M	
B: 15	NMR	2DMB	
A: 16–17	NMR: Domain association of 16–17	2K7P	**IV**
B: 16	NMR	2EE9	
C: 16	NMR	2D7N	
A: 17	X-ray: Complex with GPIbα peptide	2BP3	**I**
A: 17	NMR	2AAV	**I**
B: 17	NMR	2EEA	
C: 17	NMR	2D7O	
A: 18–19	NMR: Domain association of 18–19	2K7Q	**IV**
B: 18	NMR	2DMC	
B: 19	NMR	2DI8	
A: 19–21	X-ray: Domain association of 20–21	2J3S	Lad *et al.* 2007
B: 20	NMR	2DLG, 2E9I	
A: 21	X-ray: Complex with integrin β7 peptide	2BRQ	Kiema *et al.* 2006
A: 21	X-ray: Complex with integrin β2 peptide	2JF1	Takala *et al.* 2008
A: 21	X-ray: Complex with migfilin peptide	2W0P	Lad *et al.* 2008
A: 21	NMR: Complex with migfilin peptide	2K9U	Ithychanda *et al.* 2009a
B: 21	NMR	2EE6	
B: 22	NMR	2EEB	
C: 22	NMR	2D7P	
A: 23	NMR	2K3T	**II**
B: 23	NMR	2EEC	
C: 23	X-ray	2NQC	Sjekloca *et al.* 2007
C: 23	NMR	2D7Q	
A: 24	X-ray: Dimerization mechanism	3CNK	Seo *et al.* 2009
B: 24	NMR	2EED	
C: 24	X-ray: Dimerization mechanism	1V05	Pudas *et al.* 2005
A	X-ray: Complex with CFTR peptide (Status 16.11.2009: unreleased)	3ISW	

Dimerization mechanism of FLNs was revealed in detail in the structure of IgFLNc24 (Pudas *et al.* 2005). In the crystal structure of IgFLNc24, two domains form a compact dimer using their CD faces (Fig. 7). The two domains are arranged in antiparallel orientation. Identical domain interaction is seen in the crystal structure of IgFLNa24 (Seo *et al.* 2009). Dimerization of *Dictyostelium* ABP-120 also takes place through antiparallel interaction of the C-terminal rod repeats and involves edge-to-edge extension of the β sheets (McCoy *et al.* 1999). Atomic and topological details of the dimerization mechanisms are however drastically different. *Dictyostelium* ABP-120 dimerization takes place through strands B and G. Topology of the *Dictyostelium* ABP-120 dimerization domain (domain 6) differs from other domains: A strand is missing and there is an additional strand H. Absence of strand A liberates BG face for dimerization. Topology of IgFLNa24 and IgFLNc24 matches with other IgFLN domains and dimerization mechanism does not necessitate major structural adjustment. While the dimerization of IgFLN24 produces two β sheets with same topology ($A_1B_1E_1D_1C_2F_2G_2A'_2$) the dimerization of ABP-120 domain 6 creates two very different β sheets: $D_1E_1B_1B_2E_2D_2$ and $H_1G_1F'_1F_1C_1C_2F_2F'_2G_2H_2$. The preceding repeat 5 and the domain linker were also seen to contribute to *Dictyostelium* ABP-120 dimerization. As IgFLN24 dimerization mode, as such, produces an antiparallel orientation of the filamin monomers, but electron micrographs of filamins suggest a V-shaped structure, the role of IgFLN23 and H2 in dimerization of human FLNs was studied by Sjekloca *et al.* (Sjekloca *et al.* 2007). Their results show that IgFLNc23 does not have preference for self-association and it interacts very little with domain 24. It seems that H2 is forming a spacer or orientational guide between the two domains. They concluded that IgFLNc24 is the sole determinant for FLN dimerization. Also other cytoskeletal proteins have been found to use β sheet extension of the Ig modules for dimerization, but their detailed interaction modes are different from filamins (Zou *et al.* 2006; Pinotsis *et al.* 2008; Pinotsis *et al.* 2009). Isoform specificity of FLN dimerization has also been studied but the results are ambiguous. Himmel *et al.* have found that FLNb and FLNc are able to heterodimerize whereas FLNa only forms homodimers (Himmel *et al.* 2003). In contrast, Sheen *et al.* have shown that FLNa and FLNb are able to form heterodimers (Sheen *et al.* 2002). Their results, however, also indicate that the FLNa–FLNb heterodimerization site might be located at rod region 2, instead of domain 24. The experiments of Himmel *et al.* were conducted with constructs containing IgFLN domains 22–24.

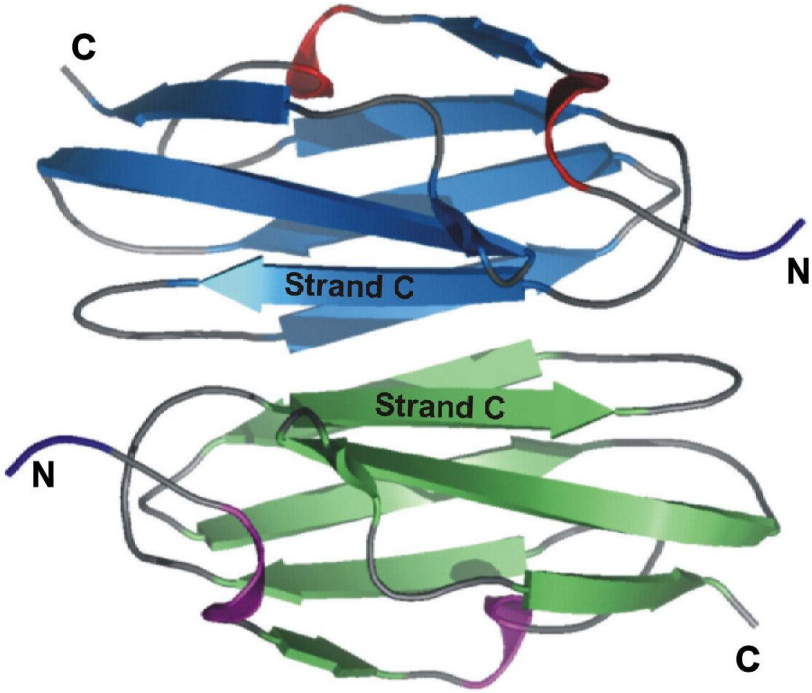

Fig. 7 The dimerization mechanism of human filamins. Crystal structure of IgFLNc24 reveals how the C-terminal IgFLN domains form an antiparallel dimer using their CD faces. Reprinted with permission from (Pudas *et al.* 2005). © 2005 Elsevier.

It has been proposed that controlled unfolding and refolding of IgFLNs could regulate filamin functions and have a role in mechanosensory signaling (Johnson *et al.* 2007). Thus stability of IgFLN fold has been of interest. The mechanical strength of *Dictyostelium* ABP-120 Ig domains has been studied both with molecular dynamics simulations (Kolahi and Mofrad 2008) and with single-molecule techniques (Schwaiger *et al.* 2004; Schwaiger *et al.* 2005). These studies show that ABP-120 Ig domains unfold before the dimer dissociates and that domain 4 with a stable folding intermediate starts to unfold with smaller force than the other domains. N-terminal unfolding of IgFLN domains under physiological forces was observed in discrete molecular dynamic simulations (Kesner *et al.* 2009a) and it was suggested that it could be a mechanism for exposure of cryptic binding sites, removal of native binding sites, and modulation of the quaternary structure. The mechanical strength of human filamins has also been studied with single-molecule techniques (Furuike *et al.* 2001; Yamazaki *et al.* 2002). Thermal stability of IgFLN domains has been studied using NMR spectroscopy (Jiang and Campbell 2008). These studies have shown that IgFLNa21 is less stable than domains 17 and 19 even if it is structurally very similar to these domains.

There are only a few structures of multi-domain IgFLN constructs available. Crystal structures of *Dictyostelium* ABP-120 multi-domain fragments (McCoy *et al.* 1999; Popowicz *et al.* 2004) show that the linkers between the

domains are relatively short and there are some inter-domain interactions between the domains. Consecutive domains form a zigzag shaped modular construction. Stability of the domain arrangement was studied with steered molecular dynamics simulations (Kolahi and Mofrad 2008) and it was noted that the repeats lose their staggered topology easily before any domain unfolding takes place. This means that the inter-domain forces are relatively weak. At next stage the domain linkers extend and lose their tertiary structure. It was speculated that despite the rigid conformation and several domain–domain interactions seen in the crystal structure, under tension, filamin rod domains become flexible, as seen in EM images (Hartwig *et al.* 1980).

Gorlin *et al.* noticed that filamin repeats 16, 18, 20, 22 and 24 have atypical N-terminal sequences (Gorlin *et al.* 1990). Nowadays, structures are available on all these domains. Domains 22 and 24 seem to have typical IgFLN folds, whereas structures of IgFLN16, 18 and 20 seem to be deprived of strand A. It has now become evident that these three domains are not structurally independent folding units, but form higher-order structures with the following domain (Lad *et al.* 2007: **IV**). First human filamin structure with multiple domains was the structure of IgFLNa19–21 (Lad *et al.* 2007). IgFLNa19 and 21 have traditional IgFLN folds but IgFLN20 is drastically different and the inter-domain organization is not linear (Fig. 8). The first β strand of IgFLNa20 is not a part of its own domain, but binds to the CD face of domain 21 blocking the integrin binding site (Kiema *et al.* 2006). Domain 20 is bound to the N-terminal end of domain 21 through a short β strand interaction between IgFLNa20 strand G and IgFLNa21 BC loop. It is worth noting that FLN splice variants lacking the inhibitory strand A of domain 20, and showing enhanced integrin binding, have been previously reported (van der Flier *et al.* 2002). This implies that the domain interaction could have an auto-inhibitory role. Also, structures of IgFLNa16–17 and 18–19 double-domains are now available and these provide yet more new domain interaction modes of IgFLN domains (see Chapter 7.2 for further details) (**IV**). Crystallization of IgFLNa14–16, which contains the H1 region, has also been reported (Aguda *et al.* 2007), but the structure is not yet available. Pentikäinen and Ylänne have studied the stability of the IgFLNa domain pairs 18–19 and 20–21 with steered molecular dynamics simulations (Pentikäinen and Ylänne 2009). They noticed that mechanical force applied to filamin can expose cryptic integrin binding sites by detaching the auto-inhibitory strand A of the even-numbered domain from the CD face of the odd-numbered domain, without unfolding the entire domains, and through this mechanism filamins could act as a mechanotransducers. Johnson *et al.* have screened for cytoskeletal proteins undergoing conformational changes due to mechanical cell stress and their results suggested that filamins could be involved in mechanosensory signaling (Johnson *et al.* 2007).

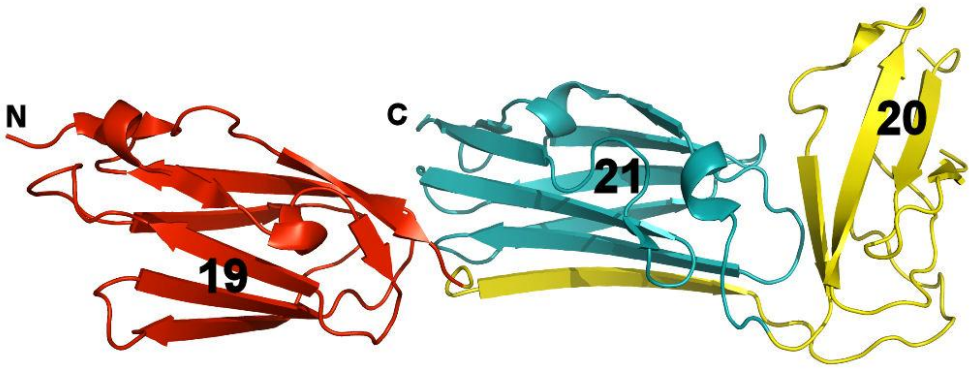

Fig. 8 The structure of IgFLNa19–21 (Lad *et al.* 2007). IgFLNa domains have been numbered and colored to emphasize the peculiar nonlinear domain organization. The locations of N- and C-termini are also indicated.

The first electron micrographs of filamins showed that the average length of filamin monomer is 80 nm (Hartwig *et al.* 1980). This is substantially less than would be expected for an almost linear array of 24 independent IgFLN domains whose approximate length is 4–5 nm. Dimensions of several filamin constructs have been studied with electron microscopy (Nakamura *et al.* 2007). Overall length of rod 2 (IgFLNa16–23) is considerably smaller than for constructs of same size from rod 1 (IgFLNa1–8 and 8–15) (Fig. 9). The average spacing of *Dictyostelium* ABP-120 Ig repeats in the three-domain construct having the zigzag arrangement was 3.7 nm (Popowicz *et al.* 2004). This would make 30 nm for eight consecutive repeats which is in pretty good agreement with IgFLNa1–18 and 8–15 construct. Average repeat spacing is however only 2.4 nm for FLN rod 2 (Nakamura *et al.* 2007). This clearly states that several domains in FLN rod 2 must exhibit more compact domain packing.

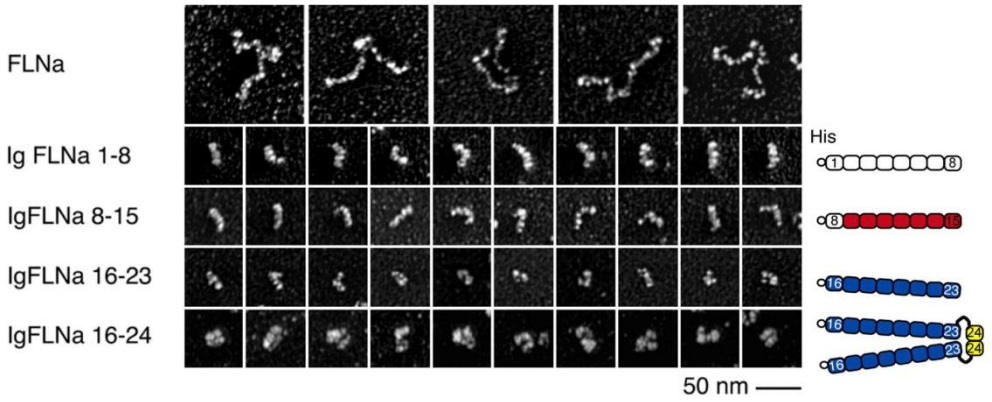

Fig. 9 Electron micrographs of rotary shadowed FLNa and truncated constructs fused to a His(hexahistidine)-tag. The rod 2 has a more globular and compact appearance. Reprinted and adapted with permission from (Nakamura *et al.* 2007). © 2007 Nakamura *et al.*

3.3. Interactions of Filamins

Filamins were first identified as actin-binding proteins but have since been shown to host a range of other interaction partners—they have even been reproached for being promiscuous (Popowicz *et al.* 2006). Interaction partners of filamins include membrane receptors and channels, enzymes, signaling intermediates and transcription factors (Stossel *et al.* 2001; Feng and Walsh 2004; Zhou *et al.* 2007a). Filamins seem to act as versatile mediators between the cytoskeleton and the proteins of the cell membrane. They anchor various transmembrane proteins, *e.g.*, cell adhesion molecules, to the cytoskeleton and thereby localize the membrane proteins to correct areas at the cell surface and mediate forces and signals from extracellular matrix to cytoskeleton. They also function as signaling scaffolds by coordinating several intracellular signaling intermediates. Different filamin related diseases are proposed to highlight different filamin interactions (Feng and Walsh 2004). Mutations localized at the binding areas of certain proteins disrupt this specific interaction, probably leaving other functions intact.

3.3.1. Interaction with Actin

Soon after identification of filamin, the actin-binding properties of the protein were characterized in more detail. Wand and Singer found that filamin collects actin filaments into thick bundles or into networks and they stated that in this way, filamins could regulate the ultrastructural state of F-actin filaments in a variety of dynamic cellular processes (Wang and Singer 1977). A decade later Hartwig and Shevlin noticed in their studies of cytoskeleton of lung macrophages that actin-binding protein, *i.e.*, filamin, is found at high-angle actin filament intersections and at points where filaments are in contact with the cell membrane (Hartwig and Shevlin 1986).

Rheological properties of filamin–actin networks have been presented in several papers. Electron micrographs of filamin–actin networks show high-angle branching of the filaments (Fig. 10) and branch distances are inversely proportional to the filamin concentration (Hartwig *et al.* 1980; Niederman *et al.* 1983). Filamin induces gelation of actin (Brotschi *et al.* 1978; Hartwig and Stossel 1981). Filamin dimerization is a prerequisite for efficient actin cross-linking, -bundling and -gelation. Hinge 1 seems to be essential for visco-elasticity of the filamin–actin networks (Goldmann *et al.* 1997; Gardel *et al.* 2006). The mechanical strength of filamin–actin interaction has been measured using single molecule techniques (Yamazaki et el. 2002; Ferrer *et al.* 2008). It was noted that the IgFLN domains unfold with less force than that needed to break the interaction with actin, and unfolding of the domains was seen to be reversible. Several studies exist where properties of filamin induced actin networks have been compared with networks generated by other ABPs. Filamin cross-linked F-actin networks are more resilient, stiffer, more solid-like and less dynamic than the actin networks generated by α-actinin and fascin (Tseng *et al.* 2004). Nakamura *et al.* have studied the differences in mechanical properties of filamin-crosslinked and Arp2/3-branched actin filaments (Nakamura *et al.* 2002). Filamin-cross-linked actin network is flexible,

orthogonal, fairly resistant meshwork adapting to morphological changes and thus enabling slow cell migration (Flanagan *et al.* 2001).

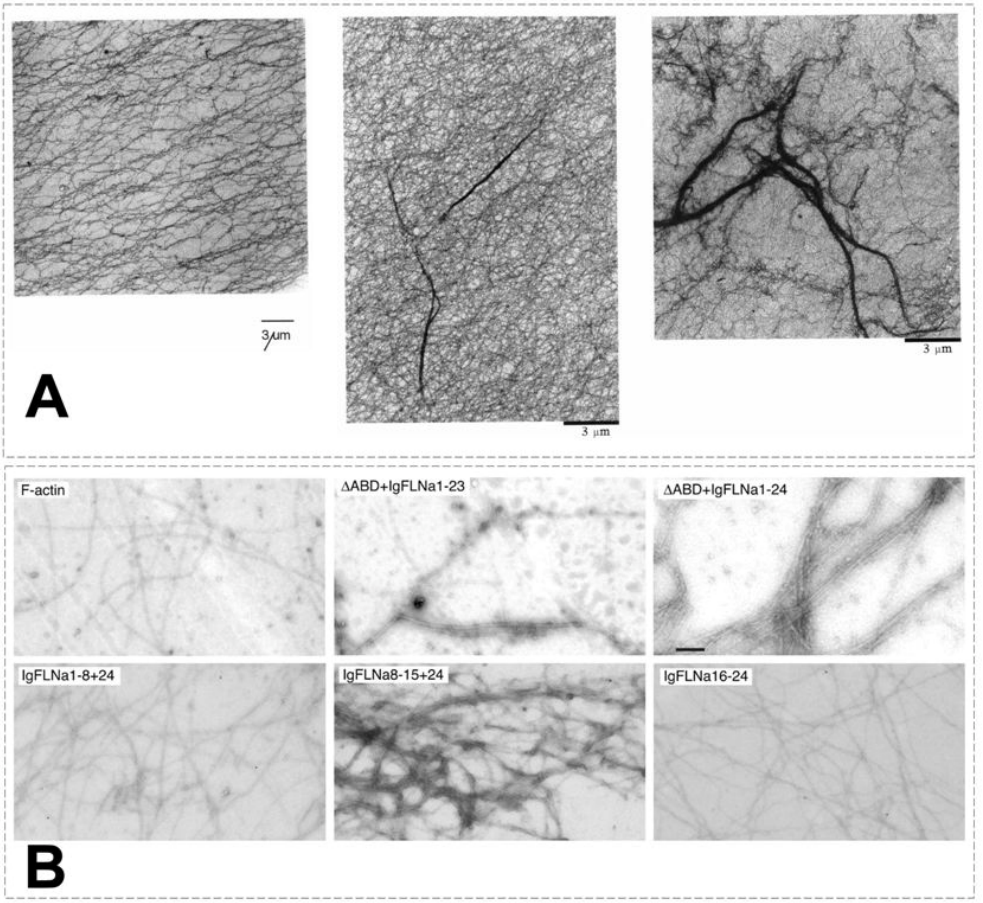

Fig. 10 Electron microscopic images of filamin–actin networks. (**A**) Actin-to-filamin concentration ratio affects morphology of actin networks: 10 μm actin in the presence of gelsolin (1:2000) without filamin (left); and with 300:1 (middle) and 20:1 (right) actin-to-filamin ratios. Reprinted and adapted with permission from (Goldmann *et al.* 1997). © 1997 Federation of European Biochemical Societies. (**B**) Also ABD deficient FLNa constructs are able to align F-actin into bundles. Another actin-binding site is located at IgFLN domains 8–15. Reprinted and adapted with permission from (Nakamura *et al.* 2007). © 2007 Nakamura *et al.*

The actin-binding site of filamin A was characterized in 1990s (Lebart *et al.* 1994). Based on sequence alignment with other ABPs it was known already that the actin-binding activity is located at the N-terminal part of the protein, *i.e.*, at the ABD. Lebart *et al.* mapped the actin-binding activity of FLNa to hydrophobic stretch of residues 121–147 (corresponding to actin-binding sequence 2 (ABS2) in Fig. 4), but they also noted that other, presumably hydrophilic, regions participate in the interaction making it sensitive to increasing salt concentrations (Lebart *et al.*

1994). Filamin–actin interaction was characterized also from the actin's point of view (Méjean *et al.* 1992). Filamin binding site was located at actin residues 105–120 and 360–372 at actin subdomain 1 (Fig. 11). Recently new light was shed on the filamin–actin interaction by Nakamura *et al.* (Nakamura *et al.* 2007). They showed that ABD of filamin is essential for actin gelation but it is not the only actin-binding region of filamin. Substantial actin-organizing activity was seen also in IgFLN domains 9–15 (Fig. 10).

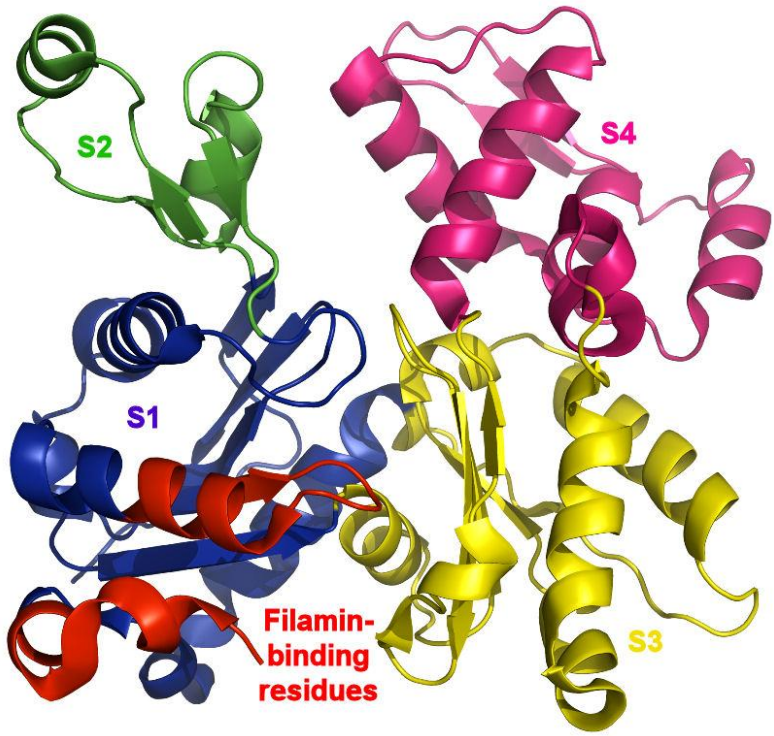

Fig. 11 The filamin binding site in actin monomer (Otterbein *et al.* 2001; Méjean *et al.* 1992). G-actin subdomains S1, S2, S3 and S4 have been indicated with different colors. Filamin-binding residues (105–120 and 360–372) are colored in red.

Structural characterization of filamin–actin interaction became possible after the structure of the FLNb ABD was solved (Sawyer *et al.* 2009). Three actin-binding sequences (ABS) have been identified in ABPs with double CH domain ABD. ABS1 and ABS2 are located near the N- and C-termini of the CH1 domain, respectively, while the ABS3 is at the CH2 domain (see Fig. 4). Both CH domains contribute to actin-binding so the entire ABD is needed for fully functional filamin–actin interaction. It should be noted that the three ABSs do not form a continuous surface, but conformational change probably aligns the actin-binding regions during binding. Lehman *et al.* have reviewed the conformation studies of CH domain-containing ABDs of several proteins (Lehman *et al.* 2004). FLNb ABD binds to F-actin at 1:1 molar ratio with dissociation constant K_d of 7.0 μM (Sawyer *et al.* 2009). The patient mutations W148R and M202V seemed to enhance the actin binding affinity of FLNb ABD. These mutations lead to autosomal dominant gain-

of-function FLNb disorders characterized by vertebral abnormalities, bone dysplasia and joint dislocations (Farrington-Rock *et al.* 2006). Enhanced actin-binding activity of FLNb explains the gain-of-function phenotype but it remains unclear how these rather remote point mutants closely retaining the fold of the native ABD can alter the affinity. FLNa ABD mutation E254K, which located at the vicinity of ABS1 and ABS3, has been shown to enhance actin-binding affinity of FLNa (Clark *et al.* 2009).

Interaction of filamin with actin can be regulated through several mechanisms. Proteolysis of filamins at hinge regions separates the dimerisation from actin-binding activity which means that filamins lose their ability to cross-link actin. Filamin–actin-filament cross-linking has been shown to be modulated by tyrosine kinase $p56^{lck}$ (Goldmann 2001; Pal Sharma and Goldmann 2004). Ca^{2+}-calmodulin has been shown to regulate the filamin–actin interaction through binding to the ABD of FLNa and thus dissociating the filamin from actin (Nakamura *et al.* 2005). Ca^{2+}-calmodulin seems to be unable to bind to the ABD of free filamin which means that it could act as a switch to release the filamin from actin filaments. Filamin activity can also be localized to certain cytoskeletal sites through the ABD. Recently, it has been shown that differences in the ABDs of filamin and α-actinin direct these proteins to different cellular locations (Washington and Knecht 2008).

3.3.2. Interactions of the Rod Domains

IgFLN domains, especially the domains 16–24, are actively interacting modules in filamins (Stossel *et al.* 2001; van der Flier and Sonnenberg 2001b; Feng and Walsh 2004; Popowicz *et al.* 2006; Zhou *et al.* 2007a). Table 5 summarizes the interaction partners of human filamins. It should be noted that some of the partners could be assigned to several categories, but the most itemized and descriptive of the suitable categories was chosen. The number of interaction partners is extensive. One has to keep in mind that there might also be some false positives, and the interaction site can be mapped to a false location. The majority of the interaction studies have used the yeast two-hybrid system (Fields and Song 1989) for identification of the interaction region and, unfortunately, domain boundaries are not always considered in these studies. Clipping of domains in parts might produce hydrophobic patches that can interact non-specifically. As the number of interactions is vast, the entirety will not be covered here in detail. The rest of this chapter will be devoted to the details of the interactions that are studied in the experimental part of this thesis. These interaction partners are glycoprotein Ibα, integrins, FilGAP, and dopamine receptors.

Table 5 Molecules that have been shown to physically interact with the rod domains of human filamins.

Interaction partner	FLN isoform: interacting repeats	References
Transcription regulators		
Androgen receptor	A/C: 16–19	Ozanne *et al.* 2000; Loy *et al.* 2003; Wang *et al.* 2007
FOXC1	A: 4–9 & 16–21	Berry *et al.* 2005
PEBP2/CBF	A: hinge2–24	Yoshida *et al.* 2005
p73α	A: 20–24	Kim *et al.* 2007b
Smad2, 3 & 5 (TGF-β signaling)	A/B: 20–23	Sasaki *et al.* 2001; Zheng *et al.* 2007
BRCA2 tumor suppressor	A: 21–24	Yuan and Shen 2001
Cell adhesion and motility		
FAP52	A: 13–16	Nikki *et al.* 2002
FILIP (Filamin A-interacting protein)	A: 15–18	Nagano *et al.* 2002; Nagano *et al.* 2004; Sato and Nagano 2005
GPIbα	A/B: 17	Fox 1985; Okita *et al.* 1985; Meyer *et al.* 1997; Takafuta *et al.* 1998; Xu *et al.* 1998; Williamson *et al.* 2002; Feng *et al.* 2003; Cranmer *et al.* 2005; Feng *et al.* 2005; **I**
Integrin β1, β2, β3, β7	A/B/C: 20–24	Pal Sharma *et al.* 1995; Loo *et al.* 1998; Pfaff *et al.* 1998; Calderwood *et al.* 2001; van der Flier *et al.* 2002; Tadokoro *et al.* 2003; Travis *et al.* 2004; Gontier *et al.* 2005; Kiema *et al.* 2006; Kim *et al.* 2008; Takala *et al.* 2008
Migfilin (filamin-binding LIM protein-1, FBLP-1)	A: 21	Takafuta *et al.* 2003; Tu *et al.* 2003; Lad *et al.* 2008; Ithychanda *et al.* 2009a
Endothelial-specific molecule-2 (ECSM2)	A: 15–16 & 19–21	Armstrong *et al.* 2008
IKAP (IκB-kinase-associated protein)	A	Johansen *et al.* 2008
CEACAM1/CD66a antigen	A: 23–24	Klaile *et al.* 2005
Vimentin	A	Kim *et al.* 2009
Tissue factor	A: 22–24	Ott *et al.* 1998

Table 5 *(continued)*

Interaction partner	FLN isoform: interacting repeats	References
Myofibril assembly		
Calsarcin-3	C: 20–24	Frey and Olson 2002
Myotilin	C: 19–21	van der Ven *et al.* 2000; Gontier *et al.* 2005
FATZ-1 (Calsarcin-2/Myozenin-1)	A/B/C: 19–24	Faulkner *et al.* 2000; Takada *et al.* 2001; Gontier *et al.* 2005
N-RAP	C: 20–24	Lu *et al.* 2003
KY protein	C: 20–22	Beatham *et al.* 2004
Titin	A/C	Labeit *et al.* 2006
Xin (cardiomyopathy associated protein)	C: 20	van der Ven *et al.* 2006
Cbl-associated protein (CAP)	C: 2	Zhang *et al.* 2007
γ- & δ-sarcoglycans	C: 20–24	Thompson *et al.* 2000
G-protein coupled receptors		
Dopamine receptors D2 & D3	A: 19	Li *et al.* 2000; Lin *et al.* 2001; Lin *et al.* 2002; Kim *et al.* 2005b; Cho *et al.* 2007
mGluR	A: 21–22	Enz 2002
μ opioid receptor	A: hinge2–24	Onoprishvili *et al.* 2003; Onoprishvili and Simon 2007; Onoprishvili *et al.* 2008
Extracellular calcium-sensing receptor	A: 14–16	Awata *et al.* 2001; Hjälm *et al.* 2001
Calcitonin receptor	A: 20–21	Seck *et al.* 2003
$P2Y_2$ nucleotide receptor	A	Yu *et al.* 2008
Ion channels		
CFTR (Cystic fibrosis transmembrane conductance regulator)	A	Thelin *et al.* 2007
Kv4.2 potassium channel	A/C: 20–24	Petrecca *et al.* 2000
Large-conductance Ca^{2+}-activated K^+ (BK_{Ca}) channels	A: 14–19	Kim *et al.* 2007a
Kir2.1 (Inwardly rectifying potassium channel)	A: 23–24	Sampson *et al.* 2003
HCN1 (pacemaker channel)	A: 23–24	Gravante *et al.* 2004
Acetylcholine receptor (AChR)	A	Shadiack and Nitkin 1991
Polycystin TRPP2	A	Sharif-Naeini *et al.* 2009
Other transmembrane proteins		
Caveolin-1	A/B: 22–24	Stahlhut and van Deurs 2000
Presenilins (causative factors in early-onset familial Alzheimer's Disease)	A/B	Zhang *et al.* 1998

Table 5 *(continued)*

Interaction partner	FLN isoform: interacting repeats	References
Intracellular signaling intermediates		
FilGAP (Rac GTPase-activating protein)	A: 23	Ohta *et al.* 2006; **II**; Shifrin *et al.* 2009
Ras-related small GTPases Rac, Rho, Cdc42, & RalA	A: hinge2–24	Ohta *et al.* 1999
RasGAP (GTPase-activating protein)	C: 15–17	Lypowy *et al.* 2005
Trio (Rac1- and RhoG-specific guanidine exchange factor)	A: 23–24	Bellanger *et al.* 2000
β-arrestin	A: 22	Kim *et al.* 2005b; Scott *et al.* 2006
LL5β (Phosphatidylinositol (3,4,5)-trisphosphate sensor)	C: 20–24	Paranavitane *et al.* 2003; Paranavitane *et al.* 2007
Phosphorylation pathways		
RSK (Ribosomal S6 kinase, filamin phosphorylation)	A: Ser2152	Woo *et al.* 2004
Insulin receptor	A: 22–24	He *et al.* 2003
ROCK/Rho-associated protein kinase	A: 24	Ueda *et al.* 2003
SHIP-2 (inositol polyphosphate 5-phosphatase)	A/B/C: 22–24	Dyson *et al.* 2001
SphK1 (Sphingosine kinase 1)	A: 22–24	Maceyka *et al.* 2008
SEK-1 (Stress-activated protein kinase activator)	A: 21–23	Marti *et al.* 1997
PTP-PEST (protein-tyrosine phosphatase)	A	Playford *et al.* 2006
Calcineurin (filamin dephosphorylation)	A: Ser2152	García *et al.* 2006
Pak1 (filamin phosphorylation)	A: Ser2152	Vadlamudi *et al.* 2002
Cyclin B1/Cdk1 (filamin phosphorylation)	A: Ser1436	Cukier *et al.* 2007
$p56^{lck}$ (Tyr kinase, filamin phosphorylation)	A	Pal Sharma and Goldmann 2004
PKA (filamin phosphorylation)	A: Ser2152	Jay *et al.* 2000; Jay *et al.* 2004
PKB-α (filamin phosphorylation)	C: Ser2213	Murray *et al.* 2004
PKC-α (filamin phosphorylation)	A & C: 1–4 & 23–24	Tigges *et al.* 2003
PKC-θ	A	Hayashi and Altman 2006
CaM kinase II (Ca^{2+}/calmodulin-dependent protein kinase II, filamin phosphorylation)		Ohta and Hartwig 1995
cAMP-dependent protein kinase (filamin phosphorylation)		Chen and Stracher 1989
Inflammatory and immune signaling		
Tc-mip (truncated c-maf inducing protein)	A: 18–19	Grimbert *et al.* 2004
CD4, HIV receptor	A: 10	Jiménez-Baranda *et al.* 2007
FcγRI (class I IgG receptor)	A	Ohta *et al.* 1991; Beekman *et al.* 2008
14-3-3		Nurmi *et al.* 2006
CD28	A: 10–12	Tavano *et al.* 2006
TRAF2 (Tumor necrosis factor (TNF) receptor-associated factor 2)	A: 15–19	Leonardi *et al.* 2000
ICAM-1 (intracellular adhesion molecule-1)	(A)/B: 19–20	Kanters *et al.* 2008
Rac1, MEKK1, MKK4, & JNK1 (Janus Tyr-kinase signaling pathway)	B: 20–24	Jeon *et al.* 2008
Lnk	A: 19–23	He *et al.* 2000

Table 5 *(continued)*

Interaction partner	FLN isoform: interacting repeats	References
Proteases and peptidases		
Epithin (membrane type-serine protease 1, matriptase)	A/B: 14–24	Kim *et al.* 2005a
Furin (protease of the *trans*-Golgi network)	A: 13–14	Liu *et al.* 1997
PMSA (Prostate-specific membrane antigen)	A: 23–24	Anilkumar *et al.* 2003
Calpain 1 & 3 (filamin proteolysis)	A: cleavage at hinge1 C: cleavage at hinge2	Gorlin *et al.* 1990; Guyon *et al.* 2003; Raynaud *et al.* 2006
Granzyme B (filamin proteolysis) and caspase	A	Browne *et al.* 2000
Miscellaneous		
Pdlim2 (PDZ and LIM domain-containing protein)	A	Torrado *et al.* 2004
Hepatitis B virus core protein	B: 23–24	Huang *et al.* 2000
Decorin (extracellular protein)	A: 22–24	Yoshida *et al.* 2002
cvHsp (Heat shock protein)	A: 23–24	Krief *et al.* 1999
Nephrocystin (mutated in juvenile nephronophthisis)	A/B: 15–16	Donaldson *et al.* 2002
Pro-PrP (cellular pro-prion protein)	A: 24	Li *et al.* 2009
Naloxone	A: 24	Wang *et al.* 2008; Wang and Burns 2009
[^{14}C]-carboplatin		Shen *et al.* 2004

Platelet Activation: Glycoprotein Ibα

Glycoprotein Ibα (GPIbα) was the first FLN binding partner identified after actin (Fox *et al.* 1985; Okita *et al.* 1985). GPIbα is an essential factor of the mechanism of platelet adhesion and activation leading eventually to blood clotting (Andrews *et al.* 1997; Du 2007). GPIbα is a part of glycoprotein Ib–IX–V (GPIb–IX–V) complex (Fig. 12). GPIb–IX–V platelet adhesion complex is a receptor for von Willebrand factor (VWF), a sub-endothelial matrix-bound multimeric adhesive glycoprotein. The absence or mutations of VWF lead to von Willebrand disease (Mannucci 2004), whereas Bernard–Soulier Syndrome is a disease caused by defects in the GPIb–V–IX complex (Lopez *et al.* 1998). A symptom of these diseases is either bleeding or increased thrombosis, presumably depending on the type of mutation (loss-of-function or gain-of-function). Inhibition of platelet GPIb–IX–V complex could potentially be used as a target for antithrombotic agents and several inhibitors, *e.g.*, monoclonal antibodies, peptides and snake venom proteins, are known (Vanhoorelbeke *et al.* 2007).

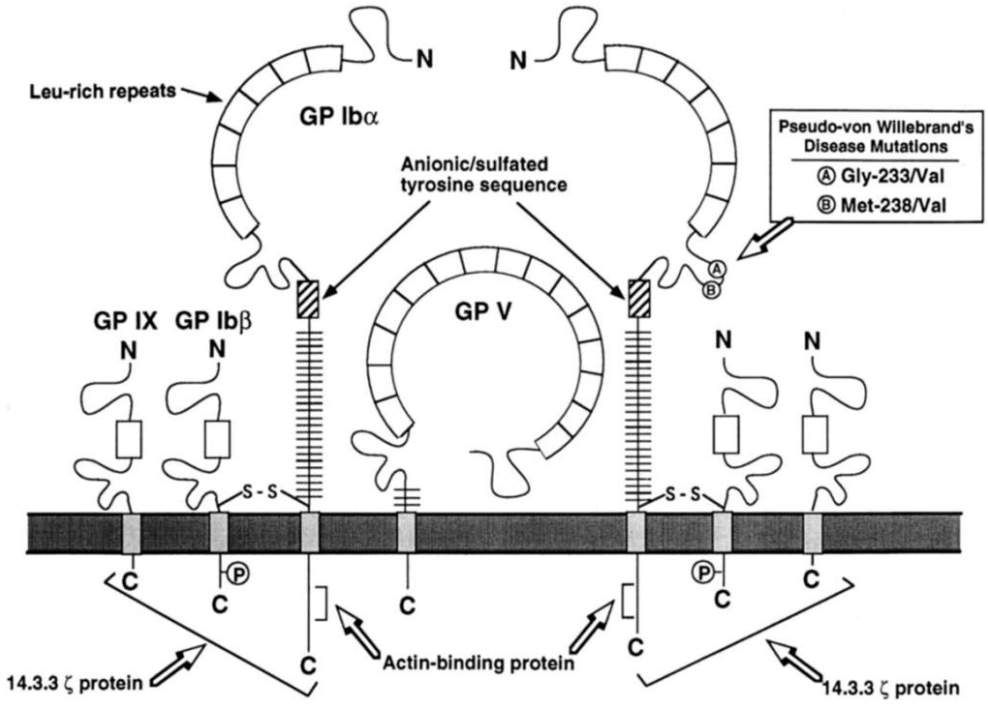

Fig. 12 Schematic diagram of platelet membrane GPIb–XI–V complex. Binding site of FLNa (actin-binding protein) on GPIbα is indicated. Reprinted with permission from (Andrews *et al.* 1997). © 1997 Elsevier.

The role of FLNa is to link the glycoproteins of the platelet plasma membrane to the cytoskeleton. FLNa binding to the cytoplasmic tail of GPIbα was noted to regulate proaggregatory tyrosine kinase signaling of platelets (Feng *et al.* 2003). GPIbα binds to FLNa already within the endoplasmic reticulum (ER) and FLNa directs the post-ER trafficking of GPIbα and cell surface expression of GPIb–IX–V (Feng *et al.* 2005). FLNa was the isoform first identified to bind GPIbα, but FLNb was also later identified as GPIbα binding protein (Takafuta *et al.* 1998; Xu *et al.* 1998). The interaction site for GPIbα was mapped to the IgFLNa domains 17–19 (Meyer *et al.* 1997). Residues 557–575 are the binding site for filamin in GPIbα (Williamson *et al.* 2002; Feng *et al.* 2003) and residues F568 and W570 were found to be especially important (Cranmer *et al.* 2005). Structure of GPIbα–IgFLNa17 complex has been solved using X-ray crystallography (**I**). Complex structure shows that GPIbα residues 560–573 bind as an additional β strand next to IgFLNa17 strand C (Fig. 13). GPIbα residues F563, L567, F568, L569, V571 and W570 make remarkable hydrophobic contacts with the CD face of IgFLNa17. Further identification of the interaction is described in Chapter 7.1.1.

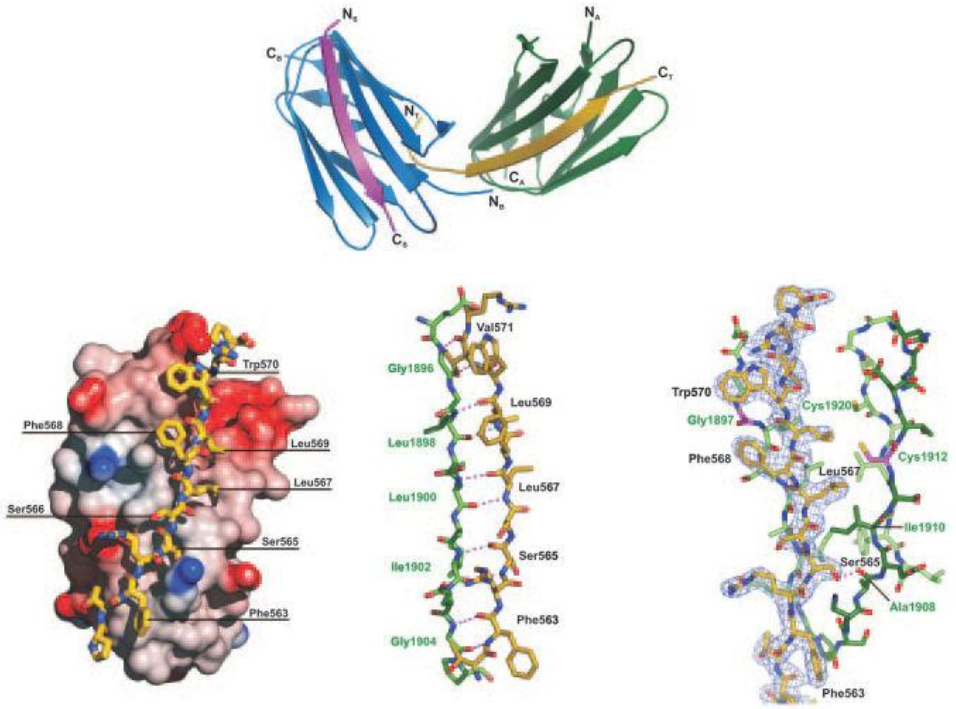

Fig. 13 The structural basis of the interaction of FLNa and GPIbα (**I**). GPIbα residues 560–573 bind as an additional β strand next to IgFLNa17 strand C (residues 1896–1904). Binding is mainly determined by hydrophobic interactions. Reprinted and adapted with permission from (**I**). © 2006 The American Society of Hematology.

Cell Adhesion Receptors: Integrins

Integrins are heterodimeric transmembrane cell adhesion molecules that link the extracellular matrix to the cytoskeleton (van der Flier and Sonnenberg 2001a; Hynes 2002). Integrins can organize cytoskeleton and control intracellular signaling pathways. There are 18 α and 8 β integrin subunits in the human genome and by forming αβ dimers they generate 24 versatile dimeric receptors for extracellular matrix ligands or counter-receptors in other cells. Integrins have an important role in cell adhesion in focal adhesions (Lo 2006) and in cell migration (Ridley *et al.* 2003). Several cytoplasmic proteins interact with the cytoplasmic domains of integrins and many of these also bind actin (Wiesner *et al.* 2005). Filamins, in concert with vimentin and PKCε, have been proposed to regulate integrin trafficking and possibly activation (Kim *et al.* 2009).

Filamins were identified as integrin binding proteins a decade ago. Cytoplasmic domain of integrins β1, β2 and β7 were shown to interact with the C-terminal part of FLNa (Pal Sharma *et al.* 1995; Loo *et al.* 1998; Pfaff *et al.* 1998). Later, integrin β3 tails were also identified as FLN binding partners (Tadokoro *et al.* 2003) and FLNc was shown to have binding activity with the β1A integrin subunit (Gontier *et al.* 2005). Filamin binding was noted to restrict integrin-dependent cell

migration by inhibiting transient membrane protrusion and cell polarization (Calderwood at al. 2001) and the effect was more pronounced with integrin β7 than with β1A or β1D. It was noted that affinity of FLNa for β7 was higher than for β1A and FLNa repeats 19–24 mediate the interaction. FLNa and FLNb splice variants which lack a 41 residue sequence between IgFLN domains 19 and 20 were noted to bind integrin β7 tails more strongly than the wild type isoforms (van der Flier *et al.* 2002; Travis *et al.* 2004) and it was speculated that alternative mRNA splicing could control the cellular localization of filamins and their interaction with integrins. Travis *et al.* also tested whether filamin phosphorylation had an effect on integrin binding but they concluded that phosphorylation of S2131 or S2152 does not play a role in regulating the interaction of filamin with the β7 integrin tail (Travis *et al.* 2004). Recently, filamin A has been shown to regulate cell spreading and survival via β1 integrins (Kim *et al.* 2008).

Calderwood *et al.* characterized the FLN binding site of integrin tails in detail (Calderwood at al. 2001). Residues 781–786 of the β7 tail are necessary for high-affinity FLNa binding and I782 and I786 seem to be especially important. It has been shown that the main integrin binding domain of FLNa is repeat 21 but repeat 19 also has some affinity for integrin β7 (Kiema *et al.* 2006). Kiema *et al.* have solved the IgFLNa21–integrin β7 complex structure using X-ray crystallography (Fig. 14). Residues 776–788 of the integrin β7 tail bind to the CD face of IgFLNa21. The interaction resembles the FLN–GPIbα interaction as integrin β7 peptide also binds as an extra β strand to the strand C of IgFLNa21. Integrin β7 residues Y778, I782 and I786 make hydrophobic contacts with the residues of IgFLNa21. T784 is also buried in the interaction interface and it was proven that phosphothreonine mimicking modification T284E abolished the interaction, which implies that phosphorylation of the β7 tail may regulate integrin–filamin interactions. Later, the mechanism behind the higher affinity of FLN splice variants towards integrins was revealed in the structure of IgFLNa19–21 (see Fig. 8) (Lad *et al.* 2007). Strand A of IgFLNa20 is bound to strand C of IgFLNa21 and it blocks the integrin binding site seen in the FLNa21–integrin β7 complex (see Fig. 8). Filamin splice variants lack the N-terminal residues of IgFLNa20 and thus the integrin binding site is not blocked (van der Flier *et al.* 2002; Travis *et al.* 2004). Also another filamin–integrin complex structure is available: IgFLNa21–integrin β2 complex (Fig. 14) (Takala *et al.* 2008). The structure of the complex is pretty much the same as in the case of β7 tail, but it was shown that phosphorylation of β2 integrin tail on T758 acts as a molecular switch to inhibit filamin affinity and promote 14-3-3 protein binding to this integrin. The regulation mechanisms of adaptor binding to β integrin cytoplasmic tails have recently been reviewed by Legate and Fässler (Legate and Fässler 2009).

All filamin interactions that have been structurally characterized so far—filamin dimerization; FLNa–GPIbα; FLNa–integrin β2; and FLNa–integrin β2 complexes—show the same interaction mode: the interaction partner binds as an additional β strand to the CD face of an IgFLN domain and extends the A'GFC β sheet (Pudas *et al.* 2005; Kiema *et al.* 2006; **I**; Takala *et al.* 2008). It has been speculated whether or not this is a general filamin interaction mode. Different interactions would localize to different Ig modules based on the sequence of the

binding partner and the structural details of CD faces of the domains. This way the different interactions could be independently regulated.

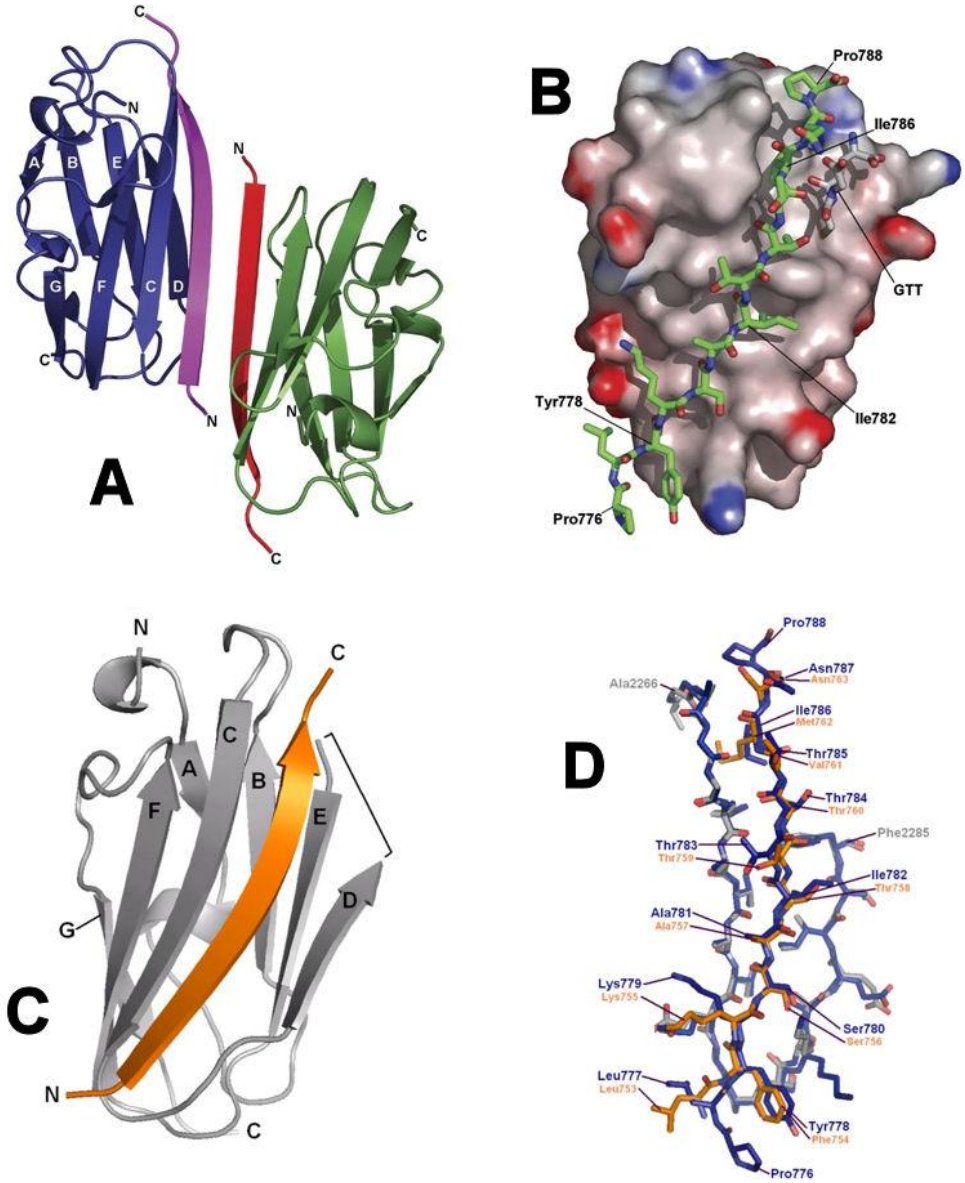

Fig. 14 IgFLNa21–integrin complexes. Cytoplasmic tails of integrin β7 (**A–B**) and β2 (**C**) bind as an additional β strand to IgFLNa21 strand C (Kiema *et al.* 2006; Takala *et al.* 2008). Panel **D** shows a superposition of the two integrin tails on the CD face of IgFLNa21. Blue, integrin β7; orange, integrin β2. A–B: reprinted and adapted with permission from (Kiema *et al.* 2006). © 2006 Elsevier. C–D: reprinted and adapted with permission from (Takala *et al.* 2008). © 2008 The American Society of Hematology.

Signaling Molecules: FilGAP

Filamins host a range of intracellular signaling intermediates (see Table 5). One of these is the recently identified GTPase-activating protein FilGAP that controls actin remodeling (Ohta *et al.* 2006). FilGAP is regulated by Rho-associated kinase ROCK and its GAP-function targets intrinsic GTPase activity of Rac. ROCK regulates FilGAP activation by phosphorylation and FilGAP controls cell polarity and movement downstream of ROCK (Fig. 14). FilGAP acts as a suppressor of Rac-mediated cell polarization. In response to cell stimulation, FLNa targets FilGAP to specific cellular sites, especially to lamellae, where FilGAP suppresses lamellae extension. FilGAP suppresses leading edge protrusion and promotes cell retraction, thereby contributing to the regulation of cell polarity. Both these processes involve actin remodeling. FLNa, a potential coordinator of actin remodeling, interacts with several signaling molecules, *e.g.*, Rho GTPases (Ridley 2006), shown to participate in actin network dynamics. FLNa seems to be a general partnering site for the Rho GTPases Rac, Rho, Cdc42, and RalA (Ohta *et al.* 1999) and colocalizes with Rho guanine nucleotide exchange factor (GEF) Lbc (Pi *et al.* 2002). FLNa also interacts with the Rac- and RhoG-specific GEF Trio (Bellanger *et al.* 2000) and kinases ROCK (Ueda *et al.* 2003) and Pak1 (Vadlamudi *et al.* 2002). FLNa seems to act as an interaction platform for all these components of the actin remodeling pathway. FLNa co-localizes FilGAP with the upstream factors that can activate and inactivate it and with Rac that can further regulate localized actin assembly. FLNa could participate in temporal–spatial regulation of signals that promote cell polarity.

FilGAP contains 748 residues and has MW of 84 kDa (Ohta *et al.* 2006). Residues 552–748 were identified as the FLNa-binding domain. By sequence homology, FilGAP also contains an N-terminal pleckstrin homology (PH) domain (residues 19–125), RhoGAP, and coiled-coil (CC) domains (Fig. 16). FLNa repeats 23–24 exhibit strong FilGAP affinity but repeat 23 alone also has some activity.

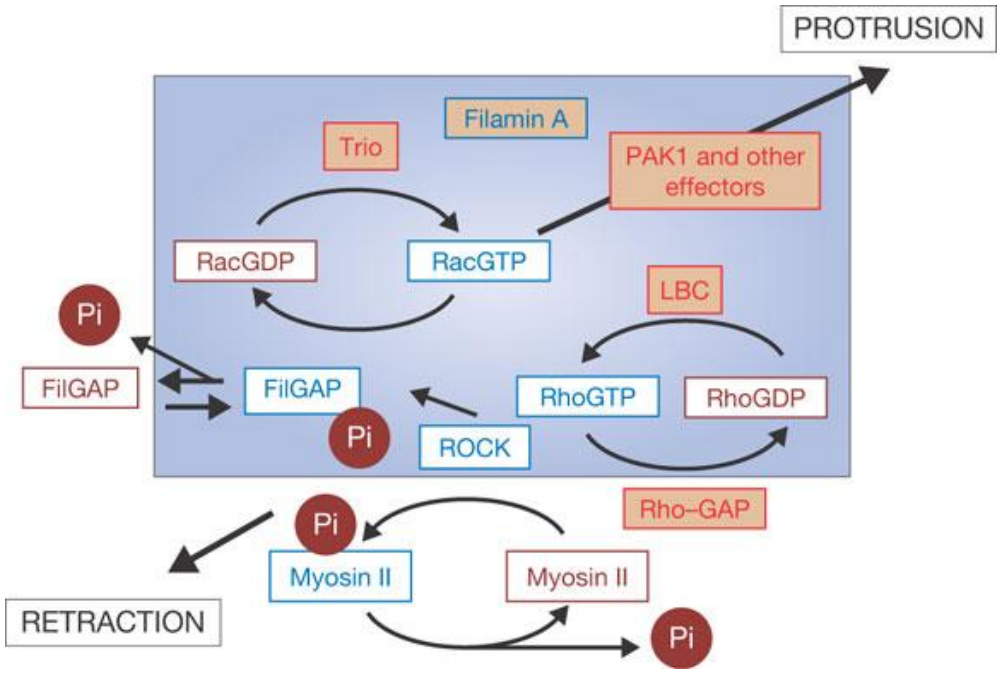

Fig. 15 The role of FilGAP and other FLNa-binding partners in determining cell polarity. Blue shading represents the FLNa platform that collects up the signaling intermediates. Blue and purple rectangles stand for activated and inactivated forms, respectively. Reprinted with permission from (Ohta *et al.* 2006). © 2006 Nature Publishing Group.

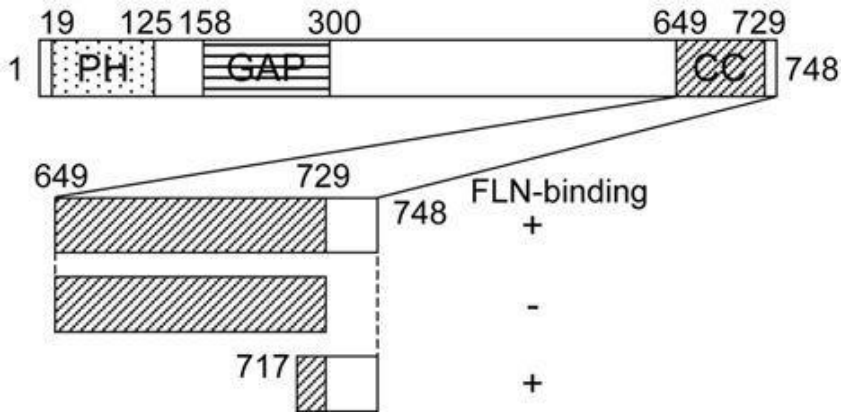

Fig. 16 Schematic structure of FilGAP: PH, pleckstrin homology domain; GAP, GTPase activating domain; CC, coiled-coil domain. FLNa binding site is located at residues 729–748. Reprinted and adapted with permission from (**II**). © 2009 Nakamura *et al.*

Filamin–FilGAP interaction was further characterized by Nakamura *et al.* (**II**). It was observed that FilGAP does not bind FLNa homologs FLNb or FLNc, even if they are sequentially very similar. It was also noted that FLNa mutations found in PVNH and FMD patients disrupt the folding of IgFLNa23 and abolish FilGAP binding. The filamin interaction site in FilGAP was further refined to the last 32 residues (717–748) of FilGAP. FilGAP was noted to dimerize using the coiled-coil domain. Affinity of isolated IgFLNa23 for monomeric FilGAP was very low, which demonstrates that both FLNa and FilGAP dimerization is required for fully efficient interaction. It was speculated that dimerization of the interaction partners defines their geometric arrangements and valences increasing avidity of the FLNa–FilGAP complex. Rac inactivation by FilGAP requires FLNa association. FilGAP V734Y mutant was noted to be unable to bind FLNa and diffuse throughout cell suppressing Rac-activity broadly, which indicates that binding of FilGAP to FLNa is important for proper spatiotemporal control of FilGAP functions. Further description of NMR characterization of FLNa–FilGAP interaction can be found in Chapter 7.1.2 (**II**).

The role of FilGAP–FLNa interaction in mechanoprotection was studied by Shiffrin *et al.* (Shifrin *et al.* 2009). Their results indicate that FLNa targets FilGAP to sites of force transfer. Force-induced redistribution of FilGAP was noted to be essential for suppression of Rac activity and lamellae formation in cells that are challenged by tensile forces. Authors state that FilGAP plays a role in protecting cells against force-induced apoptosis. The mechanoprotective role of filamins has been previously proposed by Kainulainen *et al.* (Kainulainen *et al.* 2002)

G-protein Coupled Receptors: Dopamine Receptors

Several G-protein coupled receptors (GPCR), including dopamine receptors, have been shown to interact with filamins (see Table 5). Dopaminergic signaling has a central role in the pathophysiology of Parkinson's disease and schizophrenia (Civelli *et al.* 1993; Missale *et al.* 1998). The third cytoplasmic loop of D_2-type dopamine receptors has been indicated as the binding site for FLNa (Fig. 17) (Li *et al.* 2000). There is a potential serine phosphorylation site (S238) close to the FLNa binding site and interaction with FLNa can be regulated by PKC activation. FLNa has a role in the clustering of D_2 receptors at the cell surface. Association of D_2 receptors with FLNa enhances their inhibitory coupling efficiency to adenylate cyclase. The function of filamin could be the clustering of the components of the dopaminergic signaling pathway close together.

Later it was shown that, in addition to D_2 receptors, FLNa also interacts with D_3 subtypes but not with other subtypes (Lin *et al.* 2001). The binding site was mapped to the IgFLNa domain 19. Residues 211–241 and 211–227 of D_2L (long form of D_2 receptors) and D_3 receptors, respectively, are responsible for the interaction with FLNa. FLNa seemed to be required for proper cell surface targeting and stabilization of the dopamine receptors (Lin *et al.* 2002). D_3 receptor, FLNa and β-arrestin have been shown to form a signaling complex that is destabilized by agonist- or expression-meditated increases in G-protein receptor kinase 2/3 (GRK2/3) activity (Kim *et al.* 2005b). Filamins have also been shown to directly interact with β-arrestin (Scott *et al.* 2006) and the interaction site has been mapped to IgFLNa domain 22. G-protein mediated signaling of D_2 and D_3 receptors is

terminated by binding of β-arrestin after GRK2/3 mediated phosphorylation of the receptors. This pathway can also proceed forward to endocytosis of β-arrestin–receptor complexes. Filamins may regulate the stability of receptor–G-protein signaling complexes, and in this way contribute to sensitization and desensitization of the D_3 receptors. It has been shown that physical interaction between FLNa and phosphorylated D_3 receptor is likely to participate in sequestration of D_3 receptors (Cho *et al.* 2007).

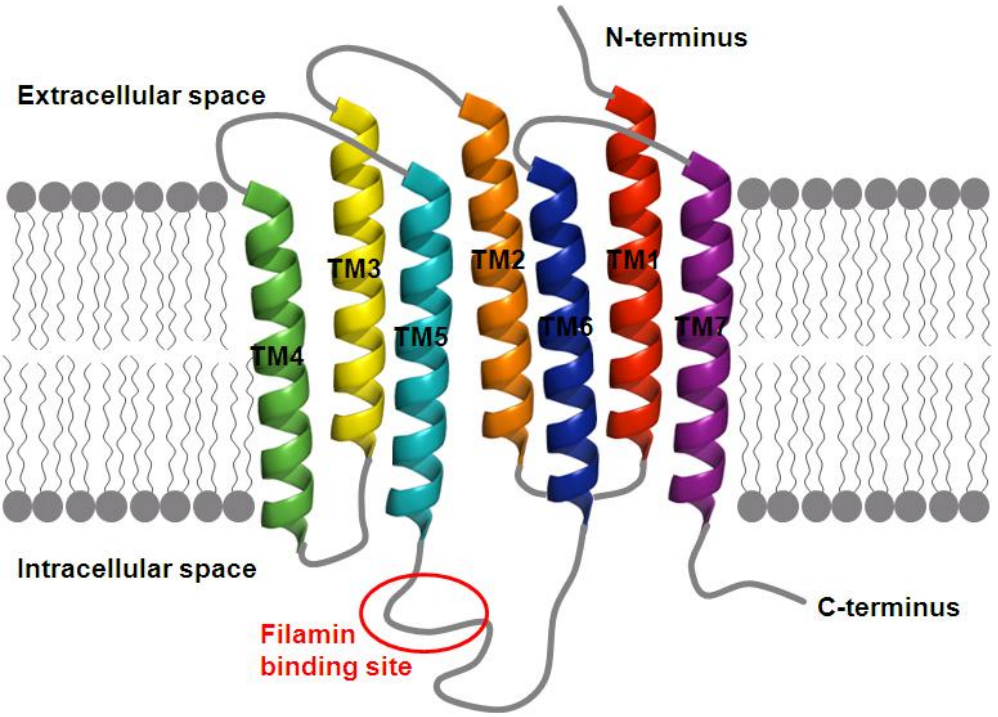

Fig. 17 The topology of D_2 dopamine receptors and the location of FLNa binding site. D_2 receptors contain seven transmembrane (TM) helices. N-terminus is located at the extracellular space and C-terminus is inside cell. Filamin binding site is located at the third intracellular loop close to the TM helix 5.

Another pharmacologically important filamin-binding GPCR is μ-opioid receptor (Onoprishvili *et al.* 2003; Onoprishvili and Simon 2007; Onoprishvili *et al.* 2008) and also in this case FLNa is involved in receptor regulation and trafficking. The μ-opioid receptor interaction site has been mapped to FLNa H2 and IgFLNa24. Interestingly, the opioid antagonist naloxone has also been shown to interact with this region of FLNa (Wang *et al.* 2008; Wang and Burns 2009).

3.4. Why All These Modules and Interactions?

We have seen that, in addition to being complex multi-domain proteins, filamins are indeed also multi-functional. All these modules and interactions raise a question over the fundamental role and purpose of filamins. Filamins clearly contribute to actin organization in a unique way and this is reflected in impairment of cell morphology and locomotion in filamin depletion. Filamins therefore have a mechanical role in the integrity of cytoskeleton. Filamins also serve as a link between the cytoskeleton and the cell membrane. They mechanically link several cell membrane receptors, participating both in cell adhesion and signaling, to the inner structures of the cell. Recently, it has been shown that filamins participate in caveolae internalization and trafficking (Sverdlov *et al.* 2009). Besides their mechanical role, filamins also function as a communicational link through coordinating organization of intracellular signaling intermediates around the receptors—they are signaling scaffolds. Filamins participate in physical connection and communication between the extracellular matrix and the cytoskeleton. Filamins are integrators of cell mechanics and signaling (Stossel *et al.* 2001). Several diseases linked to filamin defects reflect the importance of these proteins in development and physiology, and give clues about the roles of different filamin interactions. It is worth noting that several disease-causing filamin mutations are located at the N-terminal part of rod domain 1 (see Table 3), but there are not many interactions mapped to this area (see Table 5), nor there are many structures of these domains (see Table 4). These domains must, however, have a significant role if minor point mutations in the amino acids produce such drastic phenotypes. It remains to be seen whether filamin interactions, *e.g.*, physical contacts with GPCRs, could be targeted and exploited for pharmacological and pharmacotherapeutic purposes.

One of the open questions is also how filamin interactions are regulated. We have seen some examples of alternative splicing, proteolytic cleavage and phosphorylation but these mechanisms are not quite clear yet. Also, receptor occupancy, *i.e.*, competition between several ligands for the same binding site, has been shown to play a role in filamin interactions. Mechanical forces as filamin regulators have been implied in several studies. Filamin could have a role in mechanosensory signaling and mechanotransduction or even in mechanoprotection of cells from apoptosis (Glogauer *et al.* 1998). Recent findings on structures of multi-domain filamin constructs provide potential explanations of how mechanical stretching could regulate interactions. Regulation by mechanical forces could be structurally executed through inter-domain reorganization and controlled reversible unfolding of the domains. All this is crucial evidence of the fact that in order to fully understand the function of a protein, one needs to know its structure—and understand it. Structures of isolated FLN domains do provide clues on the molecular mechanisms of filamin functions, but thorough understanding of the function of this multi-module system necessitates knowledge of the complex inter-module structure, dynamics, and energetics of the entire filamin dimer.

4. NMR SPECTROSCOPY OF MULTI-DOMAIN PROTEINS

4.1. Protein NMR Spectroscopy Basics

X-ray crystallography has dominated protein structure determination for decades. During the last two decades, NMR spectroscopy has, however, evolved into a powerful structure determination technique complementing protein crystallography (Downing 2004; Cavanagh *et al.* 2006). Besides structure determination, NMR spectroscopy is also a versatile and efficient technique for studying protein interactions and dynamics, and providing the means to understand protein function (Grzesiek and Sass 2009). One of the strengths of protein NMR spectroscopy is that proteins can be studied in solution state close to physiological conditions. In the early years of protein NMR spectroscopy the technique was only applicable for small proteins. Since then, this method, and the biochemical and technical tools supporting it, have advanced a great deal and nowadays, relatively large protein systems can be studied by NMR. There are examples of NMR studies of proteins inside living cells—in the most natural environment of proteins where they are accompanied by a range of other cellular components (Dötsch 2008; Sakai *et al.* 2006; Inomata *et al.* 2009; Sakakibara *et al.* 2009). In addition, membrane proteins, pharmacologically important target proteins which have been regarded as difficult cases by both X-ray crystallographers and NMR spectroscopists, can be studied by NMR both in solution and in solid state (Opella and Marassi 2004; Sanders and Sönnichsen 2006; Hiller and Wagner 2009; McDermott 2009). It is worth mentioning that biomolecular solid state NMR spectroscopy has evolved with large leaps during the last decade (Baldus 2006; McDermott and Polenova 2007; Middleton 2007). This thesis will, however, focus on solution state protein NMR spectroscopy.

There are some well known requirements and limitations in protein studies with NMR. The first requirement for detailed protein NMR studies is isotopic labeling of the target protein with NMR active isotopes ^{13}C and/or ^{15}N (Ohki and Kainosho 2008). Some preliminary screening is of course possible with a non-labeled sample using simple ^{1}H experiments, but more advanced multi-dimensional heteronuclear NMR studies necessitate isotopically labeled protein. Usually samples are produced using well-established methods of heterologous recombinant protein production in *Escherichia coli*, but some other organisms and methods can also be used. The amount of sample needed to obtain NMR data in a reasonable time is rather large—the rule of thumb is often 250 µl of 0.5–1 mM protein sample, but this requirement has also been partly overcome by the latest technical improvements. The well known limitation of NMR studies is protein size. There is no hard-limit of protein size in NMR, but smaller proteins are easier and more straightforward to cope with, whereas a large size necessitates usage of special techniques in sample preparation and data acquisition, and can hinder the use of some techniques and studies. In order to proceed with sophisticated protein NMR studies, one has to have long-lasting good spectrum quality (*i.e.*, well-resolved

signals with high chemical shift dispersion and uniform intensities), which is an indication of a correctly folded, non-aggregated, and stable protein sample. Unfortunately, too often this is not the case. One can, usually by a trial and error approach, play around with protein construct size and sample conditions; *i.e.*, buffer type and concentration, pH, temperature, salt type and concentration, and presence of some additives; to fulfill the spectrum quality standards, but in some cases this will not give enough improvement.

If one is fortunate and obtains a well-behaved isotopically labeled protein sample, the next goal is usually resonance assignment—depending on application, either sequential assignment of the backbone resonances or full assignment of all resonances, including side chains. In the most favorable cases, *i.e.*, when spectrum quality is good enough, resonance assignment and even the whole structure determination process can be automated (Güntert 2009). There are several good books and reviews on NMR experiments and techniques used in protein studies (*e.g.*, Sattler *et al.* 1999; Berger and Braun 2004; Downing 2004; Permi and Annila 2004; Cavanagh *et al.* 2006). This thesis will not cover the basics of protein NMR spectroscopy in detail but will give a brief overview of NMR spectroscopic techniques that can be used in studies of protein structure, dynamics and interactions. More emphasis will be given to special techniques used for large modular protein systems.

4.1.1. Protein Structure Determination

Protein structure determination requires relatively concentrated and stable ^{13}C,^{15}N-labeled protein sample giving good spectra. Almost complete chemical shift assignments of the backbone and side chain signals are required to get reliable structure determination outcomes. Traditional structural restraints of NMR spectroscopic protein structure determination are distance restraints between proton pairs obtained from correlation peak intensities of ^{13}C- and ^{15}N-edited 3D NOESY spectra. The signal intensity of these spectra exploiting the nuclear Overhauser effect (NOE) is inversely proportional to the distance between the two protons ($\sim r^{-6}$), so that only protons closer than ~6 Å produce detectable correlations. These data can then be used as distance restraints in molecular dynamics, *e.g.*, torsion angle dynamics, -based structure calculations. Thus, NMR-based protein structure determination is always partially molecular modeling which is distinct from X-ray crystallographic structure determination. Several software are available for NMR structure calculation of biomolecules, *e.g.*, CYANA (Herrmann *et al.* 2002; Güntert *et al.* 2004), ARIA (Habeck *et al.* 2004), and Xplor-NIH (Schwieters and Kuszewski 2006). In addition to NOE-based restraints other restraint types can also be used; *e.g.*, dihedral angle restraints, either measured through J-couplings or calculated based on secondary chemical shifts (Shen *et al.* 2009) and hydrogen bond restraints, either measured (Cordier and Grzesiek 1999) or estimated based on *e.g.*, proton exchange rates. Other types of structural data can also be obtained with NMR experiments, *e.g.*, information on protonation and tautomeric state of histidine side chains (Shimba *et al.* 1998; Sudmeier *et al.* 2003); which, for that matter, is not detected in X-ray crystallography; and on configuration of proline rings (Schubert *et al.* 2002). The problem with all the above mentioned restraints is

that they provide relatively short-range structural information. This poses a problem; especially in structure determination of large proteins and modular systems, where potential errors and uncertainties in short range restraints may accumulate, producing imprecise or even incorrect results. New methods, *e.g.*, residual dipolar couplings (RDC) and paramagnetic probes, have been exploited to obtain long-range structural information (see Chapter 4.2.3).

NMR spectroscopic protein structure determination is by no means finished after basic structure calculation, but the ensemble of structures still has to be refined. The initial structure calculation is usually speeded up and made computationally lighter by making approximations in molecular representations, especially in non-bonded interactions such as electrostatic and van der Waals forces. In order to obtain physically more realistic structure models usable for further applications, the structure has to be refined using full molecular dynamics force fields (Xia *et al.* 2002; Linge *et al.* 2003). The final stage of structure determination is quality control and validation of the structure ensemble (Spronk *et al.* 2002). Unfortunately, too many NMR protein structures in the PDB database have not gone through these last two important steps of protein structure determination and thus may contain unreliable or even misleading structural information. There is a separate database, DRESS, for refined solution NMR structures (Nabuurs *et al.* 2004). WHAT_CHECK and PROCHECK are tools for easy and quick evaluation of protein structure quality (Hooft *et al.* 1996; Laskowski *et al.* 1996). Also guidelines for representation of NMR structures have been presented to facilitate quality estimation of published results (Markley *et al.* 1998).

NMR spectroscopic protein structure determination is a rather time-consuming and labor-intensive task. The number of structure determination targets is growing rapidly due to efficient structural genomics techniques and demand for high-throughput structure determination protocols is increasing. Several steps of NMR structure determination, *e.g.*, peak picking and resonance assignment, are straightforward and even trivial assuming that the spectrum quality is high, which means that the process can be automated. Several automation protocols and programs exist for NMR data analysis (Altieri and Byrd 2004; Donald and Martin 2009) and NMR structure determination process (Gronwald and Kalbitzer 2004; Güntert 2009). Using these automated methods NMR spectroscopy could evolve into high-throughput structure determination tool for structural proteomics (Shin *et al.* 2008). Recent studies have also revealed the potential of structural information contained in chemical shifts in protein structure determination (Cavalli *et al.* 2007).

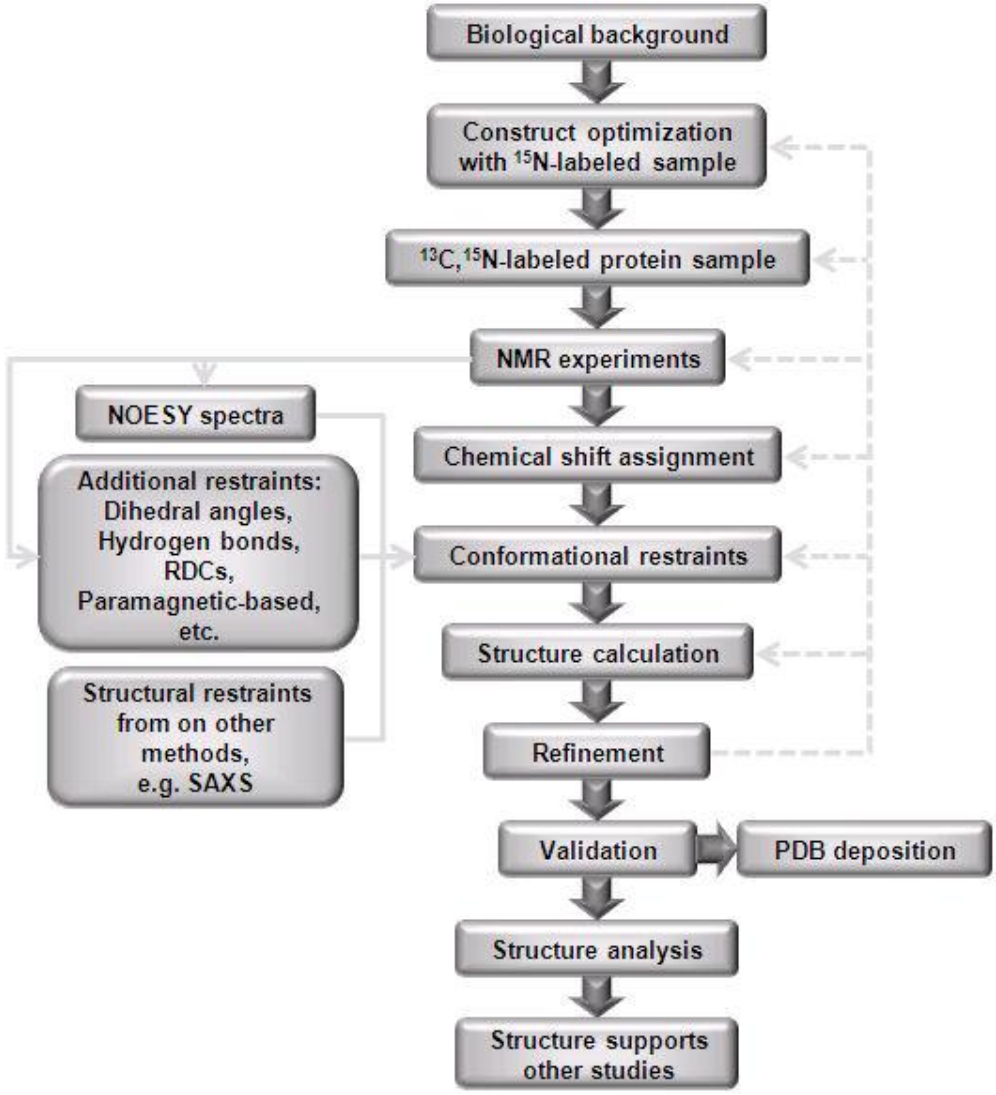

Fig. 18 Flowchart of NMR spectroscopic protein structure determination. Dashed arrows represent potential iterative cycles of the process.

4.1.2. Interaction Studies

NMR spectroscopy is a versatile tool for studying protein interactions (Zuiderweg 2002; Takeuchi and Wagner 2006). Interaction partners may include macromolecules; such as other proteins, nucleic acids and carbohydrates; molecular assemblies; like cell membranes; and small molecule ligands. The strength of NMR spectroscopy in protein interaction studies is that it gives relatively easily information on binding site and mode, and it is also powerful for detecting interactions between weakly binding components with dissociation constant $K_d > 10^{-4}$ M (Vaynberg and Qin 2006). Several NMR methods, each suited for different

combinations of settings and goals, are available for protein interaction studies (Table 6). NMR spectroscopy can be efficiently used in drug discovery, particularly for lead screening and optimization (Stockman and Dalvit 2002; Zerbe 2003; Lepre *et al.* 2004; Peng *et al.* 2004; Skinner and Laurence 2008). Drug screening can be performed either by protein-detected experiments, which can give detailed structural information on the interaction, or by ligand-detected techniques, which do not necessitate protein isotope-labeling or assignment. Many of the ligand-based experiments work only for ligands with K_d values of 10^{-6}–10^{-3} M so they are unable to detect strongly binding ligands with slow dissociation rates. Protein-detected experiments suffer from the same size limitations as all protein NMR experiments.

In many cases the ultimate goal of interaction studies is structure determination of the protein complex (Nietlispach *et al.* 2004; Bonvin *et al.* 2005). In order for the intermolecular NOEs to be detectable the complex has to be relatively tight with K_d below the micromolar range. Whereas the X-ray crystallographic complex structure determination follows the same protocol as with lone proteins, NMR spectroscopic complex structure determination often requires special techniques; such as differential labeling of the components, isotope-filtered experiments (Breeze 2000), and probably also use of additional structural restrains like residual dipolar couplings (see Chapter 4.2.3) (Clore 2000; Skrynnikov 2004) and paramagnetism-based restraints (Pintacuda *et al.* 2007). Simple chemical shift perturbation data can be also used for NMR-guided docking of the interaction partners to obtain a model of the complex structure, *e.g.*, using program HADDOCK (McCoy and Wyss 2002; Dominguez *et al.* 2003). This method enables the structure determination of weak complexes.

Table 6 NMR experiments to detect and characterize protein interactions. Gray shaded cells: ligand-detected experiments for ligand screening.

Experiment	Description	References
Saturation transfer difference (STD)	High sensitivity. Small amount of receptor needed. Saturation transfer from protein to ligand. Binding site determination with SOS-NMR.	Mayer and Meyer 1999; Hajduk *et al.* 2004
Exchange-transferred NOE (trNOE)	Only small amount of target needed. Provides information on binding conformation.	Post 2003
WaterLOGSY	Selective magnetization transfer from bulk water via the protein–ligand complex to the free ligand.	Dalvit *et al.* 2000; Dalvit *et al.* 2001
Relaxation and diffusion experiments	Relaxation and diffusion rates of small ligands are altered by binding to macromolecules.	Hajduk *et al.* 1997
^{19}F relaxation	Suitable for ^{19}F containing ligands.	Peng 2001
Paramagnetic relaxation enhancement and spin labeling	Protein attached paramagnetic spin label considerably enhances the relaxation rates of a binding ligand.	Jahnke *et al.* 2000; Jahnke *et al.* 2001
Competition binding experiments	Able to detect tight-binding ligands. Provides rapid estimate of the binding constant.	Dalvit *et al.* 2002a; Dalvit *et al.* 2002b
Chemical shift perturbations	Requires protein isotope labeling. Gives estimation of binding affinity. Gives detailed information on binding site if protein assignments are available. Can enable complex structure determination using NMR-guided docking.	Shuker *et al.* 1996; McCoy and Wyss 2002; Clore and Schwieters 2003
Transferred cross-saturation experiment (TCE)	Identification of binding sites in protein complexes. Requires isotope labeling. Experiment is based on STD.	Nakanishi *et al.* 2002
Differential line broadening	Binding epitope mapping of small (protein) ligand binding to a larger protein. Requires isotope labeling of the ligand protein. Experiment is based on enhanced relaxation at the residues at the binding epitope.	Matsuo *et al.* 1999
Transferred cross-correlated relaxation	Determination of the dihedral angles of the bound conformation. Requires isotope labeling of the protein.	Reif *et al.* 1997
Complex structure determination	Necessitates (differential) ^{13}C,^{15}N-labeling. Structure calculation based on intermolecular NOEs, RDCs and/or PRE restraints. Yields atomic resolution structure of the complex.	Nietlispach *et al.* 2004

4.1.3. Protein Dynamics

NMR spectroscopy is an excellent tool for studying the dynamic behavior of proteins and other biomolecules. Various types of NMR experiments provide information on protein motions on a broad range of timescales (Fig. 19) (Palmer 2004). Dynamics of protein folding can be also studied using NMR methods (Dyson and Wright 2004; Neudecker *et al.* 2009). NMR studies of nascent protein chains still attached to ribosomes have been conducted to understand co-translational protein folding (Hsu *et al.* 2007). A rather large share of proteins exists in cells as natively unfolded polypeptides. NMR spectroscopy has been employed to characterize the conformations of these highly dynamic molecules (Meier *et al.* 2008). Knowledge of protein dynamics provides insight into protein interactions as the dynamical behavior of the binding site residues is often distinct from the rest of the protein, and ligand binding can have an effect on the relaxation properties of the protein. Deeper understanding of enzyme function, which is an inherently dynamic process, can be gained through NMR spectroscopic analysis of enzyme dynamics (Boehr *et al.* 2006). NMR analysis of protein dynamics can also provide information on the effects of mutations on protein structure and stability (Adams *et al.* 2004).

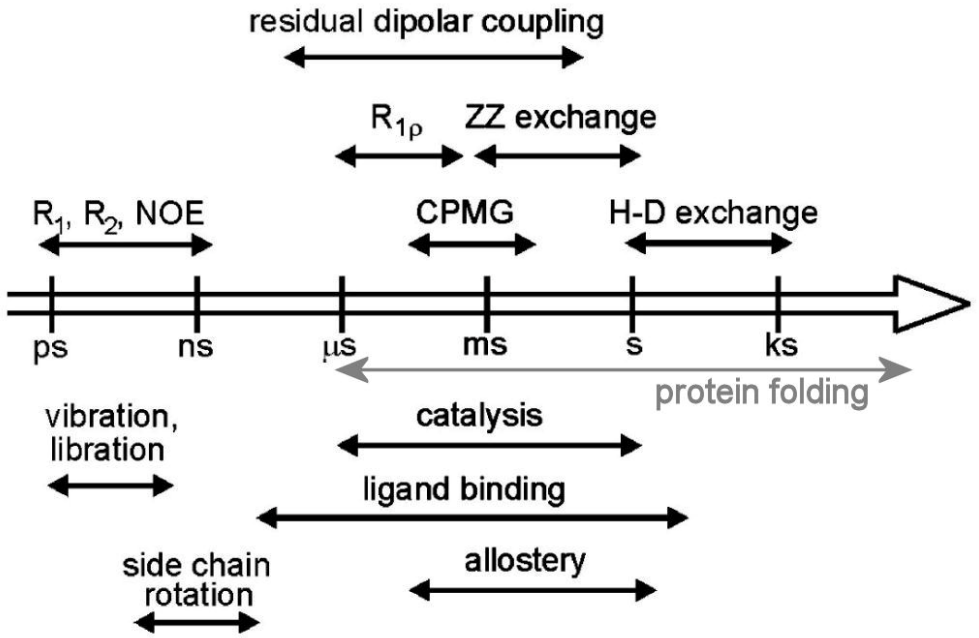

Fig. 19 NMR data timescale versus protein dynamics timescale. Reprinted and adapted with permission from (Boehr *et al.* 2006) © 2006 American Chemical Society.

Fast backbone and side chain motions can be studied by measuring relaxation rates; longitudinal relaxation rate R_1 and transverse relaxation rate R_2;

and steady-state heteronuclear NOEs (for a review of NMR studies of fast time-scale dynamics of protein backbones see Jarymowycz and Stone 2006). Most often the relaxation measurements are done for backbone $^{1}H–^{15}N$ bond vectors using $^{1}H,^{15}N$-HSQC-based experiments, but also other sites and nuclei combinations can be studied in a similar fashion and they often provide deeper and more detailed insight into protein dynamics (Igumenova *et al.* 2006). Relaxation rates provide information on motions in fast sub-ns and slow μs–ms time scales. They also reflect the overall rotational diffusion of the molecule, which is related to its size and shape. Relaxation data is often analyzed using Lipari–Szabo model-free formalism (Brüschweiler 2003). This analysis generates dynamic parameters of the protein: generalized order parameter, S^2, which describes internal motions of the protein so that value 1 denotes an absolutely rigid structure and value 0 completely free and random motion; τ_e is the timescale for the internal bond vector motion; and R_{ex} describes relaxation due to conformational exchange in μs–ms timescale. Model-free analysis requires estimation of the rotational diffusion tensor of the protein. A rough estimate is usually easily obtained from analysis of R_2/R_1 ratios of the rigid residues. Problems might be encountered in the case of highly isotropic systems or proteins undergoing large-scale internal motions. Model-free analysis provides only an estimation of R_{ex} and as many important biological processes occur at μs–ms timescales, other methods are needed to characterize these motions. $R_{1\rho}$ and R_2 relaxation dispersion analysis gives a more detailed insight into these dynamic processes (Palmer *et al.* 2001; Palmer and Massi 2006). These techniques have been used to characterize the dynamics of enzyme catalysis, a process involving motions in a wide range of timescales (Henzler-Wildman *et al.* 2007).

Very slow (ms–days) protein motions are reflected in chemical shifts and proton chemical exchange rates. If the protein under study undergoes slow motion between two states, separate signals can be detected for both forms. Sequential acquisition of NMR spectra, especially when implemented with fast-pulsing multi-dimensional techniques (Schanda 2009), can be used to follow processes slower than R_1 and R_2. Backbone amide proton exchange rates provide information on fold stability and on local structural fluctuations, *e.g.*, dynamics at secondary structure level. Relatively fast amide proton exchange rates (5–500 ms) can be studied by following the exchange of amide proton magnetization with magnetization of water protons (Dempsey 2001). Slow amide proton exchange is most easily observed through measuring a series of $^{1}H,^{15}N$-HSQC spectra of a protein freshly exchanged from water into D_2O, and following the loss of amide proton signal intensities.

Besides their popular use as structural restraints (see Chapter 4.2.3) residual dipolar couplings can also be employed to gain information on protein dynamics (Deschamps *et al.* 2005; Tolman and Ruan 2006). RDCs provide information on motions at ps–ms timescale and their strength is that they also cover the ns–μs area which is not amenable to other NMR methods. Thus RDCs can be used to study slow correlated motions often involved in enzyme catalysis, signal transduction, ligand binding and allosteric regulation (Bouvignies *et al.* 2005). Recently developed methods enable simultaneous determination of protein structure and dynamics using RDC data (Bouvignies *et al.* 2007).

4.2. Tricks for Large Proteins

It is a well known fact that size matters in protein NMR spectroscopy. But large size is no longer an absolute obstacle—it just makes things more complicated and restricts what can be done. Nowadays there are several tricks that can be employed to enable NMR studies of large proteins (Foster *et al.* 2007). The principal problem with high-molecular weight proteins in NMR is their slow tumbling rate, which causes fast relaxation of transverse magnetization. This problem has been tackled with protein deuteration and with transverse relaxation-optimized spectroscopy (TROSY). Another complication is crowded spectrum, *i.e.*, severe resonance overlap. Additional spectrum dimensions and ingenious isotope labeling approaches have been employed to overcome this problem. There are now examples of NMR studies of huge protein assemblies (Luy 2007).

Presently the largest NMR-derived structures in the PDB database are: maltose binding protein (370 residues, PDB accession code 2H25); *E. coli* transhydrogenase (393 residues, PDB accession code 2BRU); *E. coli* HSP70 (DNAK) chaperone (605 residues, PDB accession code 2KHO); and malate synthase G (MSG) (723 residues, PDB accession codes 1Y8B and 2JQX). To date, MSG is the largest protein whose structure has been determined using NMR spectroscopy. Virtually complete backbone chemical shift assignment of MSG was accomplished using 4D TROSY spectra and selective labeling strategies (Tugarinov *et al.* 2002). Residual dipolar couplings and carbonyl chemical shift changes of MSG were determined in Pf1 phage alignment medium to extract the orientational restraints for structure calculation (Tugarinov and Kay 2003a; Tugarinov and Kay 2003b). Global fold of MSG was determined using combination of different restraints: limited set of NOEs, hydrogen bond and dihedral angle restraints, RDC and carbonyl chemical shift anisotropy restraints, and radius of gyration (Tugarinov *et al.* 2005). Later the structure was also refined against combination of NMR and small-angle X-ray scattering restraints (Grishaev *et al.* 2008).

The following chapters are devoted to recent advances in NMR spectroscopy that are especially useful in NMR studies of large protein systems.

4.2.1. Sample Preparation

During the last decade, a number of new isotope labeling strategies have been employed to enable NMR studies of large protein systems (Ohki and Kainosho 2008). Deuteration can be used to simplify ^{1}H NMR spectra for example in interaction studies but more often the purpose of deuteration is to damp down protein transverse relaxation. Perdeuteration, *i.e.*, full deuteration, or random fractional deuteration can be used for the latter purpose. The problem with deuteration is that the proton density giving rise to rich NOE distance information is lost, which complicates structure determination. Several ingenious selective isotope labeling strategies, *e.g.*, amino acid-type and methyl group-selective and stereo-specific labeling schemes, have been exploited in NMR studies. Segmental labeling has become available after the development of intein technology (Iwai and Züger 2007).

The traditional, and still the most popular way of making isotope-labeled proteins for NMR spectroscopy is expression in *E. coli* cells. There are, however, some problems with prokaryotic organisms regarding protein folding and post-translational modifications. Thus, some other cells, *e.g.*, *Pichia pastoris* and *Baculovirus*-infected insect cells, have also been employed in protein production for NMR spectroscopy (Ohki and Kainosho 2008). Cell-free protein production uses the translation machinery of cells *in vitro* without the cell itself (Spirin and Swartz 2008). This method is also now used in NMR sample preparation and it can be exploited in versatile labeling schemes (Staunton *et al.* 2006). Recent developments in the cell-free systems to expand the genetic code might bring innovative labeling schemes for NMR spectroscopy (Wang *et al.* 2006; Gáspári *et al.* 2008).

4.2.2. On the Spectrometer

Technical advancements in NMR spectrometers and experiments have facilitated studies of large protein systems. Nowadays spectrometers with ^{1}H frequencies up to 1 GHz are commercially available. Higher field strengths alleviate resonance overlap and enhance sensitivity. Substantial sensitivity enhancement has been gained with cryogenically cooled probeheads (Webb 2006) which enable studies of more dilute protein samples. This means that a smaller amount of expensive isotope-labeled protein is needed, and protein aggregation problems can also be alleviated. Dynamic nuclear polarization (DNP) has been exploited to enhance NMR sensitivity especially in solid state and small-molecule solution state NMR (Maly *et al.* 2008). Recent studies have demonstrated the feasibility of DNP-enhanced high-field NMR in aqueous solutions suitable for biomolecular studies (Prandolini *et al.* 2009).

Three-dimensional NMR experiments are commonplace in protein studies, but even fourth dimension has been introduced to avoid resonance overlap and provide more specific data for resonance assignment (Konrat *et al.* 1999; Yang and Kay 1999). New pulse sequences have been developed to take full advantage of the selective isotope labeling schemes (Ohki and Kainosho 2008). Isotope-filtered experiments are exploited in extracting intermolecular NOEs for structure determination of protein complexes (Breeze 2000).

Probably the most important invention for NMR studies of large proteins has been transverse relaxation-optimized spectroscopy (TROSY) (Pervushin *et al.* 1997). TROSY is especially suited to large deuterated proteins and high spectrometer frequencies (Fernández and Wider 2003). Several pulse sequences utilizing TROSY scheme have been designed for protein studies (Zhu and Yao 2008). TROSY technique can be combined with polarization transfer by cross-correlated relaxation (CRINEPT) scheme to study even larger systems (Riek *et al.* 1999; Riek *et al.* 2002). This method enables NMR studies of systems with molecular weights approaching MDa—structure determination will probably not be feasible, but at least some useful information can be gained.

4.2.3. Long-range Conformational Restraints

The problem with traditional NOE-based distance restraints is that they provide only short-range structural information. In large systems, errors and uncertainties may accumulate, producing imprecise or even incorrect structural results. Intermolecular and inter-domain NOEs, which are usually long-range NOEs, are often difficult to detect due to their weak intensities. NOEs might be also absent due to dynamical behavior of the interface. This has created demand for long-range structural restraints for NMR spectroscopic protein structure determination.

Residual Dipolar Couplings

The principle of measuring anisotropic interactions of small organic molecules in liquid crystalline media using NMR spectroscopy was demonstrated several decades ago (Saupe and Englert 1963). The applicability of the phenomenon to obtain structural restraints for biomolecular structure determination was presented in the 1990s (Tolman *et al.* 1995). Residual dipolar coupling (RDC) and NOE restraints are different by nature: NOEs provide *distance* between two nuclei whereas RDCs represent *orientation* of a vector between two nuclei, which means that these methods provide highly *complementary* structural information. This is one of the reasons why RDCs have become so popular in biomolecular NMR studies. Strengths of RDC restraints include that they provide long-range structural information and RDCs can be also measured for heteronuclei, not just for protons, which is important in highly deuterated samples. Several excellent reviews exist on protein structure determination using RDC restraints (Lipsitz and Tjandra 2004; Prestegard *et al.* 2004). As mentioned earlier, protein dynamics can also be studied using RDCs (Tolman and Ruan 2006; Bouvignies *et al.* 2007).

The theory and applications of RDCs has been beautifully represented in a review article by Blackledge (Blackledge 2005). The basic principle of RDC restraints is encapsulated in Fig. 20. Measured RDC (D_{ij}) can be mathematically described as

$$D_{ij}(\theta,\phi) = -\frac{\gamma_i \gamma_j \mu_0 h}{16\pi^3 r_{ij,\mathrm{eff}}^3}\left[A_a\left(3\cos^2\theta - 1\right) + \frac{3}{2}A_r \sin^2\theta \cos 2\phi\right], \quad (1)$$

where r_{ij} is the distance between the two nuclei; γ_i and γ_j are the gyromagnetic ratios of the two spins; h is Planck's constant; μ_0 is the permittivity of free space; θ and ϕ are defined in Fig. 20; and A_a and A_r are the axial and rhombic components of the alignment tensor, respectively. Alignment tensor describes the extent and nature of protein alignment and it is determined by the size and shape of the protein and by the properties of the alignment medium.

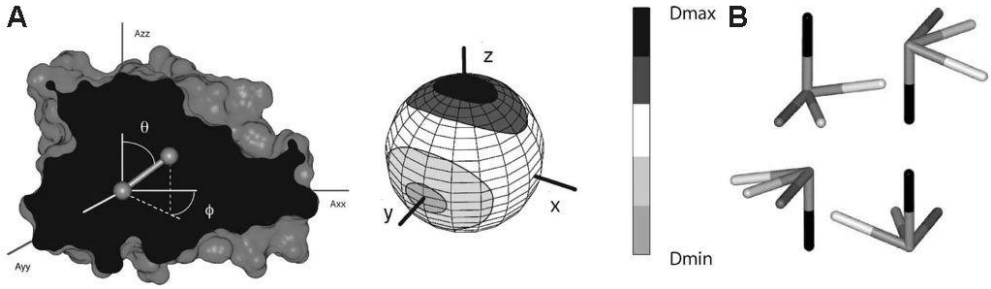

Fig. 20 The principle of RDC restraints. (**A**) Dependence of RDC values on the orientation of the inter-dipolar vector (angles θ and ϕ) and the alignment tensor with eigenvalues A_{xx}, A_{yy} and A_{zz}. The sphere depicts the range of RDC values (categorized for clarity) for different vector orientations. (**B**) The degenerate orientations resulting in equivalent RDC values. Reprinted and adapted with permission from (Blackledge 2005). © 2005 Elsevier.

Magnetic susceptibility anisotropy of some metalloproteins and nucleic acids can be large enough to provide natural alignment in magnetic field to enable measurement of RDCs, but for most proteins artificial alignment is needed, as normally proteins tumble randomly in the isotropic solution and RDCs average out. Several alignment media are available for introduction of small anisotropy for RDC measurement (see Prestegard *et al.* 2004 for comprehensive list of available media and description of their properties) and also paramagnetic tags can be used for protein alignment (see below). The most popular alignment media are phospholipic bicelles (Ottiger and Bax 1998), filamentous Pf1 bacteriophages (Hansen *et al.* 1998) and stressed polyacrylamide gels (Sass *et al.* 2000; Tycko *et al.* 2000). RDCs can be measured in theory between any NMR active atom pairs, but largest, and thus easiest and most accurately determined, RDCs are observed between directly bonded $^{1}H–^{15}N$ and $^{1}H–^{13}C$ pairs. Several pulse sequences have been developed for the measurement of RDCs (Hu and Wang 2006). TROSY-based HNCO experiments are especially well-suited for particularly large proteins (Yang *et al.* 1999; Kontaxis *et al.* 2000; Permi *et al.* 2000). Another related orientation-dependent feature that becomes available in partially aligned protein samples is non-averaged carbonyl chemical shift anisotropy, which is manifested as a residual chemical shift difference between the isotropic and anisotropic states (Cornilescu *et al.* 1998).

Paramagnetic Probes

At first paramagnetic proteins were regarded as problematic for NMR spectroscopic studies as paramagnetic centers induce paramagnetic relaxation enhancement (PRE), which substantially enhances nuclear relaxation and thus complicates NMR analysis. Protein NMR spectroscopists have, however, learned to exploit this phenomenon for several purposes. Proteins can be oriented in a magnetic field for RDC measurement using paramagnetic alignment, but natural paramagnetic metal cations in protein structures or paramagnetic tags (Su and Otting 2009) also provide another kind of long-range structural restraints (Bertini *et al.* 2008). Due to severe

paramagnetic broadening of ^{1}H signals, ^{13}C direct-detection experiments are common in studies of paramagnetic proteins. Paramagnetic enhancement of longitudinal relaxation rates and cross-correlation effects can be used as distance restraints in paramagnetic proteins (Bertini *et al.* 2005). Paramagnetic relaxation enhancement is also an efficient tool to detect molecular interactions (Clore *et al.* 2007). Certain paramagnetic metal ions have large magnetic susceptibility anisotropy and they induce position dependent pseudocontact shifts (PCS) on chemical shifts of nuclei. In favorable cases, pseudocontact shifts can be detected as far as 40 Å from the paramagnetic center, so they can provide true long-range restraints.

4.3. The Role of NMR Spectroscopy in Structural and Functional Studies of Multi-domain Proteins

Multi-domain proteins are almost always rather large systems. For X-ray crystallographic structure determination, size does not present any problems as such, but multi-domain proteins are also often somewhat dynamic and this complicates protein crystallization. NMR spectroscopy does not suffer from dynamics—on the contrary, it is a rather efficient method for the analysis of protein dynamics. Crystal structure is in principle just a snapshot of a protein undergoing conformational exchange. All previously mentioned methods for large-molecule NMR can be used to enable NMR analysis of modular proteins and NMR spectroscopy is recognized as a promising method for structural and functional analysis of multi-domain proteins (Pickford and Campbell 2004).

Several NMR methods can be used in structure elucidation of modular proteins. The problem with sole NOEs is that in many cases, especially if there are inter-module dynamics involved, the inter-domain NOEs are scarce. Segmental labeling is useful in recognizing domain interactions and inter-domain NOEs (Iwai and Züger 2007). The modular approach is a good way to proceed with structural studies of multi-domain proteins. One first measures and assigns the spectra of isolated modules and determines their structures. Chemical shift mapping between the isolated modules and the multi-domain unit gives clues on domain contacts. Domain interactions can also be recognized using domain titrations but in some cases, *e.g.*, if the domain interaction is rather weak and the domain linker has a crucial role in domain–domain interface, the interaction might not become visible in the titration. Chemical shift mapping and soft docking methods can be used in structure determination of multi-module systems (McCoy and Wyss 2002; Dominguez *et al.* 2003).

RDCs are especially well suited for structural studies of modular proteins (Fischer *et al.* 1999). RDCs provide vital information on domain orientations (Skrynnikov 2004) and they can also be used to reveal inter-module dynamics (Braddock *et al.* 2001). In addition to RDCs, spin relaxation and overall rotational diffusion tensor also gives structural data on modular assemblies and their dynamics (Fushman *et al.* 2004; Ryabow and Fushman 2007). Paramagnetic restraints can be a valuable source of long-range structural information in structure determination of modular proteins (Bertini *et al.* 2008). All this versatile atomic-resolution NMR

data can be combined with low-resolution structural data from small-angle X-ray scattering (SAXS). Combination of RDC and SAXS data has been shown to be an efficient way of solving structures of modular proteins and protein complexes (Mattinen *et al.* 2002; Grishaev *et al.* 2005; Gabel *et al.* 2008). The power of this approach in structure determination of large multi-domain proteins has recently been well demonstrated with the RDC–SAXS-refined 82-kDa structure of MSG (Grishaev *et al.* 2008).

5. AIMS OF THE STUDY

The experimental part of this thesis consists of NMR spectroscopic studies of human filamin A. Of the three filamin isoforms, we chose FLNa as it is the most ubiquitously expressed, and several FLNa interactions have been evidenced. As described in Chapter 3, Filamin A is a modular multi-functional protein with several interaction partners and versatile functions. NMR spectroscopy was employed to gain information on structure, interactions and dynamics of the protein in order to understand its function.

The specific aims of this project were:

(i) Gain high-resolution structural information on IgFLN domains in solution state (**I–II, IV**).

(ii) Learn how IgFLN domains interact with other proteins (**I, II, IV**).

(iii) Find out how consecutive IgFLN domains interact with each other and pack together to form higher-order structures (**III–V**).

In the following text the emphasis is laid on protein NMR spectroscopic aspects of the study, whereas molecular biology of filamins is covered in detail in Chapter 3 and in the original research articles.

6. EXPERIMENTAL PROCEDURES

A brief overview of the experimental procedures used in the protein NMR studies presented in this thesis is provided here to support the readability of the following chapters. More detailed descriptions can be found in the original research articles.

6.1. Expression and Purification of Isotope-labeled Proteins

6.1.1. ^{15}N- and ^{13}C,^{15}N-labeled Protein Samples

The protein constructs used in the studies are summarized in Table 7. All ^{15}N- and ^{13}C,^{15}N-labeled samples used in the study were prepared using essentially the same procedure. The fragment encoding the FLNa domain was amplified from a cDNA of human FLNA4 by PCR and cloned to PGEX2T (GE Healthcare Life Sciences) plasmid. The inserts were verified by DNA sequencing. Protein was produced in *Escherichia coli* BL21(DE3) cells in minimal media containing $^{15}NH_4Cl$ and ^{13}C-glucose (Spectra Stable Isotopes, Columbia, MD) as sole nitrogen and carbon sources, respectively. Protein expression was induced overnight at 37 °C in the presence of 0.5 mM IPTG. Cells were harvested and disrupted in PBS by using a French press. The soluble proteins were separated by ultracentrifugation. The fusion protein was purified on Glutathione Sepharose 4 Fast Flow column (Amersham Biosciences) and eluted with 10 mM glutathione in 50 mM Tris-HCl (pH 8.0). Glutathione S-transferase part of the fusion protein was removed with TEV protease. Glutathione S-transferase (GST)-His6-tag and His6-TEV were removed by passing the solution through a Ni-NTA agarose column (Qiagen). The flow-through fractions were concentrated using an Amicon Ultra-15 (Millipore) centrifugal filter with a molecular weight cutoff of 5,000 Da and applied onto a Superdex 75 HR 16/60 (Amersham Biosciences). Purified protein was concentrated with a Microcon YM-3000 centrifugal filter (Millipore). The point or deletion mutants were generated using the QuickChange site-directed mutagenesis kit (Stratagene).

Table 7 Filamin constructs and NMR sample conditions used in the studies.

Sample	IgFLNa construct	FLNa residues	Labeling	Sample and NMR conditions	Objective of the NMR experiments	Chapter	Original article
S1	**17**	1763–1756	^{13}C ^{15}N	c(protein) = 1 mM 50 mM Na-phosphate pH 6.7 10 mM DTT, 5% D_2O, T = 20 °C, 800 MHz	Structure determination	7.1.1	**I**
S2			^{15}N	As S1 but with c(protein) = 0.3 mM 600 MHz	Titration with GPIbα peptide		
S3			^{15}N	As S2, but with T = 23 °C, 500 MHz	Relaxation rate measurement		
S4	**17 G1897D C1912D**		^{15}N	As S1, but with c(protein) = 0.8 mM 500 MHz	Verification of correct folding		
S5	**23**	2427–2522	^{13}C ^{15}N	c(protein) = 1 mM 20 mM Na-phosphate pH 6.8 150 mM NaCl, 1 mM DTT, 2 mM NaN_3 7% D_2O, T = 25 °C, 800 MHz	Structure determination	7.1.2	**II**
S6			^{15}N	As S5, but with c(protein) = 0.5 mM 500 MHz	Titration with FilGAP		
S7	**23 M2474E**		^{15}N	As S5, but 600 MHz	Verification of correct folding		
S8	**23 L2439M**			As S5, but with c(protein) = 0.1 mM & 600 MHz with cryo-probe	Effect of patient mutations to domain folding		
S9	**16–17**	1772–1956	^{13}C ^{15}N	c(protein) = 1 mM 50 mM Na-phosphate pH 6.8 100 mM NaCl, 1 mM DTT, 2 mM NaN_3, 2 mM EDTA, 7% D_2O, T = 30 °C, 800 MHz	Structure determination, titration with GPIbα peptide	7.2.2	**III IV**
S10	**15–17**	1640–1956	^{13}C ^{15}N	As S9, but with c(protein) = 0.5 mM & 600 MHz	Spectrum comparison with IgFLNa16–17		Unpub. results
S11	**18–19**	1954–2141	^{13}C ^{15}N	c(protein) = 0.8 mM 50 mM Na-phosphate pH 6.8 100 mM NaCl, 1 mM DTT, 2 mM NaN_3, 7% D_2O, T = 30 °C, 750 and 800 MHz	Structure determination, titration with dopamine receptor peptides	7.2.1	**III, IV** and unpublished results
S12	**18**	1954–2045	^{13}C ^{15}N	As S11, but 600 MHz	Resonance assignment and spectrum comparison with IgFLNa18–19		
S13	**19**	2046–2141	^{15}N	As S11, but 600 MHz	Spectrum comparison with IgFLNa18–19		
S14	**16–21**	1772–2329	^{2}H ^{13}C ^{15}N	c(protein) = 0.5 mM (0.4 mM in Pf1 phage) 50 mM Na-phosphate pH 6.8 100 mM NaCl, 1 mM DTT, 2 mM NaN_3, 7% D_2O, T = 30 °C, 800 MHz	Assignment and measurement of RDCs	7.3	**V**
S15	**20–21**	2142–2329	^{13}C ^{15}N	c(protein) = 1 mM 50 mM Na-phosphate pH 6.8 100 mM NaCl, 1 mM DTT, 2 mM NaN_3, 7% D_2O, T = 30 °C, 600 MHz	Assignment and spectrum comparison with IgFLNa16–21		

6.1.2. $^{2}H,^{13}C,^{15}N$-labeled IgFLNa16–21

IgFLNa16–21 (FLNa residues 1772–2329) (**V**) was expressed from a pGEX-4T-1 vector with a TEV protease cleavage site using BL21 codon plus cells (Stratagene). Uniform $^{2}H,^{13}C,^{15}N$-labeling was achieved by growing in standard M9 minimal media with $^{15}NH_4Cl$ and D-glucose-$^{13}C_6$-1,2,3,4,5,6,6-D_7 and D_2O to replace H_2O. All isotope-labeled chemicals were supplied by Cambridge Isotope Laboratories, Inc. To achieve higher isotope labeling efficiency, all components of the cell culture were dissolved in D_2O and freeze-dried before use. One fresh colony of transformed bacteria was inoculated into 5 ml of media containing 25% D_2O as a start point. When becoming fully grown, a 100-µl culture was transferred into another fresh 5 ml of media but with 50% D_2O; this training procedure was repeated until cells grew well in 100% D_2O. Thereafter, the preparation was scaled up to 1.5 l, and IPTG was added to induce overnight expression when the OD_{600} reached 0.9. Harvested cells were lysed with hen egg lysozyme and freeze-thaw cycles. Expressed proteins were extracted from cell lysates by vortexing with a large amount of fresh PBS buffer until no more protein could be detected in the cell debris on a gel. The protein purification was done as published previously (Kiema *et al.* 2006), and the GST tag was removed by the AcTEV protease (Invitrogen). The sample was further purified by passing down a Superdex 200 column.

6.2. NMR Experiments and Data Analysis

The sample conditions used in the NMR experiments are summarized in Table 7. NMR spectra were recorded on Varian INOVA 500-, 600- and 800-MHz spectrometers equipped with 5-mm inverse z-gradient triple-resonance probeheads and Bruker DRX 750-MHz spectrometer equipped with 5-mm inverse x,y,z-gradient triple-resonance probehead. The spectra were recorded and processed using the VNMRJ 2.1 and VNMR 6.1C (Varian Inc.), and XWinNMR 3.0 (Bruker BioSpin) programs. $^{1}H,^{15}N$-HSQC spectrum of IgFLNa23-L2439M sample with low protein concentration was recorded with Varian INOVA 600-MHz spectrometer equipped with a 5-mm cryo-probe. Spectrum visualization and analysis was done with Sparky 3.110 (Goddard and Kneller 2004). The following experiments were used for the sequential backbone resonance assignment: $^{1}H,^{15}N$-HSQC, HNCA, HN(CO)CA, iHNCA, HNCACB, CBCA(CO)NH, iHNCACB, HNCO, HN(CA)CO, and HN(CA)HA (Sattler *et al.* 1999; Permi and Annila 2004). Assignment of the aliphatic side chain resonances was performed using the $^{1}H,^{13}C$-HSQC CC(CO)NH, H(CCCO)NH, HCCH-COSY, and HCCH-TOCSY spectra. The aromatic side chain resonances were assigned using the (HB)CB(CGCD)HD and (HB)CB(CGCDCE)HE spectra, and the ^{13}C-edited 3D NOESY-HSQC spectrum. The ^{15}N-edited 3D NOESY-HSQC spectrum was used in the assignment of His, Asn and Gln side chain N–H groups. The backbone resonance assignment of $^{2}H,^{13}C,^{15}N$-IgFLNa16–21 was done using the TROSY versions of $^{1}H,^{15}N$-HSQC, HNCA, HN(CO)CA, and HNCACB spectra.

6.2.1. Structure Determination

Distance restraints for structure determination were extracted from signal intensities of the ^{13}C- and ^{15}N-edited 3D NOESY-HSQC spectra. Dihedral angle constraints for χ and ψ angles were extracted from the chemical shift data using the TALOS software (Cornilescu *et al.* 1999). Structure calculation was performed using the automatic NOE assignment and torsion angle dynamics mode of the CYANA software (Herrmann *et al.* 2002). Molecular dynamics refinement of the final structures was done using a generalized Born implicit solvent model in AMBER 8.0 (Case *et al.* 2004). Quality of the structure families was verified using WHAT_CHECK (Hooft *et al.* 1996) and PROCHECK-NMR programs (Laskowski *et al.* 1996).

6.2.2. Interaction Studies

The NMR titrations to reveal FLNa interaction sites were performed by titrating (^{13}C)^{15}N-labeled protein domain sample step-wise with a concentrated solution of non-labeled peptide. The peptides were dissolved in the same buffer with the protein to be titrated. The $^{1}H,^{15}N$-HSQC spectrum of the protein was recorded at every titration point. IgFLNa17 and IgFLNa16–17 samples were titrated with glycoprotein Ibα peptide (GPIbα residues 556–577) having the sequence LRGSLPTFRSSLFLWVRPNGRV. Chemically synthesized GPIbα peptide was provided by Tufts University Core Facility, Boston, USA. IgFLNa23 was titrated with a peptide derived from FilGAP. FilGAP14 peptide, comprising residues ^{723}EQFFSTFGELTVEP^{736} of human FilGAP sequence, was purchased from EZBiolab Inc. IgFLNa19 and IgFLNa18–19 were titrated with integrin β7 peptide (Ac-^{776}PLYKSAITTTINP^{788}-NH_2, numbers denote for residues of human β7 integrin), and dopamine receptor D_2 and D_3 peptides (D_2 residues 211–230; D_3 residues 210–230). Also dopamine receptor peptides were N-teminally acetylated and C-terminally amidated. Integrin β7 peptide and dopamine receptor peptides were purchased from EZBiolab Inc. Combined chemical shift differences of the backbone N–H signals were calculated as $\Delta\delta = ((0.15*\Delta\delta_N)^2+(\Delta\delta_H)^2)^{½}$.

6.2.3. Relaxation Rate Measurements

The backbone ^{15}N R_1 and R_2 relaxation rates of IgFLNa17 and $^{2}H,^{13}C,^{15}N$-IgFLNa16–21 were measured with the conventional series of $^{1}H,^{15}N$-HSQC experiments with varied relaxation delays (Farrow *et al.* 1994). The relaxation rates of IgFLNa16–17 and 18–19 were measured using the three-dimensional relaxation rate-resolved $^{1}H,^{15}N$-HSQC spectra (Koskela *et al.* 2004). Inverse Laplace transform was applied to the relaxation dimension of the three-dimensional datasets using GIFA software (Pons *et al.* 1996). The heteronuclear NOEs of the backbone amide nitrogens were determined using conventional methods (Farrow *et al.* 1994). $\{^{1}H\}^{15}N$ heteronuclear NOEs of $^{2}H,^{13}C,^{15}N$-IgFLNa16–21 were measured using TROSY-enhanced versions of the heteronuclear NOE experiments (Zhu *et al.* 2000).

6.2.4. Residual Dipolar Couplings of IgFLNa16–21

To measure residual dipolar couplings, $^{2}H,^{13}C,^{15}N$-IgFLNa16–21 was aligned with Pf1 phage alignment media (Hansen *et al.* 1998) purchased from Asla Biotech Ltd. The phage concentration of the aligned sample was 15 mg/ml, and the protein concentration was 0.4 mM. Scalar and residual dipolar couplings between amide proton (^{1}HN) and nitrogen (^{15}N) were measured using a modified three-dimensional HNCO-TROSY-based triple-resonance experiment (Yang *et al.* 1999; Kontaxis *et al.* 2000, Permi *et al.* 2000). Data sets for selecting TROSY/TROSY and decoupled/TROSY components in ^{15}N and ^{1}H dimensions were recorded in an interleaved manner. The residual dipolar coupling contribution to the observed splitting in phage was obtained by subtracting the $^{15}N–^{1}HN$ values measured in water from the values obtained in phage.

Rigid-body modeling of the IgFLNa16–21 domain organization was done with the MODULE 2 program (Dosset *et al.* 2001). An arbitrary starting structure of IgFLNa16–21 (residues 1772–2329) was built using the structures of the IgFLNa domain pairs 16–17 (PDB accession code 2K7P, model 1, residues 1772–1955), 18–19 (2K7Q, model 1, residues 1956–2136), and 20–21 (2J3S, chain A, residues 2137–2329) by superimposing the overlapping parts of the substructures (**IV**; Lad *et al.* 2007). The structure was divided into six separate modules. The residual dipolar couplings of the backbone N–Hs were used as restraints in the rigid-body modeling of the IgFLNa16–21 domain orientations. After the alignment tensors were fitted, the domains were transformed into a common alignment frame. The inclusion and exclusion of degenerate orientations were done based on covalent and non-bonded information and chemical shift perturbations.

6.3. Preparation of Figures

All spectrum illustrations presented in this thesis were prepared with Sparky 3.110 (Goddard and Kneller 2004). The figures representing protein structures have been created with the MOLMOL (Koradi *et al.* 1996), Bodil (Lehtonen *et al.* 2004), and PyMOL (DeLano 2002) programs. The sequence alignment of dopamine receptor peptides (Fig. 29) was done using ClustalW2 (Larkin *et al.* 2007) and visualized with Jalview version 2 (Waterhouse *et al.* 2009).

7. RESULTS AND DISCUSSION

7.1. Structures of Filamin A Immunoglobulin-like Domains and Their Interactions with Other Proteins

7.1.1. Filamin A Domain 17

Filamin A domain 17 has been shown to interact with the cytoplasmic domain of glycoprotein Ibα (see Chapter 3.3.2). Our aim was to discover the structural basis of this interaction (**I**). As the first step of our study, we determined the structure of IgFLNa17 (FLNa residues 1763–1756) using NMR spectroscopy. Almost all backbone amide signals of this 10-kDa Ig domain were visible in the $^{1}H,^{15}N$-HSQC spectrum (Fig. 21) and the spectrum quality was good—an indication of a well-folded domain. Only residues Q1916 and G1918 could not be detected in the $^{1}H,^{15}N$-HSQC spectrum. Virtually complete backbone and side chain assignments were achieved and deposited in the Biological Magnetic Resonance Data Bank (BMRB accession code 6730).

The structure of IgFLNa17 was solved using distance restraints derived from ^{13}C- and ^{15}N-edited HSQC-NOESY spectra. Quality statistics of the structure family (20 substructures) represent successful structure determination (**I**: Table 1). Atomic coordinates of IgFLNa17 structure ensemble are available in the PDB database under accession code 2AAV. The structure of IgFLNa17 is a traditional filamin-type Ig domain with seven β strands forming a β sandwich with two β sheets (Fig. 22). There is also a short 3_{10} helix between strands A and A'. Except for BC and DE loops, which are somewhat looser, the structural precision is good. We also measured the backbone ^{15}N T_1 and T_2 relaxation rates to identify dynamic residues (**I**: supplemental Fig. S2). Residues of the BC loop show elevated T_2 relaxation rates, which indicates that this loop is flexible. The DE loop does not have many long-range NOE restraints and thus structural precision in this area is compromised. The surface of IgFLNa17 has many hydrophobic areas. One is located at CD face (see Fig. 13) but AG surface also contains several exposed hydrophobic residues (Fig. 22C).

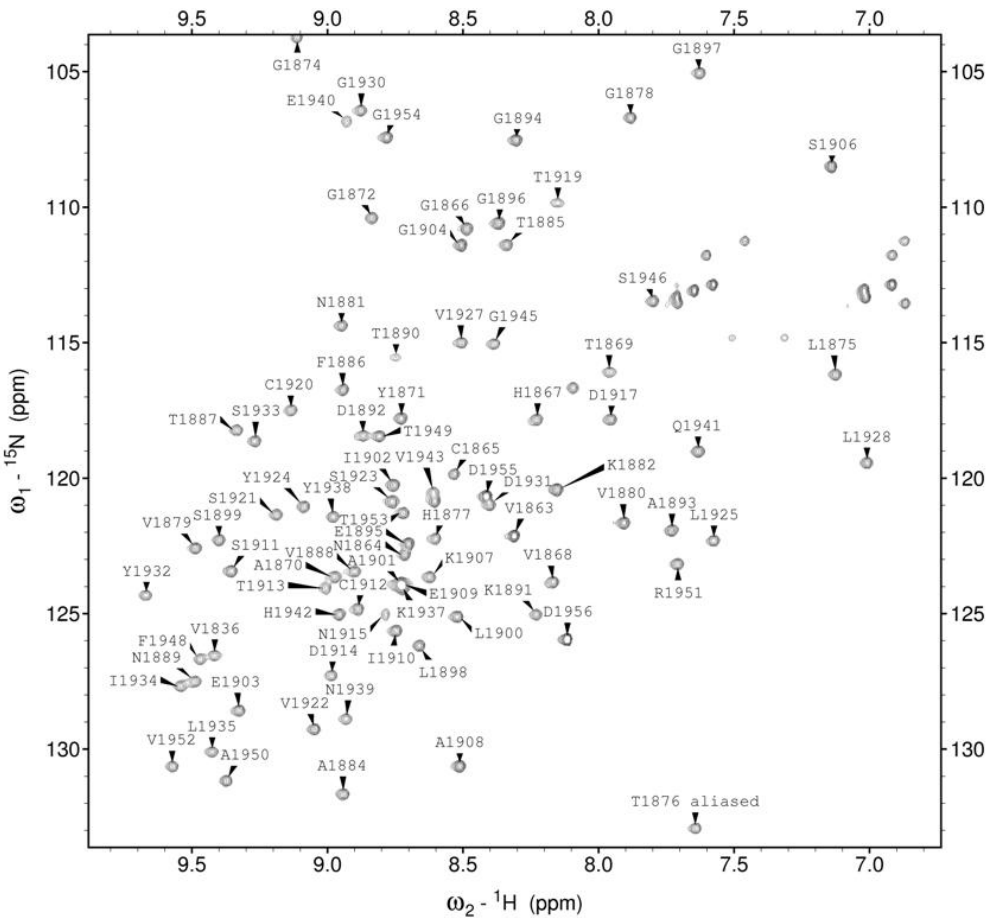

Fig. 21 The $^{1}H,^{15}N$-HSQC spectrum of IgFLNa17 with backbone resonance assignments (**I**).

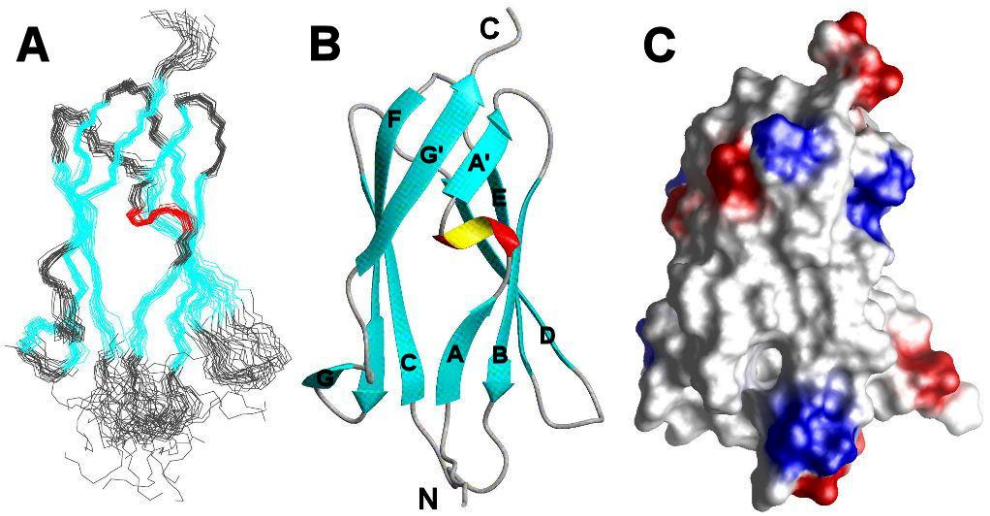

Fig. 22 The solution structure of IgFLNa17 (PDB accession code 2AAV) (**I**). All panels show the structure from the same perspective. (**A**) Superimposed backbone traces of the 20 substructures. Residues 1868–1890, 1899–1911, and 1919–1954 were superimposed. (**B**) Secondary structure elements of the mean structure. (**C**) Surface charge. Blue, positive; Red, negative.

To study the interaction of IgFLNa17 with the GPIbα we titrated IgFLNa17 with a peptide (GPIbα556–577) derived from the cytoplasmic tail of human GPIbα (^{556}LRGSLPTFRSSLFLWVRPNGRV^{577}). Interaction between IgFLNa17 and GPIbα556–577 was in the slow-exchange NMR timescale and it induced considerable changes in the ^{1}H,^{15}N-HSQC spectrum of IgFLNa17 (Fig. 23). Detailed chemical shift mapping was impossible due to drastic chemical shift changes in several cross-peaks but the most prominent changes seemed to be concentrated at residues of the CD face which indicates that GPIbα binding site is located at the CD face of IgFLNa17. There are, however, also notable chemical shift changes at other parts of the domain, which implies slight structural molding of the entire domain.

Tight interaction between IgFLNa17 and GPIbα would have enabled NMR spectroscopic structure determination of the complex. Meanwhile, crystallization of the IgFLNa17–GPIbα556–577 complex had however proven successful and the complex structure of IgFLNa17 and GPIbα556–577 was solved using X-ray crystallography (**I**). The complex structure confirmed that GPIbα binds to the CD face of IgFLNa17 (Fig. 13). GPIbα residues 560–573 bind as an additional β strand to IgFLNa17 strand C. Side chains of GPIbα also interact with the residues of IgFLNa17 strand D. This interaction closely resembles the structural basis of filamin dimerization (Pudas *et al.* 2005) and it is the first structure of IgFLN domain in complex with an interacting protein. Superposition of the NMR structure of free IgFLNa17 and the X-ray complex structure (**I**: Fig. 2C) shows that strand D slightly moves away from strand C due to peptide binding, but otherwise the two structures are very similar. Aromatic side chains of GPIbα residues F563, F268 and

W570 come into close contact with IgFLNa17, which explains the drastic chemical shift changes induced by the peptide binding.

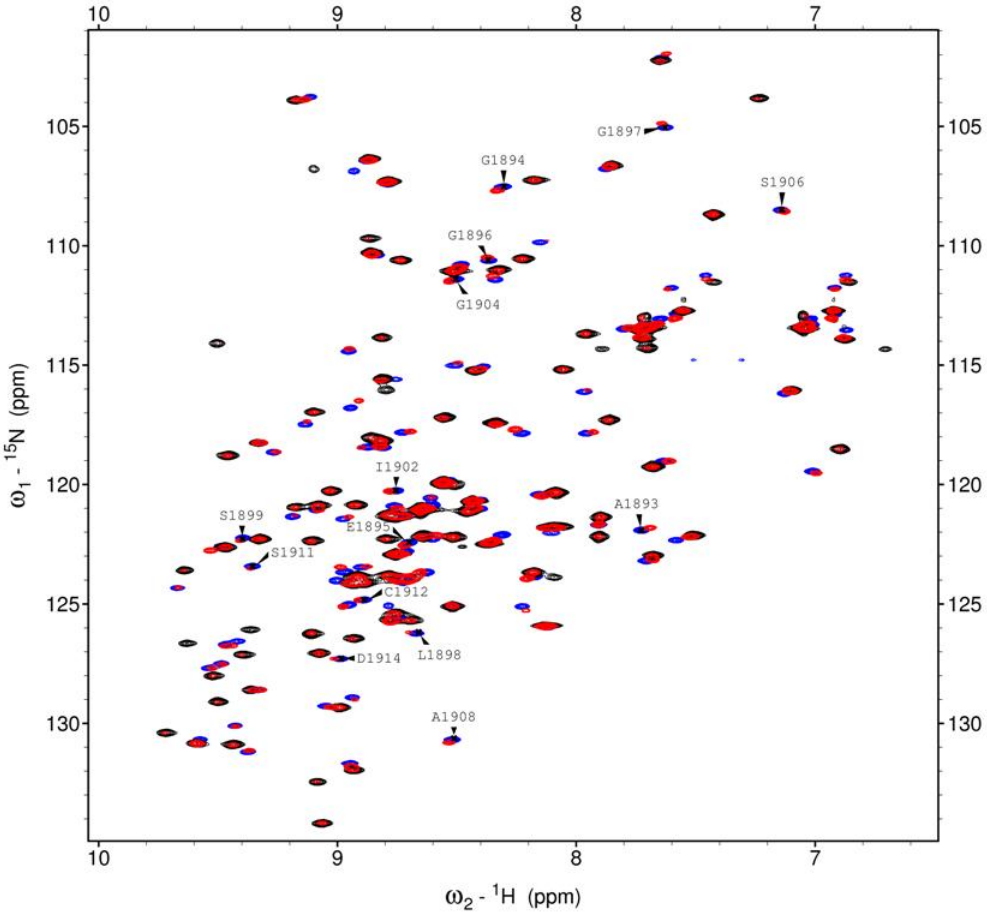

Fig. 23 Titration IgFLNa17 with GPIbα556–577. Superimposition of the $^{1}H,^{15}N$-HSQC spectra recorded during titration reveals strong slow-exchange interaction. The most notable chemical shift changes are seen in the residues of the C and D strands (1894–1914). GPIbα556–577-to-FLNa17 ratios: blue, 0%; red, 60%; black, 100%.

FLNa17–GPIbα interaction seen in the crystal structure was validated using point mutations which would disturb the interaction and prevent GPIbα binding (**I**). G1897 and C1912 are spatially closely located at IgFLNa17 strands C and D, respectively (Fig. 13). Double-mutant G1897D+C1912D was shown to abolish the interaction between FLNa and GPIbα. We wanted to confirm that this effect was not due to an impaired domain folding. We checked the $^{1}H,^{15}N$-HSQC spectrum of IgFLNa17 G1897D+C1912D double-mutant (Fig. 24). Spectrum comparison between native FLNa17 and the mutant shows that the domain is properly folded and the chemical shift changes are confined to the spatial proximity of the point

mutations. To conclude, the NMR spectroscopic studies of IgFLNa17 support the IgFLNa17–GPIbα interaction seen in the crystal structure. In the IgFLNa17 project we nicely combined NMR spectroscopy and X-ray crystallography to gain detailed information on the structure and interactions of the protein.

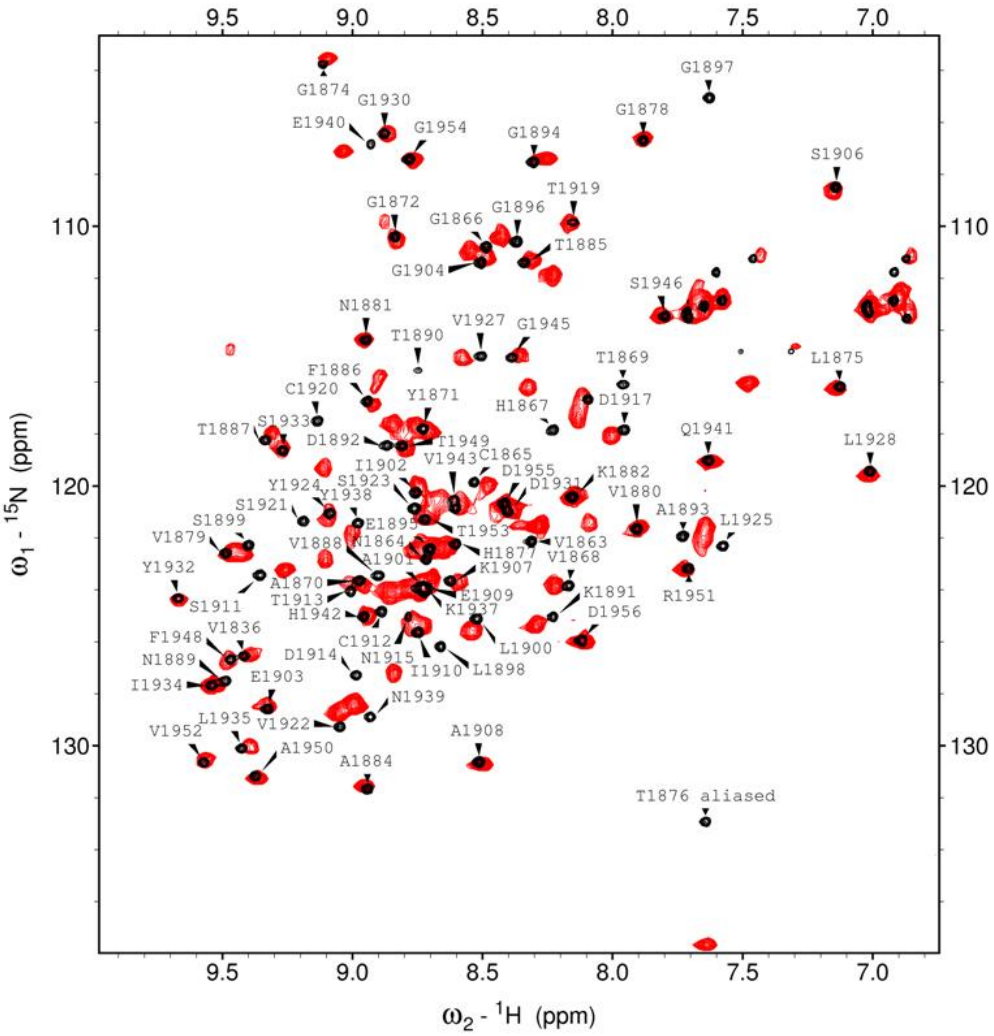

Fig. 24 Proper folding of IgFLNa17 double-mutant G1897D+C1912D was checked using $^{1}H,^{15}N$-HSQC spectrum. Overlay of the $^{1}H,^{15}N$-HSQC spectrum of native IgFLNa17 (black) and of the mutant (red). The majority of signals have retained their positions and large chemical shift changes are confined to the residues in close proximity to the mutated residues, indicating that the mutant retains the folding of the native domain. However, signals of the mutant are broadened compared to the native FLNa17, which implies some protein aggregation.

7.1.2. Filamin A Domain 23

IgFLNa domain 23 has been shown to interact with FilGAP (Ohta *et al.* 2006) and patient mutations associated with PVNH and FMD have been mapped to this domain (Zenker *et al.* 2004; Robertson *et al.* 2006). We wanted to study the structure of IgFLNa23 in order to understand the structural basis of the interaction with FilGAP and the structural effects of the disease-causing mutations (**II**). We determined the solution structure of IgFLNa23 (FLNa residues 2427–2522) using NMR spectroscopy. The spectrum quality of IgFLNa23 was excellent (Fig. 25) and essentially complete chemical shift assignments were obtained (BMRB accession code 15777).

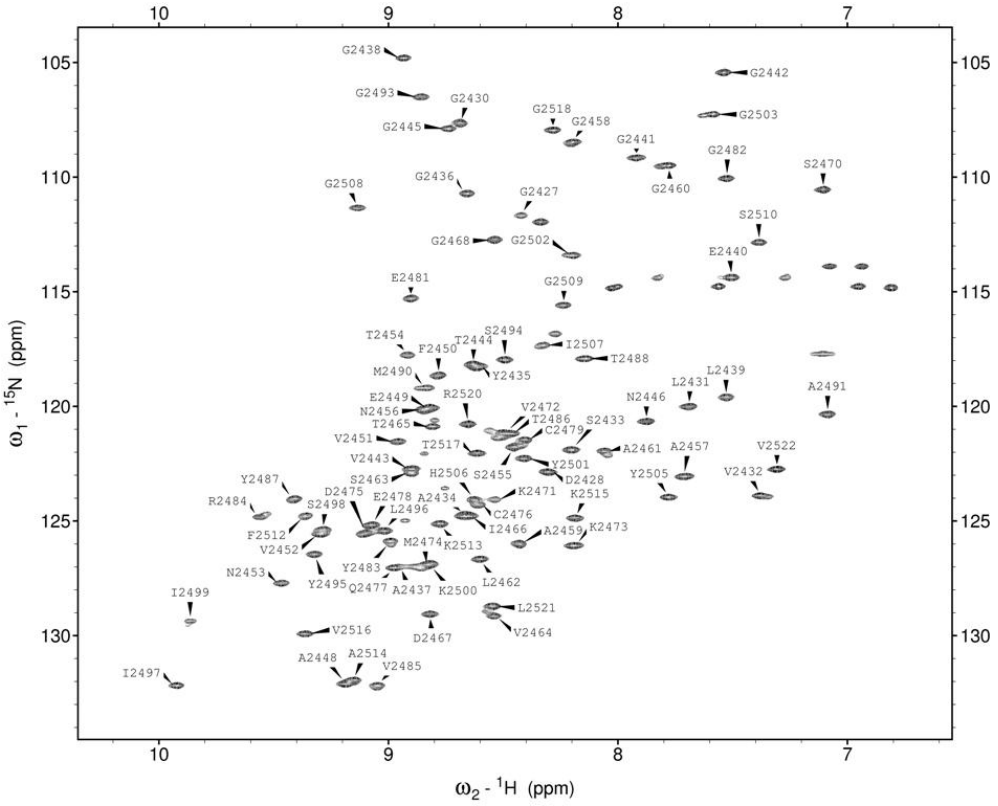

Fig. 25 The ^{1}H,^{15}N-HSQC spectrum of IgFLNa23 with backbone resonance assignments (**II**).

The structure of IgFLNa23 was solved using NOE-distance restraints from ^{13}C- and ^{15}N-edited HSQC-NOESY spectra. Due to excellent spectra, the structure determination of IgFLNa23 was straightforward and yielded a structure of excellent quality (Fig. 26; **II**: supplemental Table S1). Atomic coordinates of IgFLNa23 structure ensemble have been deposited in the PDB database (PDB accession code 2K3T). Like IgFLNa17, IgFLNa23 also holds the traditional IgFLN fold. Structural

precision is excellent throughout the sequence and side chain conformations in the hydrophobic core are also defined with high precision (Fig. 26A).

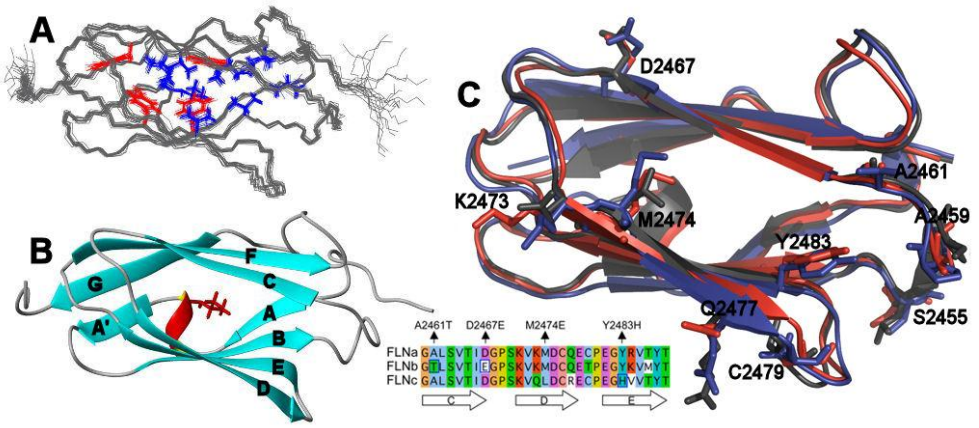

Fig. 26 The solution structure of IgFLNa23 (PDB accession code 2K3T) (**II**). All panels show the structure from the same perspective. (**A**) Superimposed backbone traces of the 20 substructures. Superposition was done for residues 2427–2520. Some of the side chains forming the hydrophobic core are also shown. (**B**) Secondary structure elements of the mean structure. L2439 is represented with stick model. (**C**) Structure superimposition of the three IgFLN23 isoforms: red, IgFLNa23; blue, IgFLNb23 (PDB entry 2EEC); black, IgFLNc23 (PDB entry 2D7Q). The inset shows sequence alignment of the isoforms. Non-conserved residues of the CD face are shown with stick models and labeled with FLNa residue codes. Reprinted and adapted with permission from (Nakamura *et al.* 2009). © 2009 Nakamura *et al.*

The interaction of IgFLNa23 with FilGAP was studied using NMR titrations. FLNa–FilGAP interaction was delineated to the 32 C-terminal residues of FilGAP (residues 717–748). This peptide, however, turned out to be highly insoluble in the buffer used for the NMR samples of IgFLNa23 and could not be used in titrations. We titrated IgFLNa23 with a more soluble shorter FilGAP peptide (FilGAP14), comprising the residues ^{723}EQFFSTFGELTVEP^{736}. Titration data indicated interaction at the fast-to-intermediate exchange region, *i.e.*, having a micromolar K_d. High excess of FilGAP14 was needed to see clear changes in the spectrum. Many ^{1}H,^{15}N-HSQC signals disappeared or divided into several peaks upon addition of FilGAP14 (**II**: supplemental Fig. S3). Spectrum quality suffered from addition of the peptide and chemical shift changes were difficult to follow. The most explicit changes were seen close to the CD face (**II**: Fig. 3), which also proves that the interaction between IgFLNa23 and FilGAP follows the general IgFLN interaction mode (Pudas *et al.* 2005; Kiema *et al.* 2006; Nakamura *et al.* 2006; Lad *et al.* 2008; Takala *et al.* 2008; Ithychanda *et al.* 2009a). As the interaction between IgFLNa23 and FilGAP14 was relatively weak and spectrum quality was compromised, complex structure determination using NMR was not possible.

FilGAP was shown to selectively interact with FLNa and not with FLNb or FLNc (**II**). The selectivity of the interaction is remarkable as the structures of the three IgFLN23 isoforms are very similar (Fig. 26C). There are few non-conserved residues at the CD face, which is the FilGAP binding site, but they are still able to delimit the interaction. Isoform-distinctive point mutations A2461T and Y2483H were shown to be enough to disrupt the FLNa–FilGAP interaction. Selectivity of FLNa–FilGAP interaction is a fine example of subtle structural features defining selectivity of protein–protein interactions.

The interaction of FLNa and FilGAP was further characterized using molecular modeling (**II**). Based on the crystal structure of IgFLNa17–GPIbα complex, *in silico* model of IgFLNa23–FilGAP complex was solved to understand the details of the interaction between FLNa and FilGAP (**II**: Fig. 3 and supplemental Fig. S4). IgFLNa23 residue M2474 is in close contact with FilGAP (Fig. 26C). As we were not able to determine the structure of FLNa–FilGAP interaction complex experimentally, we wanted to verify our interaction model with M2474E mutation. FLNa M2474E mutant was incapable of binding FilGAP, which confirms that the CD face of IgFLNa23 is indeed the binding site for FilGAP. Proper folding of IgFLNa23 domain was confirmed with NMR characterization of IgFLNa23 M2474E mutant (**II**: supplemental Fig. S5). The spectrum of the mutant proteins shows the properly folded domain and all chemical shift changes are located in close proximity to the mutated residue. M2474E point mutation does not perturb folding of IgFLNa23.

We also used NMR spectroscopy to study the effects of IgFLNa23 patient mutations on the structure of the domain (**II**). Zenker *et al.* have described *FLNa* mutation 7315C→A that leads to two aberrant transcripts: one with seven-residue (2439–2445) deletion (Δ7), and one with L2439M point mutation (Zenker *et al.* 2004). Point mutant L2439M is thought to be the cause for gain-of-function type effects observed in FMD, and deletion mutant Δ7 the cause of the loss-of-function phenotype PVNH. Residues 2439–2445 are located at IgFLNa23 strand A' and at the preceding 3_{10} helix (Fig. 26B). Highly conserved IgFLN residue L2439 is located in the middle of the 3_{10} helix pointing into the hydrophobic core of the domain. Another FLNa deletion mutation causing FMD is 7447del9, which leads to three-residue (2483–2485) deletion at IgFLNa23 (Δ3) (Robertson *et al.* 2006). These residues are located at the beginning of strand E. Attempts to record $^{1}H,^{15}N$-HSQC spectrum of Δ7 and Δ3 IgFLNa23 failed due to protein aggregation problems either during protein production and purification or in the NMR samples. It is likely that these short deletion mutations abolish the folding of IgFLNa23. Full length FLNa Δ7 and Δ3 deletion mutants were shown to eliminate the FLNa interaction with FilGAP, whereas the L2439M mutation did not affect the interaction (**II**: Fig. 7). The $^{1}H,^{15}N$-HSQC spectrum of IgFLNa23 L2439M mutant shows a well-folded domain (**II**: supplemental Fig. S7) and chemical shift differences between wild-type IgFLNa23 and the L2439M mutant are located close to the mutated residue. As the L2439M mutation does not abolish folding of IgFLNa23 or the interaction with FilGAP, there must be some other physiological mechanism that produces the phenotype of patients carrying the mutation. The mechanism might involve yet unknown FLNa interaction partner binding to the AG face of IgFLNa23.

7.2. Structures of Filamin A Tandem Immunoglobulin-like Domain Pairs

The structure of IgFLNa19–21 (see Fig. 8) showed that IgFLN domains do not live in isolation from each other (Lad *et al.* 2007). These domains can interact and organize into superstructures which influence each other's structure and function. Electron microscopy images of FLNa molecules (see Fig. 9) clearly show that the IgFLNa domains of rod 2 are more densely packed than would be expected for linearly arranged IgFLNa domains (Nakamura *et al.* 2007). By inspecting the sequence of FLNa, Gorlin *et al.* noticed that the N-terminal sequences of IgFLNa domains 16, 18, 20 and 22 are distinct from other IgFLNa domains (Gorlin *et al.* 1990). The structures of IgFLNb/c domains 16 and 18 are available in the PDB database (see Table 4). They all seem to lack the strand A of the conventional IgFLN fold—just as domain 20 does in the structure of IgFLNa19–21.

We wanted to find out whether IgFLNa domain pairs 16–17 and 18–19 share the domain packing mode of IgFLNa20–21 (**IV**). As the first step of our study, we compared the SAXS data of IgFLNa constructs 12–13, 16–17, 18–19, 20–21, and 22–23 (**IV**: Fig. 2–3 and Table 1). The construct containing domains 12–13, which are predicted to behave as two independent modules just linked together with a flexible linker, was included as a negative control. The SAXS curve of IgFLNa12–13 conformed well to dimensions of two linearly arranged conventional IgFLN domains. The dimensions of IgFLNa22–23 were similar to the dimensions of domain pair 12–13, which indicated that these domains do not form a compactly packed pair like domains 20–21. However, the dimensions of IgFLNa16–17 and 18–19 were similar to IgFLNa20–21 which implies that these domains do indeed form a compact domain pair. We studied the atomic structures of IgFLNa16–17 and IgFLNa18–19 using NMR spectroscopy (**III** and **IV**).

7.2.1. Filamin A Immunoglobulin-like Domain Pair 18–19

Chemical shift assignment, and later also structure determination, of IgFLNa18–19 was complicated by the fact that there were several signals missing from the $^{1}H,^{15}N$-HSQC spectrum (**III**: Fig. 1). Most of the missing signals are located at the N-terminal part of IgFLNa18 (S1961, H1962, L1963, V1965, G1966, A1969) and at the domain linker (S2040, Q2041, S2042, E2043, I2044). However, nearly all CH_n groups were visible in the $^{1}H,^{13}C$-HSQC spectrum and their chemical shifts were assigned. Chemical shift assignments of IgFLNa18–19 have been deposited in BMRB under accession code 15925. Our first step in revealing potential domain–domain contacts was to compare the $^{1}H,^{15}N$-HSQC spectra of the isolated IgFLN domains to the double-domain construct (Fig. 27). It was immediately obvious from the spectrum overlay that there are interactions between the domains. We also had $^{1}H,^{15}N$-HSQC assignments for isolated single IgFLNa domains 18 (FLNa residues 1954–2045) and 19 (FLNa residues 2046–2141). When chemical shift differences were plotted as a function of sequence, it was noted that the interaction between domains 18–19 resembled the domain interaction of IgFLNa20–21 (**IV**: supplemental Fig. S3). There were major chemical shift differences at IgFLNa19

strands C and D, similar to NMR titration of IgFLNa21 with IgFLNa20 (Lad *et al.* 2007: Fig. 3A). Unfortunately, the chemical shift changes at the N-terminal part of IgFLNa18 could not be tracked as these signals were not visible in the $^{1}H,^{15}N$-HSQC spectrum of IgFLNa18–19. There were also shift changes at the EF loop of IgFLNa18. The corresponding part of IgFLNa20, however, is not part of the domain interaction interface in IgFLNa20–21. This implies that there are some differences in the domain interaction modes of IgFLNa18–19 and 20–21. We also tried to attest the domain interaction with NMR titrations, but these attempts failed to show any interaction between the domains. The structure of IgFLNa18–19 will, however, provide an explanation for this behavior.

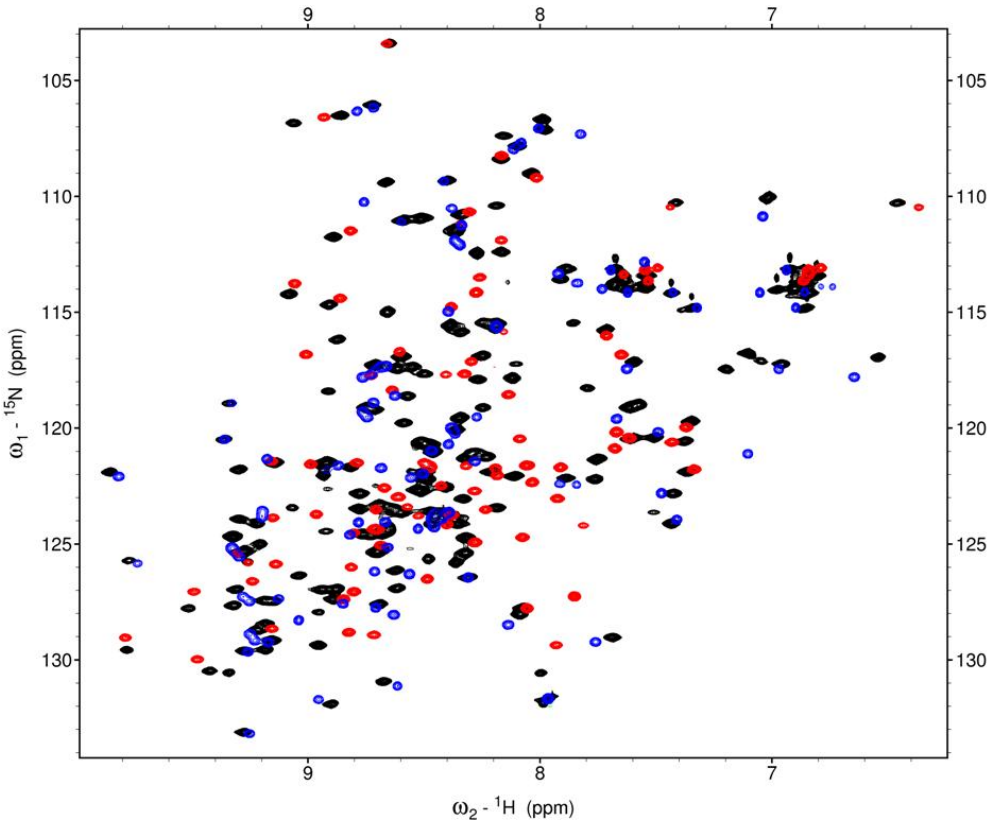

Fig. 27 Spectrum comparison demonstrates the interaction between IgFLNa domains 18 and 19. Superimposition of the $^{1}H,^{15}N$-HSQC spectra of isolated IgFLNa18 (red) and IgFLNa19 (blue) on the spectrum of IgFLNa18–19 double domain (black) reveals large chemical differences, implying strong domain–domain interaction between domains 18 and 19.

The structure of IgFLNa18–19 (FLNa residues 1954–2141) was determined by using NOE restraints from ^{13}C- and ^{15}N-edited HSQC-NOESY spectra and backbone dihedral angles derived from backbone secondary chemical shifts (**IV**). As there were some complications in the structure calculation regarding the N-terminal part of IgFLNa18 (see **IV**: supplemental methods for detailed description of the structure determination), additional hydrogen bond restraints were used between IgFLNa18 strand A and IgFLNa19 strand C. Structure quality statistics (**IV**: Table 2) show that the structure determination of IgFLN18–19 yielded a good quality result. Especially the Ramachandran diagram populations reflect a well-refined structure. Atomic coordinates of IgFLNa18–19 structure ensemble (20 structures) are available in the PDB database (accession code 2K7Q).

The overall domain arrangement of IgFLNa18–19 structure (Fig. 28) resembles that of IgFLNa20–21 (Lad *et al.* 2007). The first β strand of IgFLNa18 is not folded as part of domain 18 but is instead bound as an additional β strand to the C strand of IgFLNa19. Equally to domain pair 20–21, the domain 18 is stacked orthogonally to the N-terminal end of domain 19. The average backbone RMSD from the mean structure for the double-domain (residues 1960–2135) is 1 Å. There is some fluctuation between the two domains as the coordinate precision of single domains is better than for the double-domain. Average backbone RMSD from the mean structure is 0.8 Å for IgFLNa18 (residues 1960–2045) and 0.3 Å for IgFLNa19 (residues 2046–2135). The inter-domain fluctuation in the coordinates might be due to real physical movement or alternatively due to structural imprecision. The domain interaction of IgFLNa18–19 structure is based on 76 inter-domain NOEs, of which 42 are located between β strand A of domain 18 and the CD face of domain 19 (**IV**: supplemental Fig. S2B). The relative domain orientation of domains 18 and 19 relies on relatively few inter-domain NOEs and most of them are housed by a single residue, Y2077.

Despite the similar arrangement of the two domains in IgFLNa20–21 (Lad *et al.* 2007) and IgFLNa18–19, the details of domain interaction are completely different. The absence of β strand A leaves the hydrophobic core of domain 18 partly exposed. The side chain of Y2077 is pointing outwards from the BC loop of IgFLNa19 and it sticks into the hydrophobic core of domain 18, attaching the domains together (Fig. 28C). This domain–domain interaction is totally different from IgFLNa20–21 where the domain interaction is mainly determined by the β strand interaction between IgFLNa20 strand G and the BC loop of IgFLNa21 (Fig. 8). The relative domain orientations also differ substantially in these two domain pairs (**IV**: Fig. 7). On this account the domain linkers and the AB loops of the even-numbered domains take completely different paths in the two structures. In IgFLNa18–19, both the domain linker and the AB loop of domain 18 participate in the domain interface (Fig. 28C). In contrast, in IgFLNa20–21 the AB loop of domain 20 and the domain linker are exposed to solvent (Fig. 8). In addition, the IgFLNa18 EF loop, housing the hydrophobic residues (F2011, P2013) in contact with the side chain of Y2077, is an important part of the domain interface, which explains the chemical shift differences observed in this area (**IV**: supplemental Fig. S3). The crucial role of the domain linker in the domain interaction of IgFLNa18–19 explains why our attempts to demonstrate the domain–domain interaction using NMR titrations failed: the extra residues introduced to the N-terminal end of

domain 19 in protein production disturb the interaction interface. Linking the domains together also increases the effective concentration of the domains enhancing the interaction.

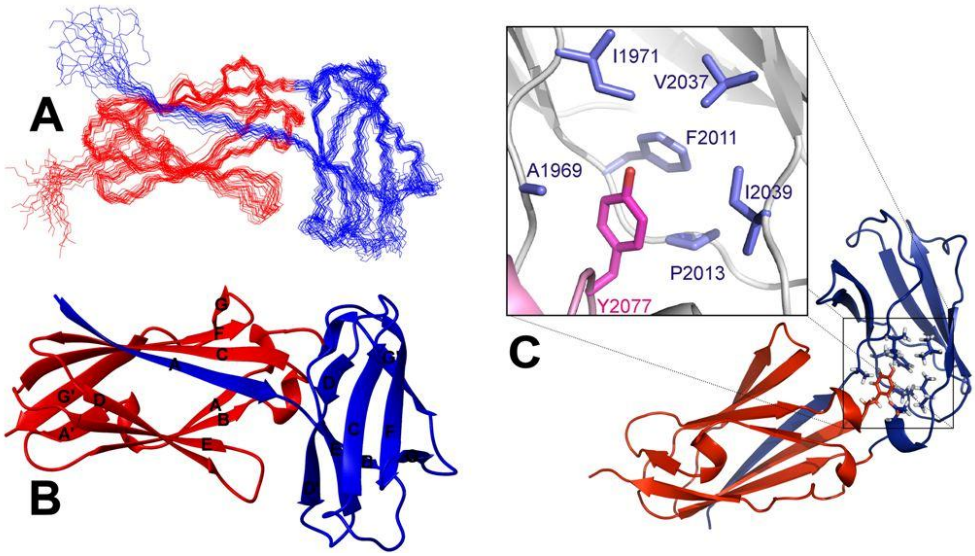

Fig. 28 The solution structure of IgFLNa18–19 (PDB accession code 2K7Q) (**IV**). Panels (**A**) and (**B**) show the structure from the same perspective. Panel (**C**) shows the opposite view to pick out the essentials of domain–domain interaction. Domains (defined by the sequence) are differentially colored: 18, blue; 19, red. (**A**) Superimposed backbone traces of the 20 substructures. Superposition was done using residues 1960–2135. (**B**) Secondary structure elements of the mean structure. (**C**) Y2077 is the main determinant of the domain–domain interaction between IgFLNa domain 18 and 19. Reprinted and adapted with permission from (**IV**). © 2009 The American Society for Biochemistry and Molecular Biology.

We measured the backbone ^{15}N R_1 and R_2 relaxation rates and $\{^1H\}$–^{15}N heteronuclear NOEs to elucidate the dynamicity of IgFLNa18–19, and also to verify the structure of IgFLNa18–19. The relaxation rates of IgFLNa18–19 (**IV**: supplemental Fig. S7) are in the expected range for a 20-kDa tightly-folded protein. Relaxation analysis was complicated by many overlapping and missing ^1H,^{15}N-HSQC signals especially in those areas which would have been the most interesting, *i.e.*, at the IgFLNa18 strand A and at the domain linker. The relaxation data accords with the domain association model of IgFLNa18–19, where the N-terminal part of domain 18 is bound to the domain 19 and the two domains are tightly bound together. Observed relaxation rates imply a compact domain pairing and do not reveal any highly flexible loops or long tails. We attempted to carry out full model-free analysis of the relaxation data, but successful analysis was hampered, presumably due to high rotational anisotropy of the molecule or due to large-scale inter-domain motions.

IgFLNa18–19 Interaction with β7 Integrin and Dopamine Receptors

IgFLNa19 is known to participate in the interaction between FLNa and integrin tails, even if the main integrin binding site is located at domain 21 (see Chapter 3.3.2). With similarity to IgFLNa20–21 (Lad *et al.* 2007), the first β strand of IgFLNa18 is blocking the integrin binding site at the C strand of domain 19. It has been shown that the presence of IgFLNa20 strand A effectively blocks the integrin binding site of domain 21, inhibiting integrin binding, even if integrin tails are able to displace strand A of domain 20 from domain 21 to some extent (Lad *et al.* 2007). Integrin tails bind to IgFLNa18–19 even if binding is weaker than to isolated domain 19. We tested the interaction between IgFLNa18–19 and integrin β7 peptide (Ac-^{776}PLYKSAITTTINP^{788}-NH_2) using NMR titrations (**IV**: supplemental methods and supplemental Fig. S4). In our experiments we could not detect interaction between integrin β7 peptide and IgFLNa18–19; even when under equivalent conditions the peptide clearly interacted with the strand C of isolated IgFLNa19. This confirms that IgFLNa18 strand A is able to at least inhibit, if not totally block, the interaction between IgFLNa and integrin β7.

IgFLNa19 has also been proven to be the binding site for dopamine receptors D_2 and D_3 (see Chapter 3.3.2) (Lin *et al.* 2001). The point mutation experiments of Lin *et al.* showed that the interaction site is located at the CD face of domain 19 (Lin *et al.* 2002). FLNa binding site has been mapped to the third intracellular loop of the dopamine receptor, *i.e.*, to the D_2 and D_3 residues 211–344 and 211–227, respectively. When we compared these residues, we noted highly conserved sequences, which contain a polyarginine repeat resembling the N-terminal sequence of IgFLNa20 (Fig. 29).

Fig. 29 The dopamine receptor peptides tested for interaction with IgFLNa18–19.

We wanted to confirm the dopamine receptor binding site at IgFLNa19 and to see whether dopamine receptor peptides are able to displace the IgFLNa18 strand A from the CD face of domain 19. We performed NMR titrations of IgFLNa18–19 using dopamine receptor peptides described in Fig. 29 (unpublished results). The titration results are presented in Fig. 30. Both D_2 and D_3 peptides interacted with IgFLNa18–19 with high affinity and were able to displace the strand A of IgFLNa18 from the CD face of IgFLNa19. The binding site for dopamine receptors is located at the CD face of domain 19. Some chemical shift changes are also found at the residues of domain 18. All affected residues are located close to CD face of domain 19. This verifies the dopamine receptor interaction site at the CD face of IgFLNa19 and suggests that this interaction also follows the general interaction mode of IgFLN domains. A more detailed view of the interaction could be gained from a complex structure of IgFLNa19 and dopamine receptor peptide.

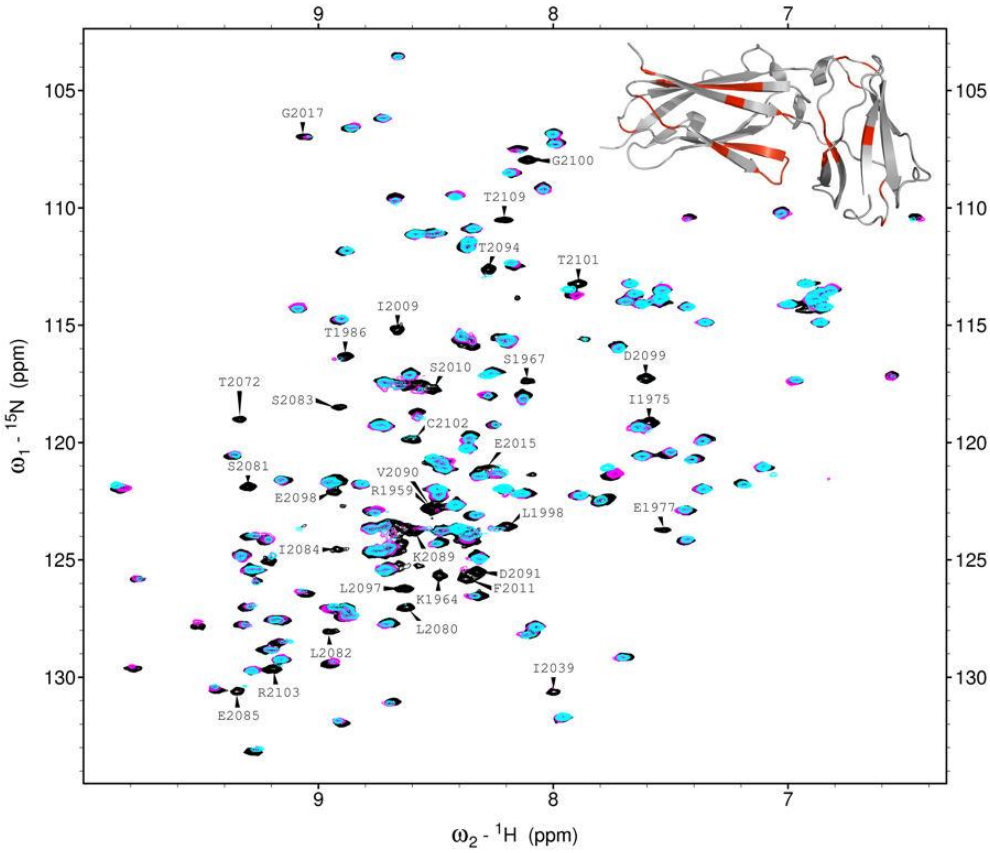

Fig. 30 Dopamine receptors D_2 and D_3 interact with the CD face of IgFLNa19. IgFLNa18–19 was titrated with the peptides derived from the third intracellular loop of dopamine receptors D_2 and D_3 (Fig. 29). Spectrum overlay reveals the residues with chemical shift changes: black, IgFLNa18–19 in the absence of ligands; magenta, 1.6:1 D_2-to-IgFLNa18–19; cyan, 1.6:1 D_3-to-FLNa18–19. Both peptides bind to the same site with similar affinities. Inset shows the location of the residues with affected resonances.

7.2.2. Filamin A Immunoglobulin-like Domain Pair 16–17

The spectra of IgFLNa16–17 were remarkably good (**III**: Fig. 1B). All cross-peaks except K1801, G1866 and Q1916 were visible in the $^{1}H,^{15}N$-HSQC spectrum and essentially complete backbone and side chain assignments were attained (BMRB accession code 15924). As we already had assignments for IgFLNa17 (see Chapter 7.1.1), we compared the chemical shifts of domain 17 in isolation and in the IgFLNa16–17 domain pair. We expected to see something comparable to the changes of IgFLNa19 and 21, but the results were rather the opposite (**III**: Fig. 2). All chemical shift changes were located at the AG face of domain 17 and the resonances of the CD face remained practically unchanged. This implied that the domain–domain interaction mode of domains 16 and 17 is drastically different from IgFLNa18–19 and 20–21.

Structure determination of IgFLNa16–17 (FLNa residues 1772–1956) was relatively straightforward owing to good spectrum quality and yielded a structure of excellent quality (**IV**). NOE restraints from ^{13}C- and ^{15}N-edited HSQC-NOESY spectra and chemical shift-based backbone dihedral angle restraints were used as constraints in the structure calculation. Both Ramachandran map populations and coordinate precision indicate successful structure determination (**IV**: Table 2). Atomic coordinates of IgFLNa16–17 structure ensemble (40 structures) are available in the PDB database (accession number 2K7P). Ninety-nine inter-domain distance restraints were found (**IV**: supplemental Fig. S2A), and all of them were located between β strands A and G of IgFLNa17 and B and G of IgFLNa16. These were enough to define the inter-domain orientation in comparable precision to the individual domains.

As in IgFLNa18 and 20, the first predicted β strand of domain 16 does not fold as in conventional IgFLNs. Residues 1772–1785, corresponding to β strand A of IgFLNa16, lack long range distance restraints and do not hold any regular secondary structure (Fig. 31). Due to missing strand A, the hydrophobic core of domain 16 is exposed, and it binds tightly to the AG face of domain 17. The two IgFLN domains are stacked on to each other so that their β sheets are approximately parallel. The domain interaction is mostly based on hydrophobic interactions. The side chains of H1877 and T1876 from IgFLNa17 are located particularly close to the exposed hydrophobic core of IgFLNa16 (Phe1791, Leu1793, Ile1795, Leu1856, and Phe1858) (**IV**: Fig. 5C). There are several hydrophobic and aromatic residues at the AG surface of IgFLNa17, much more than in the corresponding parts of domains 19 and 21 (Fig. 22 and **IV**: supplemental Fig. S1), which establishes prerequisites for the domain interaction of IgFLNa16–17. The structure of domain 17 in IgFLNa16–17 is remarkably similar to the structure of isolated IgFLNa17. In fact it is somewhat surprising that the solubility of isolated IgFLNa17, with relatively hydrophobic exposed AG face, was sufficient for successful NMR studies. In conclusion, the structure of IgFLNa16–17 revealed a novel domain–domain interaction mode of IgFLNs.

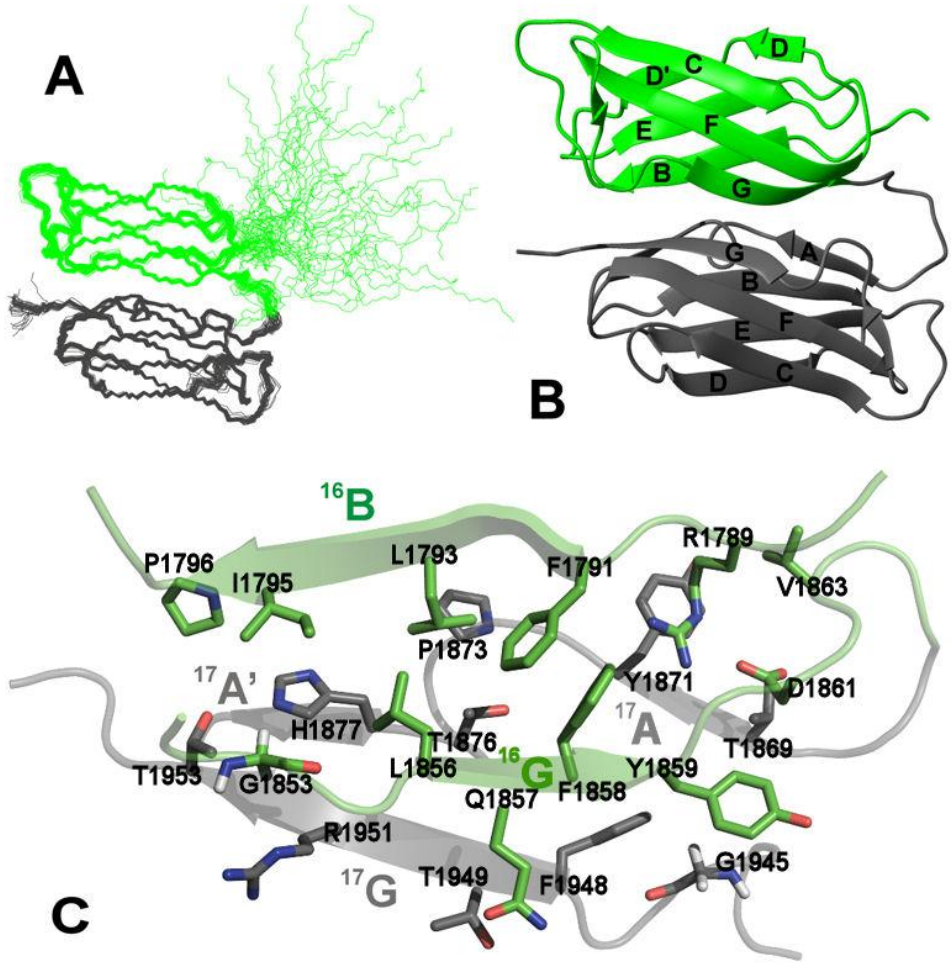

Fig. 31 The solution structure of IgFLNa16–17 (PDB accession code 2K7P) (**IV**). Panels (**A**) and (**B**) show the structure from the same perspective. Panel (**C**) shows a top view through domain 16 to pick out the essentials of the domain interaction. Domains are colored as: 16, green; 17, gray. (**A**) Superimposed backbone traces of the 40 substructures. Superimposition was done using residues 1787–1954. (**B**) Secondary structure elements of the mean structure. (**C**) Exposed hydrophobic core of IgFLNa16 stacks on to the AG face of domain 17. Residues of the domain interface are represented with stick models. Reprinted and adapted with permission from (**IV**). © 2009 The American Society for Biochemistry and Molecular Biology.

In order to characterize the dynamic behavior of IgFLNa16–17 we measured the backbone ^{15}N R_1 and R_2 relaxation rates and $\{^1H\}–^{15}N$ heteronuclear NOEs. There were some overlapping $^1H,^{15}N$-HSQC signals which hindered relaxation analysis of those residues, but overall almost complete relaxation data was achieved (**IV**: supplemental Fig. S6). Measured relaxation rates conform well to the characteristic values of 20-kDa globular proteins. Relaxation analysis clearly

shows that the N-terminal residues of domain 16 undergo rapid motions, which confirms that IgFLNa16 strand A is unfolded. R_2 relaxation rates and heteronuclear NOEs have a slight decrease at the BC loop of IgFLNa17, indicating that this loop is more flexible than the rest of the structure. Coordinate precision of this loop is, however, almost as good as at other parts of the structure even if it was somewhat floppy in the structure of isolated IgFLNa17 (see Fig. 22). In conclusion, the relaxation analysis along with the abundance of inter-domain NOEs and the excellent spectrum quality, support the view that the two domains of IgFLNa16–17 are tightly bound together.

Interaction of IgFLNa16–17 with GPIbα

We had previously shown that glycoprotein Ibα binds to the CD face of IgFLNa17 (**I**) and we also verified the interaction with NMR titrations (see Fig. 23). As the CD face of domain 17 is free in IgFLNa16–17 and essentially structurally identical to isolated IgFLNa17, we were confident that GPIbα also binds to IgFLNa16–17. To confirm the interaction we performed NMR titration of IgFLNa16–17 with GPIbα556–577 peptide. The results of the titration are comparable to the ones achieved with isolated IgFLNa17 (**IV**: supplemental Fig. S5). The strength of the interaction was further verified with biochemical experiments (**IV**: Fig. 6).

Potential Influence of Domain 15 and Hinge 1 on Structure of IgFLNa16–17

The peculiar structure of IgFLNa16–17 raised questions about whether the presence of domain 15 or H1 preceding domain 16 could have any effect on the domain interaction of IgFLNa16–17. The structure of IgFLNb15 (PDB code 2DMB) shows a conventional IgFLN fold, but nothing is known about the structure of H1. We compared the $^{1}H,^{15}N$-HSQC spectra of IgFLNa15–17 and IgFLNa16–17 to see if the residues of domains 16–17 undergo any chemical shift changes (unpublished results). $^{1}H,^{15}N$-spectrum of IgFLNa15–17 shows >250 well-resolved backbone signals of which around one-third have higher intensity and narrower line-width. Spectrum comparison shows that the chemical shifts of domains 16–17 are essentially the same in both IgFLNa15–17 and IgFLNa16–17 constructs (Fig. 32). This indicates that the folding pattern of IgFLNa16–17 pair is also retained in this longer construct and IgFLNa15 or H1 do not interact with this domain pair. There are some minor changes at 16–17 linker (*e.g.*, residue H1867) and at BC loop of IgFLNa17 (*e.g.*, residue T1890). These are presumably due to slightly different experimental conditions which have the most pronounced effect on the resonances of these flexible loops. It is also evident that the cross-peaks belonging to domain pair 16–17 are considerably broader than the rest of the peaks, indicating faster transverse relaxation. This confirms that domain 15 behaves independently on domains 16–17—it is just linked to them with a flexible linker H1. We are planning to sequentially assign the spectra of IgFLNa15–17 and to measure the $\{^{1}H\}$–^{15}N heteronuclear NOEs to find out if H1 has some structured parts or whether it is just a flexible linker sequence.

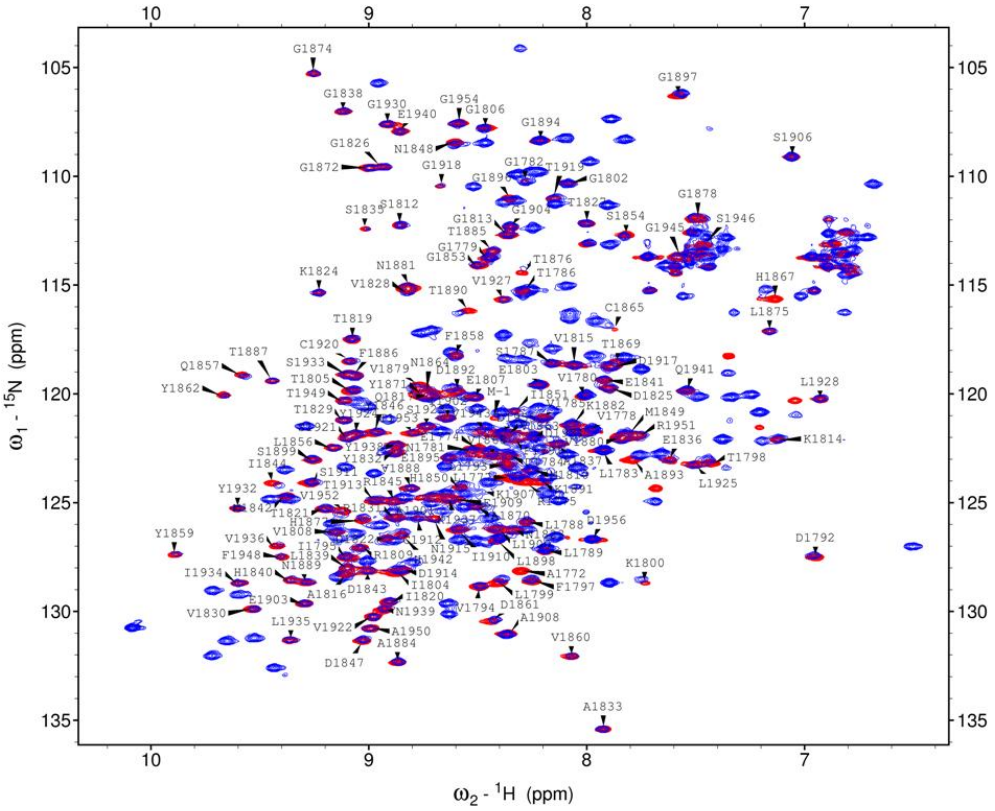

Fig. 32 ^{1}H,^{15}N-HSQC spectrum comparison of IgFLNa15–17 (blue) and IgFLNa16–17 (red) shows that domain 15 or H1 do not interact with the domain pair 16–17. Also, the narrow line-width of the signals of domain 15 support the conclusion that domain 15 behaves independently from the domain pair 16–17. Resonance assignments of IgFLNa16–17 signals are shown.

7.2.3. Similarities and Differences of the Three IgFLNa Domain Pairs

The three IgFLNa domain pair structures characterized so far have all surprised us with new structural features. There are two common denominators of the three domain pairs IgFLNa16–17, IgFLNa18–19, and IgFLNa20–21: (i) the two domains interact tightly with each other and form relatively compact structures, and (ii) the β strand A of the even-numbered domain is not folded with its own domain but is either unstructured (IgFLNa16) or folds together with the following domain (IgFLNa18–19 and IgFLNa20–21). If one dissects the structures in more detail, some additional similarities can be found. In all three domain pairs the strand D of the even-numbered domain is split into two parts: beginning of strand D is part of β sheet CFG and D' makes a β strand interaction with strand E (Fig. 28; Fig. 31; Fig. 33; Lad *et al.* 2007). In conventional IgFLN domains, and also in the odd-numbered domains of the domain pairs, the strand D is continuous and binds next to the strand E. Another unifying trait of the even-numbered domains is that the tyrosine corner (Hemmingsen *et al.* 1994), one of the highly conserved features in the Ig-like

domains, is replaced by histidine (H1840, H2019 and H2210) (Fig. 33). In odd-numbered domains of all three domain pairs the corresponding residue is tyrosine (Y1932, Y2114 and Y2305). Chemical shifts of H1840 and H2019 (**III**) indicate that these histidines are protonated at the δ nitrogen of the imidazole ring, which is the more infrequent histidines tautomer. Sequence alignment of IgFLN domains (van der Flier and Sonnenberg 2001b) shows that the tyrosine corner is also replaced by histidine in domains 1, 2, 5 and 11 in all FLN isoforms and depending on isoform by histidine or some other residue in domains 7 and 22. Structures of domains 11 and 22 are available in the PDB database and they also have a discontinuous D strand, but otherwise the structures seem to be fully folded IgFLN domains.

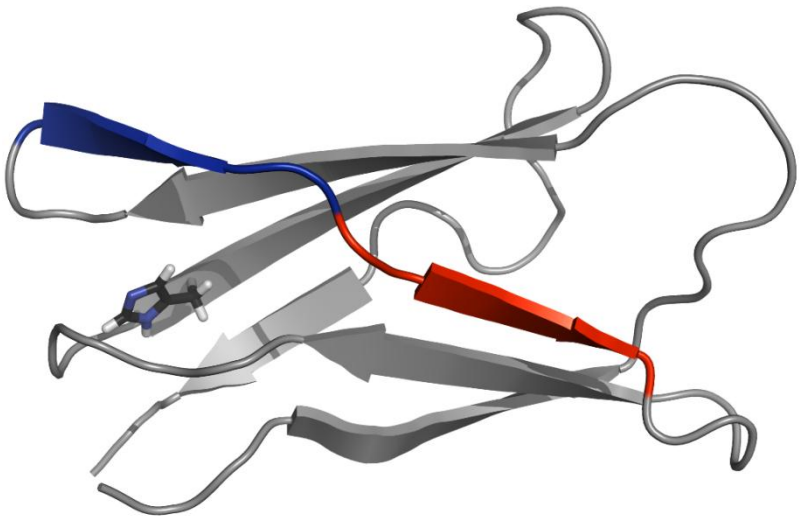

Fig. 33 The odd-numbered domains of the IgFLNa domain pairs 16–17, 18–19, and 20–21 have discontinuous strand D and δ protonated histidine replacing the tyrosine corner. The structure of IgFLNa16 is shown here as an example. H1840 is represented with a stick model. Blue, strand D; red, strand D'.

Despite these similarities it is obvious that all three IgFLN domain pairs are remarkably different and no general pattern of IgFLN domain–domain interaction was recognized. Sequence comparison of IgFLN domains, however, shows that some of the key residues involved in domain interactions have been conserved in all human filamin isoforms and also in filamins of other organisms (**IV**: Fig. 4 and supplemental Fig. S1). It seems that the concept of three filamin domain pairs at the C-terminal end of filamins could be evolutionally conserved because this feature has specific functions in regulating protein binding to filamins.

7.3. Domain Organization in Filamin A Immunoglobulin-like Domains 16–21

After unveiling the structures of the IgFLNa domain pairs 16–17, 18–19, and 20–21, it became obvious that IgFLNa domains 16–21 are forced to pack into a compact cluster of domains. In their recent article, Kesner *et al.* presented a homology modeling-based full-length filamin model that includes the compact packing of domain pairs 18–19 and 20–21 (Kesner *et al.* 2009b). Even if it roughly matches with the experimentally detected dimensions of filamin dimers, this sketchy structure model is not able to provide details on domain interactions and it fails to reproduce the compact domain packing of IgFLNa16–17. We wanted to characterize the structure of IgFLNa16–21 domain sextet to find out whether the domain pairs also remain intact in this larger construct, and what the consequences of dense domain packing for FLNa interactions might be. As previous attempts to crystallize IgFLNa16–21 had not succeeded, we decided to look into the structure of this 60-kDa protein using NMR spectroscopy (**V**). Residual dipolar couplings provide ideal conformational restraints for NMR studies of protein domain organization of large modular systems (Fischer *et al.* 1999; Skrynnikov 2004; Blackledge 2005).

Due to the high molecular weight of IgFLNa16–21 (FLNa residues 1772–2329), perdeuteration of the protein was mandatory to suppress extensive transverse relaxation. Triply-labeled (^{2}H,^{13}C,^{15}N-labeling) sample of IgFLNa16–21 was produced for resonance assignment and measurement of RDC restraints. As there are no deeply buried areas in this protein, sufficient deuterium–proton exchange was attained simply by buffer exchange, eliminating the need for elaborate sample pretreatment and protein denaturation. The overall transverse relaxation rate of ^{2}H,^{13}C,^{15}N-IgFLNa16–21 was in the range of 30–40 s^{-1}, which necessitated the use of TROSY-based NMR experiments in the sequential assignment, in the relaxation measurements, and in determination of residual dipolar couplings. With the TROSY-based experiments, however, a relatively good and complete NMR dataset was gained.

The ^{1}H,^{15}N-HSQC-TROSY spectrum of triply-labeled IgFLNa16–21 shows approximately 450 well-resolved cross-peaks with relatively uniform intensities, and assignments were found for 88% of the 514 non-proline residues of IgFLNa16–21 (**V**: Fig. 3). To find out whether the three domain pairs specifically interact with each other in the larger constructs and to locate the interaction sites, we compared the ^{1}H,^{15}N-HSQC spectra of the isolated IgFLNa domain pairs 16–17, 18–19, and 20–21 with the spectrum of IgFLNa16–21 (Fig. 34). The spectrum of IgFLNa16–21 is almost the sum of its subcomponents and most of the signals have retained their locations. The similarity of the spectra was of great help in the sequential assignment of IgFLNa16–21. Assignment from scratch would not have been feasible, or at least it would have been extremely challenging. Clearly, no dramatic structural differences are present between IgFLNa16–21 and its isolated substructures. Closer inspection of the chemical shift differences gave clues about the domain interaction interfaces (**V**: Fig. 5). In general, not many chemical shift differences can be detected between the domain pairs and the IgFLNa16–21. The

only significant differences are found in domains 19 and 21. The absence of major chemical shift differences suggests that the interactions between the domain pairs are rather weak and the domain organization of the IgFLNa16–21 is mainly determined by the covalent linkages of the short linker sequences between the domains.

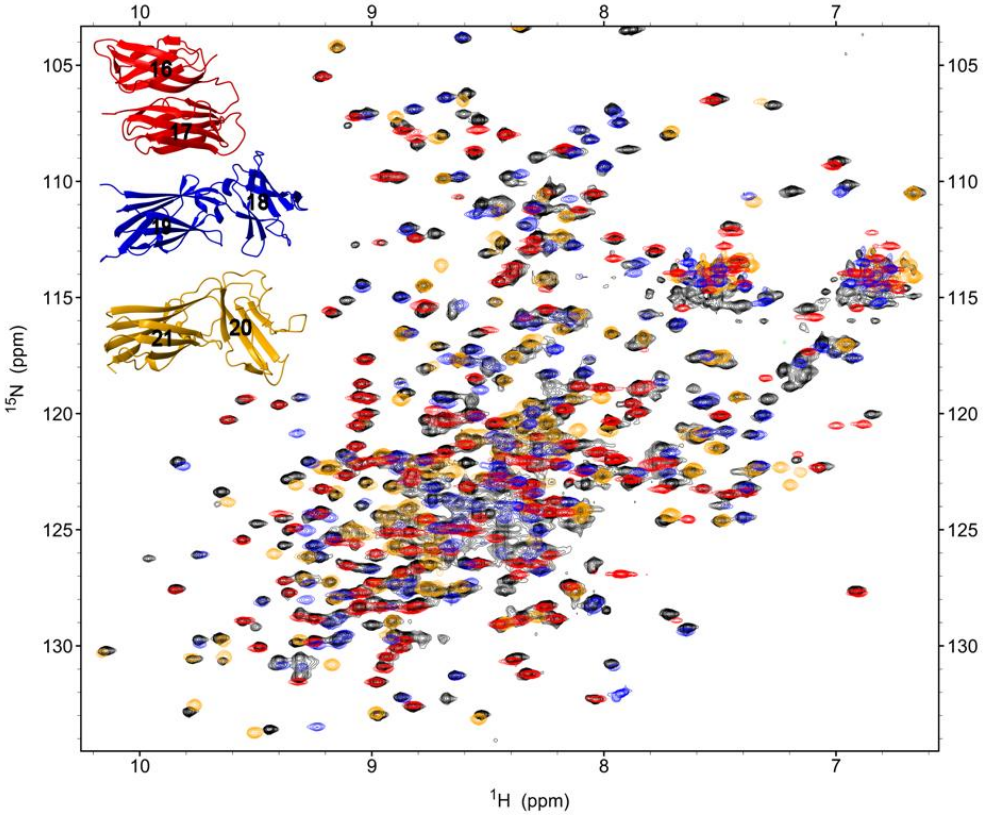

Fig. 34 Superimposition of the ^{1}H,^{15}N-HSQC-TROSY spectrum of ^{2}H,^{13}C,^{15}N-IgFLNa16–21 (black) and the ^{1}H,^{15}N-HSQC spectrum of IgFLNa16–17 (red), IgFLNa18–19 (blue), and IgFLNa20–21 (yellow) (**V**). The structures of the isolated domain pairs are shown in the inset.

The calculated pI of IgFLNa16–21 is 5.7 making it negatively charged in the sample pH of 6.8. Negatively charged Pf1 phages (Hansen *et al.* 1998) were thus chosen to introduce residual alignment into the IgFLNa16–21 sample for the RDC determination. The scalar and residual dipolar couplings between the amide proton (^{1}HN) and nitrogen (^{15}N) were measured using three-dimensional HNCO-TROSY-based triple-resonance experiment (Yang *et al.* 1999; Kontaxis *et al.* 2000, Permi *et al.* 2000). Backbone amide ^{1}HN–^{15}N RDCs were determined in total for 430 residues. The distribution of RDCs indicated that the alignment was stronger for domains 20–21 than for domains 16–19 (**V**: Fig. 6).

For rigid-body modeling of the IgFLNa16–21 domain organization, an arbitrary starting structure was built using the structures of IgFLNa domain pairs 16–17, 18–19 and 20–21 by superimposing the overlapping parts of the substructures (**IV**; Lad *et al.* 2007). We first attempted to carry out the alignment tensor fitting and the determination of domain pair orientations with three modules formed from domain pairs 16–17, 18–19, and 20–21. It, however, turned out to be impossible to find the proper fit of the RDCs in this way. There were no problems in domain pair 16–17, but domain pair 18–19 and especially 20–21 yielded poor fits of the RDCs. We supposed that this could be an indication of the altered domain orientations of the double-domains. Thus, we fitted the RDCs using six modules composed of individual domains (Fig. 35).

The closely similar alignment tensors of domains 16 and 17 confirm that these domains form a compact tightly packed domain pair, and the domain orientation determined by the NOE restraints is close to the real structure (Fig. 35). A slight adjustment of the domain orientation was suggested by the alignment tensors (**V**: Fig. 9A). The domain orientations in domain pairs 18–19 and 20–21 required closer inspection, as in these domain pairs, the alignment tensors of the two domains seem to be different. The alignment tensor components of domain 18 are of a smaller magnitude than for domain 19, suggesting that domain 18 wobbles slightly relative to domain 19. Alignment of the tensor axes twists domain 18 to a slightly more open conformation relative to domain 19 (**V**: Fig. 9B). Obviously, the low number of inter-domain NOE restraints between domains 18 and 19 was not quite enough to determine the domain orientation with high accuracy (see Chapter 7.2.1). The inter-domain orientation of domain pair 20–21 was affected even more by the alignment of the tensors (**V**: Fig. 9C). Relative to domain 21, domain 20 is twisted along its longitudinal axis and turns more towards domain 21. As the chemical shifts of domains 20 and 21 are very similar in the isolated double domain 20–21 and IgFLNa16–21, the domain orientation cannot be markedly affected by the presence of other domains. According to the RDC data, the domain arrangement in solution differs from the orientation seen in the crystal structure. Interestingly, the molecular dynamics simulations performed by Lad *et al.* for the structure of IgFLNa19–21 to see whether the crystal contacts had affected the structure, gave structure alterations that were similar to those in as our RDC analysis (Lad *et al.* 2007).

Parallelization of the alignment tensors and selection between the combinations of degenerate orientations produced a clover-leaf-shaped organization of the three domain pairs (Fig. 35B). The compact shape and dimensions (maximum dimension approximately 100 Å) of the IgFLNa16–21 structure model match nicely with the previously published electron microscopy images of the IgFLNa constructs (Nakamura *et al.* 2007). In this domain organization mode, the interaction sites at the CD faces of domains 17, 19 and 21 are freely exposed to solvent, and available for interactions.

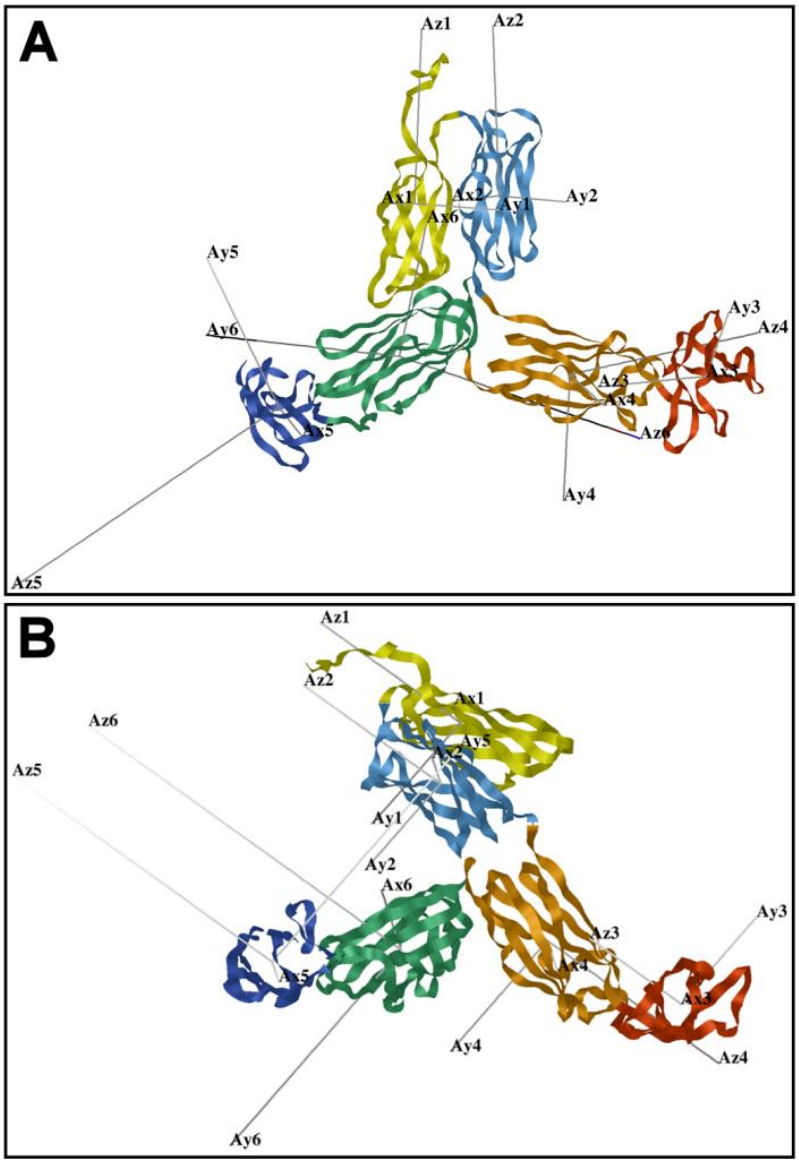

Fig. 35 Rigid-body modeling of the IgFLNa16–21 domain orientations using RDC restraints (**V**). Separate modules are color coded as: yellow, domain 16; light blue, domain 17; orange, domain 19 and the A strand of domain 18; red, domain 18; green, domain 21 and the A strand of domain 20; navy, domain 20. (**A**) Arbitrary structure of IgFLNa16–21 showing the alignment tensors of modules. (**B**) Parallelized alignment tensors. The figure shows one plausible combination of degenerate orientations that fulfills covalent and non-covalent structural confines and chemical shift data. The figures were created with the MODULE program (Dosset *et al*. 2001).

To characterize its dynamic behavior we measured the backbone amide ^{15}N R_1 and R_2 relaxation rates and $\{^1HN\}^{15}N$ heteronuclear NOEs of IgFLNa16–21 (**V**: Fig. 8). Some differences can be noted in the relaxation properties of the different domains. Domain pair 16–17 has on average slower transverse relaxation than domain pairs 18–19 and 20–21, which suggests that domain pair 16–17 is more dynamic than the other two domain pairs. The flexibility of domain pair 16–17 enables it to give way for the interaction partners to bind to the CD faces of the odd-numbered domains. Faster transverse relaxation in domain pairs 18–19 and 20–21 implies that these domain pairs could be bound together as they exhibit relaxation properties of a larger unit than domain pair 16–17. There is, however, some flexibility between domain pairs 18–19 and 20–21, as the alignment tensors of these domains are not equal. Except for the 15 N-terminal residues, the relaxation properties of domains 16 and 17 are similar, which confirms that the domains form a compact domain pair. The relaxation properties of the even- and odd-numbered domains of domain pairs 18–19 and 20–21 are more distinct. In general, the even-numbered domains seem to have somewhat reduced heteronuclear NOEs than the odd-numbered domains and have regions with elevated R_1 (especially domain 18) and lowered R_2 (domain 20). Altered relaxation properties indicate that the fold of the domains 18 and 20 is not as fixed as folding in other domains. Similar behavior of these domains was noted in structures of the isolated domain pairs (**IV**; Lad *et al.* 2007).

Even if the changes in the domain orientations produced by RDC analysis are notable, the structural details of the domain interactions could also be, in principle, fulfilled in these domain conformations. However, more elaborate analysis and refinement of the structures are needed to focus on the structural details as the rigid-body modeling performed here is only a crude way to model the domain orientations. The A strands of domains 18 and 20 escaped detailed analysis as their signals were not visible in the spectra. As these parts of the protein are more flexible, it is possible that the A strands of domains 18 and 20 are detached from the corresponding even-numbered domains in this larger construct. This would allow large freedom in domain arrangement. The chemical shift and relaxation data of IgFLNa16–21, however, suggest that the A strands of domains 18 and 20 remain bound to the CD face of domains 19 and 21, respectively.

Another phenomenon becoming available in the aligned protein samples is the residual anisotropy of the carbonyl chemical shift (Cornilescu *et al.* 1998). These effects can be also used as structural restraints in the refinement of protein structures. We detected a clear trend comparable with the RDCs in the changes of amide carbonyl chemical shifts between the isotropic and anisotropic sample, but the resolution of the HNCO-TROSY spectra in the carbon dimension was not sufficient to provide reliable restraints.

The structural characterization of IgFLNa16–21 could be further elaborated by refining the starting structures against the RDCs and NOE restraints simultaneously. Only NOEs between the exchanging protons (in practice, the backbone amides) can be recorded for perdeuterated IgFLNa16–21, and laborious selective labeling approaches should be used to obtain more NOE restraints. Extensive transverse relaxation and dynamicity of the domain interactions might, however, prevent detection of the inter-domain NOEs. A more fruitful approach to

refine the structure model would be combination of RDC and small-angle X-ray scattering (SAXS) restraints (Mattinen *et al.* 2002; Grishaev *et al.* 2005; Gabel *et al.* 2008). SAXS provides information on the dimensions of the protein, nicely complementing the orientational information gained from RDCs. In this particular case, SAXS would help in determining the integrity of the domain interactions and in fixing the positions of the domain pairs relative to each other.

7.4. Implications of Our Structural Findings for Filamin Functions

The structures of the IgFLNa domains 17, 19 and 23 all have traditional IgFLN fold and they closely resemble each other and domain 21 with average pairwise Cα RMSD of ~1.2 Å (**I, II, IV**). All filamin protein–protein interactions studied were discovered to take place through the same interaction mechanism—binding of the extended peptide as an additional β strand next to the C strand of the domain in question. Both the sequences of the interacting peptides, and the sequences of the IgFLNa domains seem to have some homology. Similarities of the interaction partners open up a possibility that the interactions can be at least partly indiscriminate. Ithychanda *et al.* have recently shown that IgFLNa domains 4, 9, 12, 17, 19, 21 and 23 form a homologous subgroup of IgFLNa domains and GPIbα, integrin β7, and migfilin peptides can all bind to several of these domains (Ithychanda *et al.* 2009b). The authors speculated that simultaneous binding to several IgFLN domains could promote receptor clustering. However, it should be noted that these studies were done with isolated single IgFLN domains and in full-length filamin the situation might be different. Our structural findings clearly indicate that IgFLN domains can exert an influence on the interactions and function of their fellow domains. The A strands of IgFLNa domains 18 and 20 block the protein binding site at the following domain and hinder the interactions at these binding sites. In full length filamin the inter-domain contacts can have even more complex consequences for the interactions and the function of the protein. IgFLN domains do not live in isolation, and thus should not be studied as such without further consideration of the effect of domain–domain interactions. In light of domain promiscuity of the filamin interactions, the FLN isoform selectivity seen with FilGAP is remarkable. Subtle differences in the structure of the CD face of IgFLN domain 23 discriminate between the isoforms so that only FLNa, but not FLNb or FLNc, binds to FilGAP (**II**).

IgFLNa domain pairs 16–17, 18–19 and 20–21 all have peculiar domain–domain interaction modes. Filamins have been speculated to be involved in mechanosensory signaling (Johnson *et al.* 2007) and IgFLN domain pairing could, in principle, act as a sensor for mechanical force. Pentikäinen and Ylänne have studied the effect of mechanical force on folding of IgFLNa domain pairs 18–19 and 20–21 using steered molecular dynamics simulations (Pentikäinen and Ylänne 2009). They noted that the A strands of the even-numbered domains detached relatively easily from the CD faces of the corresponding odd-numbered domains, exposing the binding sites for filamin interaction partners without disturbing the overall folding of the domains. Further stretching caused partial unfolding of the even-numbered domain, elongating the domain pair. Reversible dissolution of domain interaction and unfolding of the domains could act as a mechanism

introducing elasticity to filamin–actin networks. Domain interaction between IgFLNa domains 16–17 appears tighter than in other domain pairs and it is not interfering with the interaction site at the CD face. The function of this domain interaction is not obvious from the structure alone. The large planar surface formed by the parallel β sheets could in principle serve as a docking site for protein–protein interactions and there are some clefts at the domain interface that could be imagined to function as binding sites for small ligands. This is, however, only speculation.

Relatively compact dimensions of the filamin rod domain 2 are nicely explained by the tight domain packing of IgFLNa16–21 domain sextet (**V**). These domains form a cluster of domains having maximum dimension of 100 Å. IgFLNa domains 16–21 contain interaction sites for several filamin interaction partners (see Table 5). Domain contacts in IgFLNa16–21 can have considerable effects on filamin interactions mediated by these domains. Close domain packing can block access to interaction sites. Liberation of domain contacts through detachment of the A strands of domains 18 or 20 from the CD face of the corresponding odd-numbered domain by one interaction partner could open up the domain cluster to reveal other interaction sites buried in the domain interfaces. It is also possible that the A strands of domains 18 and 20 could swap between the CD faces of different odd-numbered domains, raising the complexity of domain organization even more.

It is intriguing that domains 16–21 house numerous filamin interaction sites but only a few disease-causing filamin mutations have been found in these domains (Table 3). There could be two opposing explanations for this: either these interactions are not that essential for normal human physiology, making the mutations irrelevant; or mutations in these domains cause devastating consequences for normal development, eliminating these mutants at early stages.

8. CONCLUDING REMARKS

This project is a demonstration of the power and versatility of NMR spectroscopy in studies of modular proteins. In order to fully understand the structure, interactions and function of multi-domain proteins, one needs to know the structure of the entire system. Even if it is harder and more time-consuming, protein structure determination projects should turn their focus from isolated single domains to larger systems. This is unlikely to lead to greater success in terms of number of PDB entries, but will certainly provide richer and more informative structural data.

We have used a bottom-up approach to elucidate the architecture of filamin A immunoglobulin-like domains. We started the project by studying single IgFLN domains and their interactions. As a lot of structural data is available on isolated FLN domains, we wanted to move from single domains to larger systems. This approach was successful as we were able to reveal the structures of two novel filamin domain pairs. As a final challenge, we wanted to see the big picture: we used NMR spectroscopy to find out how the three filamin domain pairs arrange themselves into even higher superstructures. This is still work in progress, but it has already provided clues on the structural organization of 60-kDa multi-domain IgFLNa16–21 housing binding sites for several interaction partners of filamins. This study has certainly made clear that filamin immunoglobulin-like domains, like most protein modules, are more than just beads on a string.

"An expert is one who knows
more and more about less and less."

- Nicholas Murray Butler 1862–1947 -

9. REFERENCES

Adams PD, Loh AP, Oswald RE (2004) Backbone dynamics of an oncogenic mutant of Cdc42Hs shows increased flexibility at the nucleotide-binding site. Biochemistry 43:9968–9977

Aguda AH, Sakwe AM, Rask L, Robinson RC (2007) Expression, crystallization and preliminary crystallographic data analysis of filamin A repeats 14–16. Acta Crystallogr F F63:291–293

Alper Ö, Stetler-Stevenson WG, Harris LN, Leitner WW, Özdemirli M, Hartmann D *et al.* (2009) Novel anti-filamin-A antibody detects a secreted variant of filamin-A in plasma from patients with breast carcinoma and high-grade astrocytoma. Cancer Sci 100:1748–1756

Altieri AS, Byrd RA (2004) Automation of NMR structure determination of proteins. Curr Opin Struct Biol 14:547–552

Andrews RK, López JA, Berndt MC (1997) Molecular mechanisms of platelet adhesion and activation. Int J Biochem Cell Biol 29:91–105

Anilkumar G, Rajasekaran SA, Wang S, Hankinson O, Bander NH, Rajasekaran AK (2003) Prostate-specific membrane antigen association with filamin A modulates its internalization and NAALADase activity. Cancer Res 63:2645–2648

Aricescu AR, Jones EY (2007) Immunoglobulin superfamily cell adhesion molecules: zippers and signals. Curr Opin Cell Biol 19:543–550

Armstrong L-J, Heath VL, Sanderson S, Kaur S, Beesley JFJ, Herbert JMJ *et al.* (2008) ECSM2, an endothelial specific filamin A binding protein that mediates chemotaxis. Arterioscler Thromb Vasc Biol 28:1640–1646

Awata H, Huang C, Handlogten ME, Miller RT (2001) Interaction of the calcium-sensing receptor and filamin, a potential scaffolding protein. J Biol Chem 276:34871–34879

Bachmann AS, Howard JP, Vogel C-W (2006) Actin-binding protein filamin A is displayed on the surface of human neuroblastoma cells. Cancer Sci 97:1359–1365

Baldassarre M, Razinia Z, Burande CF, Lamsoul I, Lutz PG, Calderwood DA (2009) Filamins regulate cell spreading and initiation of cell migration. PLoS ONE 4:e7830

Baldus M (2006) Molecular interactions investigated by multi-dimensional solid-state NMR. Curr Opin Struct Biol 16:618–623

Barclay AN (2003) Membrane proteins with immunoglobulin-like domains – A master superfamily of interaction molecules. Semin Immunol 15:215–223

Barends TRM, Dunn MF, Schlichting I (2008) Tryptophan synthase, an allosteric molecular factory. Curr Opin Chem Biol 12:593–600

Bashton M, Chothia C (2007) The generation of new protein functions by the combination of domains. Structure 15:85–99

Batey S, Randles LG, Steward A, Clarke J (2005) Cooperative folding in a multi-domain protein. J Mol Biol 349:1045–1059

Beatham J, Romero R, Townsend SKM, Hacker T, van der Ven PFM, Blanco G (2004) Filamin C interacts with the muscular dystrophy KY protein and is abnormally distributed in mouse KY deficient muscle fibres. Hum Mol Genet 13:2863–2874

Bechtel PJ (1979) Identification of a high molecular weight actin-binding protein in skeletal muscle. J Biol Chem 254:1755–1758

Beekman JM, van der Poel CE, van der Linden JA, van den Berg DLC, van den Berghe PVE, van de Winkel JGJ, Leusen JHW (2008) Filamin A stabilizes FcγRI surface expression and prevents its lysosomal routing. J Immunol 180:3938–3945

Bellanger J-M, Astier C, Sardet C, Ohta Y, Stossel TP Debant A (2000) The Rac1- and RhoG-specific GEF domain of Trio targets filamin to remodel cytoskeletal actin. Nat Cell Biol 2:888–892

Berger S, Braun S (2004) 200 and more NMR experiments: A practical course. Wiley-VCH, Weinheim

Berry FB, O'Neill MA, Coca-Prados M, Walter MA (2005) FOXC1 Transcriptional regulatory activity is impaired by PBX1 in a filamin A-mediated manner. Mol Cell Biol 25:1415–1424

Bertini I, Luchinat C, Parigi G, Pierattelli R (2005) NMR spectroscopy of paramagnetic metalloproteins. ChemBioChem 6:1536–1549

Bertini I, Luchinat C, Parigi G, Pierattelli R (2008) Perspectives in paramagnetic NMR of metalloproteins. Dalton Trans 3782–3790

Bicknell LS, Farrington-Rock C, Shafeghati Y, Rump P, Alanay Y, Alembik Y *et al.* (2007) A molecular and clinical study of Larsen syndrome caused by mutations in FLNB. J Med Genet 44:89–98

Bicknell LS, Morgan T, Bonafé L, Wessels MW, Bialer MG, Willems PJ *et al.* (2005) Mutations in FLNB cause boomerang dysplasia. J Med Genet 42:e43

Blackledge M (2005) Recent progress in the study of biomolecular structure and dynamics in solution from residual dipolar couplings. Prog Nucl Magn Reson Spectrosc 46:23–61

Boehr DD, Dyson HJ, Wright PE (2006) An NMR perspective on enzyme dynamics. Chem Rev 106:3055–3079

Bonvin AMJJ, Boelens R, Kaptein R (2005) NMR analysis of protein interactions. Curr Opin Chem Biol 9:501–508

Bork P, Holm L, Sander C (1994) The immunoglobulin fold: Structural classification, sequence patterns and common core. J Mol Biol 242:309–320

Bouvignies G, Bernadó P, Meier S, Cho K, Grzesiek S, Brüschweiler R, Blackledge M (2005) Identification of slow correlated motions in proteins using residual dipolar and hydrogen-bond scalar couplings. Proc. Natl. Acad. Sci. U. S. A. 102:13885–13890

Bouvignies G, Markwick PRL, Blackledge M (2007) Simultaneous definition of high resolution protein structure and backbone conformational dynamics using NMR residual dipolar couplings. ChemPhysChem 8:1901–1909

Braddock DT, Cai M, Baber JL, Huang Y, Clore GM (2001) Rapid identification of medium- to large-scale interdomain motion in modular proteins using dipolar couplings. J Am Chem Soc 123:8634–8635

Breeze AL (2000) Isotope-filtered NMR methods for the study of biomolecular structure and interactions. Prog Nucl Magn Reson Spectrosc 36:323–372

Brotschi EA, Hartwig JH, Stossel TP (1978) The gelation of actin by actin-binding protein. J Biol Chem 253:8988–8993

Browne KA, Johnstone RW, Jans DA, Trapani JA (2000) Filamin (280-kDa actin-binding protein) is a caspase substrate and is also cleaved directly by the cytotoxic T lymphocyte protease granzyme B during apoptosis. J Biol Chem 275:39262–39266

Brüschweiler R (2003) New approaches to the dynamic interpretation and prediction of NMR relaxation data from proteins. Curr Opin Struct Biol 13:175–183

Bröcker F, Bardenheuer W, Vieten L, Jülicher K, Werner N, Marquitan G *et al.* (1999) Assignment of human filamin gene FLNB to human chromosome band 3p14.3 and identification of YACs containing the complete FLNB transcribed region. Cytogenet Cell Genet 85:267–268

Caetano-Anollés G, Wang M, Caetano-Anollés D, Mittenthal JE (2009) The origin, evolution and structure of the protein world. Biochem J 417:621–637

Calderwood DA, Huttenlocher A, Kiosses WB, Rose DM, Woodside DG, Schwartz MA, Ginsberg MH (2001) Increased filamin binding to β-integrin cytoplasmic domains inhibits cell migration. Nat Cell Biol 3:1060–1068

Case DA, Darden TA, Cheatham TE, Simmerling CL, Wang J, Duke RE *et al.* (2004) AMBER 8. University of California, San Francisco, CA

Cavalli A, Salvatella X, Dobson CM, Vendruscolo M (2007) Protein structure determination from NMR chemical shifts. Proc Natl Acad Sci U S A 104:9615–9620

Cavanagh J, Fairbrother WJ, Palmer AG, Rance M, Skelton NJ (2007) Protein NMR spectroscopy: principles and practice, 2nd ed., Elsevier Academic Press, London

Chayen NE, Saridakis E (2008) Protein crystallization: from purified protein to diffraction-quality crystal. Nat Methods 5:147–153

Chen M, Stracher A (1989) In situ phosphorylation of platelet actin-binding protein by cAMP-dependent protein kinase stabilizes it against proteolysis by calpain. J Biol Chem 264:14282–14289

Chiang W, Greaser ML, Lyons G (2000) Filamin isogene expression during mouse myogenesis. Dev Dyn 217:99–108

Cho E-Y, Cho D-I, Park JH, Kurose H, Caron MG, Kim K-M (2007) Roles of protein kinase C and actin-binding protein 280 in the regulation of intracellular trafficking of dopamine D_3 receptor. Mol Endocrinol 21:2242–2254

Chothia C, Gelfand I, Kister A (1998) Structural determinants in the sequences of immunoglobulin variable domain. J Mol Biol 278:457–479

Chothia C, Lesk AM (1986) The relation between the divergence of sequence and structure in proteins. EMBO J 5:823–826

Civelli O, Bunzow JR, Grandy DK (1993) Molecular diversity of the dopamine receptors. Annu Rev Pharmacol Toxicol 32:281–307

Clark AR, Sawyer GM, Robertson SP, Sutherland-Smith AJ (2009) Skeletal dysplasias due to filamin A mutations result from a gain-of-function mechanism distinct from allelic neurological disorders. Hum Mol Genet, in press

Clore GM (2000) Accurate and rapid docking of protein-protein complexes on the basis of intermolecular nuclear Overhauser enhancement data and dipolar couplings by rigid body minimization. Proc Natl Acad Sci U S A 97:9021–9025

Clore GM, Schwieters CD (2003) Docking of protein-protein complexes on the basis of highly ambiguous intermolecular distance restraints derived from $^{1}HN/^{15}N$ chemical shift mapping and backbone ^{15}N-^{1}H residual dipolar couplings using conjoined rigid body/torsion angle dynamics. J Am Chem Soc 125:2902–2912

Clore GM, Tang C, Iwahara J (2007) Elucidating transient macromolecular interactions using paramagnetic relaxation enhancement. Curr Opin Struct Biol 17:603–616

Cordier F, Grzesiek S (1999) Direct observation of hydrogen bonds in proteins by interresidue $^{3h}J_{NC'}$ scalar couplings. J Am Chem Soc 121:1601–1602

Cornilescu G, Delaglio F, Bax A (1999) Protein backbone angle restraints from searching a database for chemical shift and sequence homology. J Biomol NMR 13:289–302

Cornilescu G, Marquardt JL, Ottiger M, Bax A (1998) Validation of protein structure from anisotropic carbonyl chemical shifts in a dilute liquid crystalline phase. J Am Chem Soc 120:6836–6837

Cranmer SL, Pikovski I, Mangin P, Thompson PE, Domagala T, Frazzetto M, Salem HH, Jackson SP (2005) Identification of a unique filamin A binding region within the cytoplasmic domain of glycoprotein Ibα. Biochem J 387:849–858

Cuff AL, Sillitoe I, Lewis T, Redfern OC, Garratt R, Thornton J, Orengo CA (2009) The CATH classification revisited – Architectures reviewed and new ways to characterize structural divergence in superfamilies. Nucleic Acids Res 37:D310–314

Cukier IH, Li Y, Lee JM (2007) Cyclin B1/Cdk1 binds and phosphorylates Filamin A and regulates its ability to cross-link actin. FEBS Lett 581:1661–1672

Cunningham CC, Gorlin JB, Kwiatkowski DJ, Hartwig JH, Janmey PA, Byers HR, Stossel TP (1992) Actin-binding protein requirement for cortical stability and efficient locomotion. Science 255:325–327

Dalkilic I, Schienda J, Thompson TG, Kunkel LM (2006) Loss of filamin C (FLNc) results in severe defects in myogenesis and myotube structure. Mol Cell Biol 26:6522–6534

Dalvit C, Fasolini M, Flocco M, Knapp S, Pevarello P, Veronesi M (2002a) NMR-based screening with competition water-ligand observed via gradient spectroscopy experiments: Detection of high-affinity ligands. J Med Chem 45:2610–2614

Dalvit C, Flocco M, Knapp S, Mostardini M, Perego R, Stockman BJ, Veronesi M, Varasi M (2002b) High-throughput NMR-based screening with competition binding experiments. J Am Chem Soc 124:7702–7709

Dalvit C, Fogliatto G, Stewart A, Veronesi M, Stockman B (2001) WaterLOGSY as a method for primary NMR screening: Practical aspects and range of applicability. J Biomol NMR 21:349–359

Dalvit C, Pevarello P, Tatò M, Veronesi M, Vulpetti A, Sundström M (2000) Identification of compounds with binding affinity to proteins via magnetization transfer from bulk water. J Biomol NMR 18:65–68

Davies PJA, Wallach D, Willingham MC, Pastan I (1978) Filamin-actin interaction: Dissociation of binding from gelation by Ca^{2+}-activated proteolysis. J Biol Chem 253:4036–4042

DeLano WL (2002) The PyMOL molecular graphics system. DeLano Scientific, Palo Alto, CA, USA

Dempsey CE (2001) Hydrogen exchange in peptides and proteins using NMR spectroscopy. Prog Nucl Magn Reson Spectrosc 39:135–170

Deschamps M, Campbell ID, Boyd J (2005) Residual dipolar couplings and some specific models for motional averaging. J Magn Reson 172:118–132

Dobbs MB, Boehm S, Grange DK, Gurnett CA (2008) Congenital knee dislocation in a patient with Larsen syndrome and a novel filamin B mutation. Clin Orthop Relat Res 466:1503–1509

Dominguez C, Boelens R, Bonvin AM (2003) HADDOCK: A protein-protein docking approach based on biochemical or biophysical information. J Am Chem Soc 125:1731–1737

Donald BR, Martin J (2009) Automated NMR assignment and protein structure determination using sparse dipolar coupling constraints. Prog Nucl Magn Reson Spectrosc 55:101–127

Donaldson JC, Dise RS, Ritchie MD, Hanks SK (2002) Nephrocystin-conserved domains involved in targeting to epithelial cell-cell junctions, interaction with filamins, and establishing cell polarity. J Biol Chem 277:29028–29035

dos Remedios CG, Chhabra D, Kekic M, Dedova IV, Tsubakihara M, Berry DA, Nosworthy NJ (2003) Actin binding proteins: Regulation of cytoskeletal microfilaments. Physiol Rev 83:433–473

dos Remedios CG, Thomas DD (Eds.) (2001) Molecular interactions of actin: Actin structure and actin-binding proteins. Springer-Verlag, Heidelberg

Dosset P, Hus J-C, Marion D, Blackledge M (2001) A novel interactive tool for rigid-body modeling of multi-domain macromolecules using residual dipolar couplings. J Biomol NMR 20:223–231

Downing AK (Ed.) (2004) Protein NMR Techniques, 2nd ed., Humana Press Inc, Totowa

Drenth J (Ed.) (2007) Principles of protein X-ray crystallography, 3rd ed. Springer Science+Business Media, LCC, New York

Du X (2007) Signaling and regulation of the platelet glycoprotein Ib-IX-V complex. Curr Opin Hematol 14:262–269

Dyson HJ, Wright PE (2004) Unfolded proteins and protein folding studied by NMR. Chem Rev 104:3607–3622

Dyson JM, O'Malley CJ, Becanovic J, Munday AD, Berndt MC, Coghill ID *et al.* (2001) The SH2-containing inositol polyphosphate 5-phosphatase, SHIP-2, binds filamin and regulates submembraneous actin. J Cell Biol 155:1065–1079

Dötsch V (2008) Investigation of proteins in living bacteria with in-cell NMR experiments. Top Curr Chem 273:203–229

Edman P (1950) Method for determination of the amino acid sequence in peptides. Acta Chem Scand 4:283–293

Enz R (2002) The actin-binding protein Filamin-A interacts with the metabotropic glutamate receptor type 7. FEBS Lett 514:184–188

Farrington-Rock C, Firestein MH, Bicknell LS, Superti-Furga A, Bacino CA, Cormier-Daire V *et al.* (2006) Mutations in two regions of FLNB result in atelosteogenesis I and III. Hum Mutat 27:705–710

Farrington-Rock C, Kirilova V, Dillard-Telm L, Borowsky AD, Chalk S, Rock MJ, Cohn DH, Krakow D (2008) Disruption of the *Flnb* gene in mice phenocopies the human disease spondylocarpotarsal synostosis syndrome. Hum Mol Genet 17:631–641

Farrow NA, Muhandiram R, Singer AU, Pascal SM, Kay CM, Gish G, Shoelson SE, Pawson T, Forman-Kay JD, Kay LE (1994) Backbone dynamics of a free and a phosphopeptide-complexed Src homology 2 domain studied by ^{15}N NMR relaxation. Biochemistry 33:5984–6003

Faulkner G, Pallavicini A, Comelli A, Salamon M, Bortoletto G, Ievolella C *et al.* (2000) FATZ, a filamin-, actinin-, and telethonin-binding protein of the Z-disc of skeletal muscle. J Biol Chem 275:41234–41242

Feng S, Lu X, Kroll MH (2005) Filamin A binding stabilizes nascent glycoprotein Ibα trafficking and thereby enhances its surface expression. J Biol Chem 280:6709–6715

Feng S, Reséndiz JC, Lu X, Kroll MH (2003) Filamin A binding to the cytoplasmic tail of glycoprotein Ibα regulates von Willebrand factor-induced platelet activation. Blood 102:2122–2129

Feng Y, Chen MH, Moskowitz IP, Mendonza AM, Vidali L, Nakamura F, Kwiatkowski DJ, Walsh CA (2006) Filamin A (FLNA) is required for cell-cell contact in vascular development and cardiac morphogenesis. Proc Natl Acad Sci U S A 103:19836–19841

Feng Y, Walsh CA (2004) The many faces of filamin: A versatile molecular scaffold for cell motility and signalling. Nat Cell Biol 6:1034–1038

Fernández C, Wider G (2003) TROSY in NMR studies of the structure and function of large biological macromolecules. Curr Opin Struct Biol 13:570–580

Ferrer JM, Lee H, Chen J, Pelz B, Nakamura F, Kamm RD, Land MJ (2008) Measuring molecular rupture forces between single actin filaments and actin-binding proteins. Proc Natl Acad Sci U S A 105:9221–9226

Fields S, Song O (1989) A novel genetic system to detect protein-protein interactions. Nature 340:245–246

Findlay JB, Geisow MJ (Eds.) (1989) Protein sequencing: A practical approach. Oxford University Press, New York

Fischer MWF, Losonczi JA, Weaver JL, Prestegard JH (1999) Domain orientation and dynamics in multidomain proteins from residual dipolar couplings. Biochemistry 38:9013–9022

Fitter J (2009) The perspectives of studying multi-domain protein folding. Cell Mol Life Sci 66:1672–1681

Flanagan LA, Chou J, Falet H, Neujahr R, Hartwig JH, Stossel TP (2001) Filamin A, the Arp2/3 complex, and the morphology and function of cortical actin filaments in human melanoma cells. J Cell Biol 155:511–517

Foster MP, McElroy CA, Amero CD (2007) Solution NMR of large molecules and assemblies. Biochemistry 46:331–340

Fox JEB (1985) Identification of actin-binding protein as the protein linking the membrane skeleton to glycoproteins on platelet plasma membranes. J Biol Chem 260:11970–11977

Fox JW, Lamperti ED, Eksioglu YZ, Hong SE, Feng Y, Graham DA *et al.* (1998) Mutations in filamin 1 prevent migration of cerebral cortical neurons in human periventricular heterotopia. Neuron 21:1315–1325

Frey N, Olson EN (2002) Calsarcin-3, a novel skeletal muscle-specific member of the calsarcin family, interacts with multiple Z-disc proteins. J Biol Chem 277:13998–14004

Fucini P, Renner C, Herberhold C, Noegel AA, Holak TA (1997) The repeating segments of the F-actin cross-linking gelation factor (ABP-120) have an immunoglobulin-like fold. Nat Struct Biol 4:223–230

Furuike S, Ito T, Yamazaki M (2001) Mechanical unfolding of single filamin A (ABP-280) molecules detected by atomic force microscopy. FEBS Lett 498:72–75

Fushman D, Varadan R, Assfalg M, Walker O (2004) Determining domain orientation in macromolecules by using spin-relaxation and residual dipolar coupling measurements. Prog Nucl Magn Reson Spectrosc 44:189–214

Gabel F, Simon B, Nilges M, Petoukhov M, Svergun D, Sattler M (2008) A structure refinement protocol combining NMR residual dipolar couplings and small angle scattering restraints. J Biomol NMR 41:199–208

García E, Stracher A, Jay D (2006) Calcineurin dephosphorylates the C-terminal region of filamin in an important regulatory site: A possible mechanism for filamin mobilization and cell signaling. Arch Biochem Biophys 446:140–150

Gardel ML, Nakamura F, Hartwig JH, Crocker JC, Stossel TP, Weitz DA (2006) Prestressed F-actin networks cross-linked by hinged filamins replicate mechanical properties of cells. Proc Natl Acad Sci U S A 103:1762–1767

Gariboldi M, Maestrini E, Canzian F, Manenti G, De Gregorio L, Rivella S *et al.* (1994) Comparative mapping of the actin-binding protein 280 denes in human and mouse. Genomics 21:428–430

Gáspári Z, Pál G, Perczel A (2008) A redesigned genetic code for selective labeling in protein NMR. BioEssays 30:772–780

Gelfand IM, Chothia C, Kister AE (2007) Immunoglobulin fold: Structures of proteins in the immunoglobulin superfamily. In Cox MM, Phillips JG (Eds.) Handbook of proteins, John Wiley & Sons Ltd, Chichester, pp. 51–57

Gérard-Blanluet M, Sheen V, Machinis K, Neal J, Apse K, Danan C *et al.* (2006) Bilateral periventricular heterotopias in an X-linked dominant transmission in a family with two affected males. Am J Med Genet A 140A:1041–1046

Gerstein M, Lesk AM, Chothia C (1994) Structural mechanisms for domain movements in proteins. Biochemistry 33:6739–6749

Glogauer M, Arora P, Chou D, Janmey PA, Downey GP, McCulloch CAG (1998) The role of actin-binding protein 280 in integrin-dependent mechanoprotection. J Biol Chem 273:1689–1698

Goddard TD, Kneller DG (2004) SPARKY 3. University of California, San Francisco, USA

Goldmann WH (2001) Phosphorylation of filamin (ABP-280) regulates the binding to the lipid membrane, integrin, and actin. Cell Biol Int 25:805–808

Goldmann WH, Tempel M, Sprenger I, Isenberg G, Ezzell RM (1997) Viscoelasticity of actin-gelsolin networks in the presence of filamin. Eur J Biochem 246:373–379

Gómez-Garre P, Seijo M, Gutiérrez-Dalicado E, Castro del Río M, de la Torre C, Gómez-Abad C *et al.* (2006) Ehlers-Danlos syndrome and periventricular nodular heterotopia in a Spanish family with a single FLNA mutation. J Med Genet 43:232–237

Gontier Y, Taivainen A, Fontao L, Sonnenberg A, van der Flier A, Carpén O, Faulkner G, Borradori L (2005) The Z-disc proteins myotilin and FATZ-1 interact with each other and are connected to the sarcolemma via muscle-specific filamins. J Cell Sci 118:3739–3749

Gorlin JB, Yamin R, Egan S, Stewart M, Stossel TP, Kwiatkowski DJ, Hartwig JH (1990) Human endothelial actin-binding protein (ABP-280, nonmuscle filamin): A molecular leaf spring. J Cell Biol 111:1089–1105

Gravante B, Burbuti A, Milanesi R, Zappi I, Viscomi C, DiFrancesco D (2004) Interaction of the pacemaker channel HCN1 with filamin A. J Biol Chem 279:43847–43853

Grimbert P, Valanciute A, Audard V, Lang P, Guellaën G, Sahali, D (2004) The filamin-A is a partner of Tc-mip, a new adapter protein involved in c-maf-dependent Th2 signaling pathway. Mol Immunol 40:1257–1261

Grishaev A, Tugarinov V, Kay LE, Trewhella J, Bax A (2008) Refined solution structure of the 82-kDa enzyme malate synthase G from joint NMR and synchrotron SAXS restraints. J Biomol NMR 40:95–106

Grishaev A, Wu J, Trewhella J, Bax A (2005) Refinement of multidomain protein structures by combination of solution small-angle X-ray scattering and NMR data. J Am Chem Soc 127:16621–16628

Gronwald W, Kalbitzer HR (2004) Automated structure determination of proteins by NMR spectroscopy. Prog Nucl Magn Reson Spectrosc 44:33–96

Grzesiek S, Sass H-J (2009) From biomolecular structure to functional understanding: New NMR developments narrow the gap. Curr Opin Struct Biol 19:585–595

Guerrini R, Mei D, Sisodiya S, Sicca F, Harding B, Takahashi Y *et al.* (2004) Germline and mosaic mutations of FLN1 in men with periventricular heterotopia. Neurology 63:51–56

Guyon JR, Kudryashova E, Potts A, Dalkilic I, Brosius M, Thompson TG *et al.* (2003) Calpain 3 cleaves filamin C and regulates its ability to interact with γ- and δ-sarcoglycans. Muscle Nerve 28:472–283

Güntert P (2004) Automated NMR structure calculation with CYANA. In Downing AK (Ed.) Protein NMR techniques, 2nd ed., Humana Press Inc, Totowa, pp. 353–378

Güntert P (2009) Automated structure determination from NMR spectra. Eur Biophys J 38:129–143

Habeck M, Rieping W, Linge JP, Nilges M (2004) NOE assignment with ARIA 2.0: The nuts and bolts. In Downing AK (Ed.) Protein NMR techniques, 2nd ed., Humana Press Inc, Totowa, pp. 379–402

Hadley C, Jones DT (1999) A systematic comparison of protein structure classifications: SCOP, CATH and FSSP. Structure 7:1099–1112

Hajduk PJ, Mack JC, Olejniczak ET, Park C, Dandliker PJ, Beutel BA (2004) SOS-NMR: A saturation transfer NMR-based method for determining the structures of protein-ligand complexes. J Am Chem Soc 126:2390–2398

Hajduk PJ, Olejniczak ET, Fesik SW (1997) One-dimensional relaxation- and diffusion-edited NMR methods for screening compounds that bind to macromolecules. J Am Chem Soc 119:12257–12261

Halaby DM, Mornon JPE (1998) The immunoglobulin superfamily: An insight on its tissular, species, and functional diversity. J Mol Evol 46:389–400

Halaby DM, Poupon A, Mornon J-P (1999) The immunoglobulin fold family: sequence analysis and 3D structure comparisons. Protein Eng 12:563–571

Han J-H, Batey S, Nickson AA, Teichmann SA, Clarke J (2007) The folding and evolution of multidomain proteins. Nat Rev Mol Cell Biol 8:319–330

Hansen MR, Mueller L, Pardi A (1998) Tunable alignment of macromolecules by filamentous phage yields dipolar coupling interactions. Nat Struct Biol 5:1065–1074

Hart AW, Morgan JE, Schneider J, West K, McKie L, Bhattacharya S, Jackson IJ, Cross SH (2006) Cardiac malformations and midline skeletal defects in mice lacking filamin A. Hum Mol Genet 15:2457–2467

Hartwig JH, Shevlin P (1986) The architecture of actin filaments and the ultrastructural location of actin-binding protein in the periphery of lung macrophages. J Cell Biol 103:1007–1020

Hartwig JH, Stossel TP (1975) Isolation and properties of actin, myosin, and a new actin-binding protein in rabbit alveolar macrophages. J Biol Chem 250:5696–5705

Hartwig JH, Stossel TP (1981) Structure of macrophage actin-binding protein molecules in solution and interacting with actin filaments. J Mol Biol 145:563–581

Hartwig JH, Tyler J, Stossel TP (1980) Actin-binding protein promotes the bipolar and perpendicular branching of actin filaments. J Cell Biol 87:841–848

Hasegawa H, Holm L (2009) Advances and pitfalls of protein structural alignment. Curr Opin Struct Biol 19:341–348

Hawkins AR, Lamb HK (1995) The molecular biology of multidomain proteins. Eur J Biochem 232:7–18

Hayashi K, Altman A (2006) Filamin A is required for T cell activation mediated by protein kinase C-θ. J Immunol 177:1721–1728

He H-J, Kole S, Kwon Y-K, Crow MT, Bernier M (2003) Interaction of filamin A with the insulin receptor alters insulin-dependent activation of the mitogen-activated protein kinase pathway. J Biol Chem 278:27096–27104

He X, Li Y, Schembri-King J, Jakes S, Hayashi J (2000) Identification of actin binding protein, ABP-280, as a binding partner of human Lnk adaptor protein. Mol Immunol 37:603–612

Hehr U, Hehr A, Uyanik G, Phelan E, Winkler J, Reardon W (2006) A filamin A splice mutation resulting in a syndrome of facial dysmorphism, periventricular nodular heterotopia, and severe constipation reminiscent of cerebro-fronto-facial syndrome. J Med Genet 43:541–544

Hemmingsen JM, Gernert KM, Richardson JS, Richardson DC (1994) The tyrosine corner: A feature of most Greek key β-barrel proteins. Protein Sci 3:1927–1937

Henzler-Wildman KA, Lei M, Thai V, Kerns SJ, Karplus M, Kern D (2007) A hierarchy of timescales in protein dynamics is linked to enzyme catalysis. Nature 450:913–916

Herrmann T, Güntert P, Wüthrich K (2002) Protein NMR structure determination with automated NOE assignment using the new software CANDID and the torsion angle dynamics algorithm DYANA. J Mol Biol 319:209–227

Heuzé ML, Lamsoul I, Baldassarre M, Lad Y, Lévêque S, Razinia Z *et al.* (2008) ASB2 targets filamins A and B to proteasomal degradation. Blood 112:5130–5140

Hidalgo-Bravo A, Pompa-Mera EN, Kofman-Alfaro S, Gonzalez-Bonilla CR, Zenteno JC (2005) A novel filamin A D203Y mutation in a female patient with otopalatodigital type 1 syndrome and extremely skewed X chromosome inactivation. Am J Med Genet A 136A:190–193

Hiller S, Wagner G (2009) The role of solution NMR in the structure determinations of VDAC-1 and other membrane proteins. Curr Opin Struct Biol 19:1–6

Himmel M, van der Ven PFM, Stöcklein W, Fürst DO (2003) The limits of promiscuity: Isoform-specific dimerization of filamins. Biochemistry 42:430–439

Hjälm G, MacLeod RJ, Kifor O, Chattopadhyay N, Brown EM (2001) Filamin-A binds to the carboxyl-terminal tail of the calcium-sensing receptor, an interaction that participates in CaR-mediated activation of mitogen-activated protein kinase. J Biol Chem 276:34880–34887

Holland TA, Veretnik S, Shindyalov IN, Bourne PE (2006) Partitioning protein structures into domains: Why is it so difficult? J Mol Biol 361:562–590

Holm L, Sander C (1998) Dictionary of recurrent domains in protein structures. Proteins 33:88–96

Hooft RW, Vriend G, Sander C, Abola EE (1996) Errors in protein structures. Nature 381:272

Hsu S-TD, Fucini P, Cabrita LD, Launay H, Dobson CM, Christodoulou J (2007) Structure and dynamics of a ribosome-bound nascent chain by NMR spectroscopy. Proc Natl Acad Sci U S A 104:16516–16521

Hu W, Wang L (2006) Residual dipolar couplings: Measurements and applications to biomolecular studies. Annual Reports on NMR Spectroscopy 58:231–304

Huang C-J, Chen Y-H, Ting L-P (2000) Hepatitis B virus core protein interacts with the C-terminal region of actin-binding protein. J Biomed Sci 7:160–168

Hynes RO (2002) Integrins: Bidirectional, allosteric signaling machines. Cell 110:673–687

Igumenova TI, Frederick KK, Wand AJ (2006) Characterization of the fast dynamics of protein amino acid side chains using NMR relaxation in solution. Chem Rev 106:1672–1699

Inomata K, Ohno A, Tochio H, Isogai S, Tenno T, Nakase I *et al.* (2009) High-resolution multi-dimensional NMR spectroscopy of proteins in human cells. Nature 458:106–109

Ithychanda SS, Das M, Ma Y-Q, Ding K, Wang X, Gupta S *et al.* (2009a) Migfilin, a molecular switch in regulation of integrin activation. J Biol Chem 284:4713–4722

Ithychanda SS, Hsu D, Li H, Yan L, Liu D, Das M, Plow EF, Qin J (2009b) Identification and characterization of multiple similar ligand binding repeats in filamin: implication on filamin-mediated receptor clustering and cross-talk. J Biol Chem, in press.

Iwai H, Züger S (2007) Protein ligation: Applications in NMR studies of proteins. Biotechnol Genet Eng Rev 24:129–146

Jahnke W, Perez LB, Paris CG, Strauss A, Fendrich G, Nalin CM (2000) Second-site NMR screening with a spin-labeled first ligand. J Am Chem Soc 122:7394–7395

Jahnke W, Rüdisser S, Zurini M (2001) Spin label enhanced NMR screening. J Am Chem Soc 123:3149–3150

Jarymowycz VA, Stone MJ (2006) Fast time scale dynamics of protein backbones: NMR relaxation methods, applications, and functional consequences. Chem Rev 106:1624–1671

Jay D, García EJ, de la Luz Ibarra M (2004) In situ determination of a PKA phosphorylation site in the C-terminal region of filamin. Mol Cell Biochem 260:49–53

Jay D, García EJ, Lara JE, Medina MA, de la Luz Ibarra M (2000) Determination of a cAMP-dependent protein kinase phosphorylation site in the C-terminal region of human endothelial actin-binding protein. Arch Biochem Biophys 377:80–84

Jeon YJ, Choi JS, Lee JY, Yu KR, Ka SH, Cho Y *et al.* (2008) Filamin B serves as a molecular scaffold for type I interferon-induced c-Jun NH_2-terminal kinase signaling pathway. Mol Biol Cell 19:5116–5130

Jiang P, Campbell ID (2008) Integrin binding immunoglobulin type filamin domains have variable stability. Biochemistry 47:11055–11061

Jiménez-Baranda S, Gómez-Moutón C, Rojas A, Martínez-Prats L, Mira E, Lacalle RA *et al.* (2007) Filamin-A regulates actin-dependent clustering of HIV receptors. Nat Cell Biol 9:838–846

Johansen LD, Naumanen T, Knudsen A, Westerlund N, Gromova I, Junttila M *et al.* (2008) IKAP localizes to membrane ruffles with filamin A and regulates actin cytoskeleton organization and cell migration. J Cell Sci 121:854–864

Johnson CP, Tang H-Y, Carag C, Speicher DW, Discher DE (2007) Forced unfolding of proteins within cells. Science 317:663–666

Jonic S, Vénien-Bryan C (2009) Protein structure determination by electron cryo-microscopy. Curr Opin Pharmacol 9:1–7

Kainulainen T, Pender A, D'Addario M, Feng Y, Lekic P, McCulloch A (2002) Cell death and mechanoprotection by filamin A in connective tissues after challenge by applied tensile forces. J Biol Chem 277:21998–22009

Kanters E, van Rijssel J, Hensbergen PJ, Hondius D, Mul FPJ, Deelder AM *et al.* (2008) Filamin B mediates ICAM-1-driven leukocyte transendothelial migration. J Biol Chem 283:31830–31839

Kern D, Zuiderweg ERP (2003) The role of dynamics in allosteric regulation. Curr Opin Struct Biol 13:748–757

Keskin O, Gursoy A, Ma B, Nussinov R (2008) Principles of protein-protein interactions: What are the preferred ways for proteins to interact? Chem Rev 108:1225–1244

Kesner BA, Ding F, Temple BR, Dokholyan NV (2009a) N-terminal strands of filamin Ig domains act as a conformational switch under biological forces. Proteins, in press

Kesner BA, Milgram SL, Temple BR, Dokholyan NV (2009b) Isoform divergence of the filamin family of proteins. Mol Biol Evol, in press

Khurana S (2006) Aspects of the cytoskeleton. Elsevier, San Diego

Kiema T, Lad Y, Jiang P, Oxley CL, Baldassarre M, Wegener KL *et al.* (2006) The molecular basis of filamin binding to integrins and competition with talin. Mol Cell 21:337–347

Kim C, Cho Y, Kang C-H, Kim MG, Lee H, Cho E-G, Park D (2005a) Filamin is essential for shedding of the transmembrane serine protease, epithin. EMBO Rep 6:1045–1051

Kim E-J, Park J-S, Um S-J (2007b) Filamin A negatively regulates the transcriptional activity of p73a in the cytoplasm. Biochem Biophys Res Commun 362:1101–1106

Kim EY, Ridgway LD, Dryer SE (2007a) Interactions with filamin A stimulate surface expression of large-conductance Ca^{2+}-activated K^{+} channels in the absence of direct actin binding. Mol Pharmacol 72:622–630

Kim H, Nakamura F, Lee W, Shifrin Y, Arora P, McCulloch CA (2009) Filamin A is required for vimentin-mediated cell adhesion and spreading. Am J Physiol Cell Physiol, in press

Kim H, Sengupta A, Glogauer M, McCulloch CA (2008) Filamin A regulates cell spreading and survival via β1 integrins. Exp Cell Res 314:834–846

Kim K-M, Gainetdinov RR, Laporte SA, Caron MG, Barak LS (2005b) G protein-coupled receptor kinase regulates dopamine D_3 receptor signaling by modulating the stability of a receptor-filamin-β-arrestin complex. J Biol Chem 280:12774–12780

Kirschner K, Bisswanger H (1976) Multifunctional proteins. Annu Rev Biochem 45:143–166

Klaile E, Müller MM, Kannicht C, Singer BB, Lucka L (2005) CEACAM1 functionally interacts with filamin A and exerts a dual role in the regulation of cell migration. J Cell Sci 118:5513–5524

Kley RA, Hellenbroich Y, van der Ven PFM, Fürst DO, Huebner A, Bruchertseifer B *et al.* (2007) Clinical and morphological phenotype of the filamin myopathy: a study of 31 German patients. Brain 130:3250–3264

Kolahi KS, Mofrad MRK (2008) Molecular mechanics of filamin's rod domain. Biophys J 94:1075–1083

Konrat R, Yang D, Kay LE (1999) A 4D TROSY-based pulse scheme for correlating $^{1}HN_i$,$^{15}N_i$,$^{13}C^{\alpha}$, $^{13}C'_{i-1}$ chemical shifts in high molecular weight, ^{15}N,^{13}C,^{2}H labeled proteins. J Biomol NMR 15:309–313

Kontaxis G, Clore MG, Bax A (2000) Evaluation of cross-correlation effects and measurement of one-bond couplings in proteins with short transverse relaxation times. J Magn Reson 143:184–196

Koradi R, Billeter M, Wüthrich K (1996) MOLMOL: A program for display and analysis of macromolecular structures. J Mol Graph 14:51–55

Koskela H, Kilpeläinen I, Heikkinen S (2004) Evaluation of protein ^{15}N relaxation times by inverse Laplace transformation. Magn Reson Chem 42:61–65

Koteliansky VE, Clukhova MA, Gneushev GN, Samuel J-L, Rappaport L (1986) Isolation and localization of filamin in heart muscle. Eur. J. Biochem 156:619–623

Koteliansky VE, Glukhova MA, Shirihsky VP, Babaev VR, Kandalenko VF, Rukosuev VS, Smirnov VN (1981a) Identification of a filamin-like protein in chicken heart muscle. FEBS Lett 125:44–48

Koteliansky VE, Shirinsky VP, Gneushev GN, Smirnov VN (1981b) Filamin, a high relative molecular mass actin-binding protein from smooth muscles, promotes actin polymerization. FEBS Lett 136:98–100

Krakow D, Robertson SP, King LM, Morgan T, Sebald ET, Bertolotto C *et al.* (2004) Mutations in the gene encoding filamin B disrupt vertebral segmentation, joint formation and skeletogenesis. Nature Genet 36:405–410

Krief S, Faivre J-F, Robert P, Le Douarin B, Brument-Larignon N, Lefrère I *et al.* (1999) Identification and characterization of cvHsp. J Biol Chem 274:36592–36600

Kyndt F, Gueffet J-P, Probst V, Jaafar P, Legendre A, Le Bouffant F *et al.* (2007) Mutations in the gene encoding filamin A as a cause for familial cardiac valvular dystrophy. Circulation 115:40–49

Kyte J (2007) Structure in protein chemistry, 2nd ed., Garland Science, New York

Labeit S, Kolmerer B (1995) Titins: Giant proteins in charge of muscle ultrastructure and elasticity. Science 270:293–296

Labeit S, Lahmers S, Burkart C, Fong C, McNabb M, Witt S *et al.* (2006) Expression of distinct classes of titin isoforms in striated and smooth muscles by alternative splicing, and their conserved interaction with filamins. J Mol Biol 362:664–681

Lad Y, Jiang P, Ruskamo S, Harburger DS, Ylänne J, Campbell ID, Calderwood DA (2008) Structural basis of the migfilin-filamin interaction and competition with integrin β tails. J Biol Chem 283:35154–35163

Lad Y, Kiema T, Jiang P, Pentikäinen OT, Coles CH, Campbell ID, Calderwood DA, Ylänne J (2007) Structure of three tandem filamin domains reveals auto-inhibition of ligand binding. EMBO J 26:3993–4004

Larkin MA, Blackshields G, Brown NP, Chenna R, McGettigan PA, McWilliam H *et al.* (2007) Clustal W and Clustal X version 2.0. Bioinformatics 23:2947–2948

Laskowski RA, Rullmann JAC, MacArthur MW, Kaptein R, Thornton JM (1996) AQUA and PROCHECK-NMR: Programs for checking the quality of protein structures solved by NMR. J Biomol NMR 8:477–486

Lebart M-C, Méjean C, Casanova D, Audemard E, Derancourt J, Roustan C, Benyamin Y (1994) Characterization of the actin binding site on smooth muscle filamin. J Biol Chem 269:4279–4284

Legate KR, Fässler R (2009) Mechanisms that regulate adaptor binding to β-integrin cytoplasmic tails. J Cell Sci 122:187–198

Lehman W, Craig R, Kendrick-Jones J, Sutherland-Smith AJ (2004) An open or closed case for the conformation of calponin homology domains on F-actin? J Muscle Res Cell Motil 25:351–358

Lehtonen JV, Still DJ, Rantanen VV, Ekholm J, Björklund D, Iftikhar Z *et al.* (2004) BODIL: A molecular modeling environment for structure-function analysis and drug design. J Comput Aided Mol Des 18:401–419

Leonardi A, Ellinger-Ziegelbauer H, Franzoso G, Brown K, Siebenlist U (2000) Physical and functional interaction of filamin (actin-binding protein-280) and tumor necrosis factor receptor-associated factor 2. J Biol Chem 275:271–278

Lepre CA, Moore JM, Peng JW (2004) Theory and applications of NMR-based screening in pharmaceutical research. Chem Rev 104:3641–3676

Levitt M (2009) Nature of the protein universe. Proc Natl Acad Sci U S A 106:11079–11084

Li C, Yu S, Nakamura F, Yin S, Xu J, Petrolla AA *et al.* (2009) Binding of pro-prion to filamin A disrupts cytoskeleton and correlates with poor prognosis in pancreatic cancer. J Clin Invest 119:2725–2736

Li M, Bermak JC, Wang ZW, Zhou QY (2000) Modulation of dopamine D_2 receptor signaling by actin-binding protein (ABP-280). Mol Pharmacol 57:446–452

Lin R, Canfield V, Levenson R (2002) Dominant negative mutants of filamin A block cell surface expression of the D2 dopamine receptor. Pharmacology 66:173–181

Lin R, Karpa K, Kabbani N, Goldman-Rakic P, Levenson R (2001) Dopamine D2 and D3 receptors are linked to the actin cytoskeleton via interaction with filamin A. Proc Natl Acad Sci U S A 98:5258–5263

Linge JP, Williams MA, Spronk CAEM, Bonvin AMJJ, Nilges M (2003) Refinement of protein structures in explicit solvent. Proteins 50:496–506

Lipsitz RS, Tjandra N (2004) Residual dipolar couplings in NMR structure analysis. Annu Rev Biophys Biomolec Struct 33:387–413

Liu G, Thomas L, Warren RA, Enns CA, Cunningham CC, Hartwig JH, Thomas G (1997) Cytoskeletal protein ABP-280 directs the intracellular trafficking of furin and modulates proprotein processing in the endocytic pathway. J Cell Biol 139:1719–1733

Lo SH (2006) Focal adhesions: what's new inside. Dev Biol 294:280–291

Loo DT, Kanner SB, Aruffo A (1998) Filamin binds to the cytoplasmic domain of the β_1-integrin. J Biol Chem 273:23304–23312

López JA, Andrews RK, Afshar-Kharghan V, Berndt MC (1998) Bernard-Soulier syndrome. Blood 91:4397–4418

Loy CJ, Sim KS, Yong EL (2003) Filamin-A fragment localizes to the nucleus to regulate androgen receptor and coactivator functions. Proc Natl Acad Sci U S A 100:4562–4567

Lu J, Lian G, Lenkinski R, De Grand A, Vaid RR, Bryce T *et al.* (2007) Filamin B mutations cause chondrocyte defects in skeletal development. Hum Mol Genet 16:1661–1675

Lu S, Carroll SL, Herrera AH, Ozanne B, Horowitz R (2003) New N-RAP-binding partners α-actinin, filamin and Krp1 detected by yeast two-hybrid screening: implications for myofibril assembly. J Cell Sci 116:2169–2178

Luy B (2007) Approaching the megadalton: NMR spectroscopy of protein complexes. Angew Chem Int Edit 46:4214–4216

Lypowy J, Chen I-Y, Abdellatif M (2005) An alliance between Ras GTPase-activating protein, filamin C, and Ras GTPase-activating protein SH3 domain-binding protein regulates myocyte growth. J Biol Chem 280:25717–25728

Löwe T, Kley RA, van der Ven PFM, Himmel M, Huebner A, Vorgerd M, Fürst DO (2007) The pathomechanism of filaminopathy: altered biochemical properties explain the cellular phenotype of a protein aggregation myopathy. Hum Mol Genet 16:1351–1358

Maceyka M, Alvarez SE, Milstien S, Spiegel S (2008) Filamin A links sphingosine kinase 1 and sphingosine-1-phosphate receptor 1 at lamellipodia to orchestrate cell migration. Mol Cell Biol 28:5687–5697

Maestrini E, Patrosso C, Mancini M, Rivella S, Rocchi M, Repetto M *et al.* (1993) Mapping of two genes encoding isoforms of the actin binding protein ABP-280, a dystrophin like protein, to Xq28 and to chromosome 7. Hum Mol Genet 2:761–766

Majumdar I, Kinch LN, Grishin NV (2009) A database of domain definitions for proteins with complex interdomain geometry. PLoS ONE 4:e5084

Maly T, Debelouchina GT, Bajaj VS, Hu K-N, Joo C-G, Mak-Jurkauskas ML *et al.* (2008) Dynamic nuclear polarization at high magnetic fields. J Chem Phys 128:052211

Mannucci PM (2004) Treatment of von Willebrand's disease. N Engl J Med 351:683–94

Markley JL, Bax A, Arata Y, Hilbers CW, Kaptein R, Sykes BD, Wright PE, Wüthrich K (1998) Recommendations for the presentation of NMR structures of proteins and nucleic acids. J Biomol NMR 12:1–23

Marti A, Luo Z, Cunningham C, Ohta Y, Hartwig J, Stossel TP, Kyriakis JM, Avruch J (1997) Actin-biding protein-280 binds the stress-activated protein kinase (SAPK) activator SEK-1 and is required for tumor necrosis factor-a activation of SAPK in melanoma cells. J Biol Chem 272:2620–2628

Masruha M, Caboclo LOSF, Carrete HJ, Cendes ÍL, Rodrigues MG, Garzon E *et al.* (2006) Mutation in filamin A causes periventricular heterotopia, developmental regression, and West syndrome in males. Epilepsia 47:211–214

Matsuo H, Walters KJ, Teruya K, Tanaka T, Gassner GT, Lippard SJ, Kyogoku Y, Wagner G (1999) Identification by NMR spectroscopy of residues at contact surfaces in large, slowly exchanging macromolecular complexes. J Am Chem Soc 121:9903–9904

Mattinen M-L, Pääkkönen K, Ikonen T, Craven J, Drakenberg T, Serimaa R, Waltho J, Annila A (2002) Quaternary structure built from subunits combining NMR and small-angle X-ray scattering data. Biophys J 83:1177–1183

Mayer M, Meyer B (1999) Characterization of ligand binding by saturation transfer difference NMR spectroscopy. Angew Chem Int Ed 38:1784–1788

McCammon JA, Harvey SC (1988) Dynamics of proteins and nucleic acids. Cambridge University Press, Cambridge

McCoy AJ, Fucini P, Noegel AA, Stewart M (1999) Structural basis for dimerization of the Dictyostelium gelation factor (ABP120) rod. Nat Struct Biol 6:836–841

McCoy MA, Wyss DF (2002) Structures of protein-protein complexes are docked using only NMR restraints from residual dipolar coupling and chemical shift perturbations. J Am Chem Soc 124:2104–2105

McDermott A (2009) Structure and dynamics of membrane proteins by magic angle spinning solid-state NMR. Ann Rev Biophys 38:385–403

McDermott A, Polenova T (2007) Solid state NMR: New tools for insight into enzyme function. Curr Opin Struct Biol 17:617–622

Meier JL, Burkart MD (2009) The chemical biology of modular biosynthetic enzymes. Chem Soc Rev 38:2012–2045

Meier S, Blackledge M, Grzesiek S (2008) Conformational distributions of unfolded polypeptides from novel NMR techniques. J Chem Phys 128:052204

Méjean C, Lebart M-C, Boyer M, Roustan C, Benyamin Y (1992) Localization and identification of actin structures involved in the filamin-actin interaction. Eur J Biochem 209:555–562

Meyer SC, Zuerbig S, Cunningham CC, Hartwig JH, Bissell T, Gardner K, Fox JEB (1997) Identification of the region in actin-binding protein that binds to the cytoplasmic domain of glycoprotein Ib_{α}. J Biol Chem 272:2914–2919

Middleton DA (2007) Solid-state NMR spectroscopy as a tool for drug design: from membrane-embedded targets to amyloid fibrils. Biochem Soc Trans 35:985–990

Missale C, Nash SR, Robinson SW, Jaber M, Caron MG (1998) Dopamine receptors: From structure to function. Physiol Rev 78:189–225

Murray JT, Campbell DG, Peggie M, Alfonso M, Cohen P (2004) Identification of filamin C as a new physiological substrate of PKBα using KESTREL. Biochem J 384:489–494

Murzin AG, Brenner SE, Hubbard T, Chothia C (1995) SCOP: A structural classification of proteins database for the investigation of sequences and structures. J Mol Biol 247:536–540

Nabuurs SB, Nederveen AJ, Vranken W, Doreleijers JF, Bonvin AMJJ, Vuister GW, Vriend G, Spronk CAEM (2004). DRESS: A database of refined solution NMR structures. Proteins 55:483–486

Nagano T, Morikubo S, Sato M (2004) Filamin A and FILIP (filamin A-interacting protein) regulate cell polarity and motility in neocortical subventricular and intermediate zones during radial migration. J Neurosci 24:9648–9657

Nagano T, Yoneda T, Hatanaka Y, Kubota C, Murakami F, Sato M (2002) Filamin A-interacting protein (FILIP) regulates cortical cell migration out of the ventricular zone. Nat Cell Biol 4:495–501

Nakamura F, Hartwig JH, Stossel TP, Szymanski PT (2005) Ca^{2+} and calmodulin regulate the binding of filamin A to actin filaments. J Biol Chem 280:32426–32433

Nakamura F, Osborn E, Janmey PA, Stossel TP (2002) Comparison of filamin A-induced cross-linking and Arp2/3 complex-mediated branching on the mechanics of actin filaments. J Biol Chem 277:9148–9154

Nakamura F, Osborn TM, Hartemink CA, Hartwig JH, Stossel TP (2007) Structural basis of filamin A functions. J Cell Biol 179:1011–1025

Nakanishi T, Miyazawa M, Sakakura M, Terasawa H, Takahashi H, Shimada I (2002) Determination of the interface of a large protein complex by transferred cross-saturation measurements. J Mol Biol 318:245–249

Neudecker P, Lundström P, Kay LE (2009) Relaxation dispersion NMR spectroscopy as a tool for detailed studies of protein folding. Biophys J 96:2045–2054

Niederman R, Amrein PC, Hartwig J (1983) Three-dimensional structure of actin filaments and of an actin gel made with actin-binding protein. J Cell Biol 96:1400–1413

Nietlispach D, Mott HR, Stott KM, Nielsen PR, Thiru A, Laue ED (2003) Structure determination of protein complexes by NMR. In Downing AK (Ed.) Protein NMR techniques, 2nd ed., Humana Press Inc, Totowa, pp. 255–288

Nikki M, Meriläinen J, Lehto V-P (2002) FAP52 regulates actin organization via binding to filamin. J Biol Chem 277:11432–11440

Nurmi SM, Gahmberg CG, Fagerholm SC (2006) 14-3-3 proteins bind both filamin and $\alpha_L\beta_2$ integrin in activated T cells. Ann NY Acad Sci 1090:318–325

Ohki S, Kainosho M (2008) Stable isotope labeling methods for protein NMR spectroscopy. Prog Nucl Magn Reson Spectrosc 53:208–226

Ohta Y, Hartwig JH (1995) Actin filament crosslinking by chicken gizzard filamin is regulated by phosphorylation in vitro. Biochemistry 34:6745–6754

Ohta Y, Hartwig JH, Stossel TP (2006) FilGAP, a Rho- and ROCK-regulated GAP for Rac binds filamin A to control actin remodelling. Nat Cell Biol 8:803–814

Ohta Y, Stossel TP, Hartwig JH (1991) Ligand-sensitive binding of actin-binding protein to immunoglobulin G Fc receptor I (FcγRI). Cell 67:275–282

Ohta Y, Suzuki N, Nakamura S, Hartwig JH, Stossel TP (1999) The small GTPase RalA targets filamin to induce filopodia. Proc Natl Acad Sci U S A 96:2122–2128

Okita JR, Picard D, Newman PJ, Montgomery RR, Kunicki TJ (1985) On the association of glycoprotein Ib and actin-binding protein in human platelets. J Cell Biol 100:317–321

Onoprishvili I, Ali S, Andria ML, Shpigel A, Simon EJ (2008) Filamin A mutant lacking actin-binding domain restores Mu opioid receptor regulation in melanoma cells. Neurochem Res 33:2054–2061

Onoprishvili I, Andria ML, Kramer HK, Ancevska-Taneva N, Hiller JM, Simon EJ (2003) Interaction between the μ opioid receptor and filamin A is involved in receptor regulation and trafficking. Mol Pharmacol 64:1092–1100

Onoprishvili I, Simon EJ (2007) Chronic morphine treatment up-regulates mu opioid receptor binding in cells lacking filamin A. Brain Res 1177:9–18

Opella SJ, Marassi FM (2004) Structure determination of membrane proteins by NMR spectroscopy. Chem Rev 104:3587–3606

Orengo CA, Michie AD, Jones S, Jones DT, Swindells MB, Thornton JM (1997) CATH - A hierarchic classification of protein domain structures. Structure 5:1093–1108

Ott I, Fischer EG, Miyagi Y, Mueller BM, Ruf W (1998) A role for tissue factor in cell adhesion and migration mediated by interaction with actin-binding protein 280. J Cell Biol 140:1241–1253

Otterbein LR, Graceffa P, Dominguez R (2001) The crystal structure of uncomplexed actin in the ADP state. Science 293:708–711

Ottiger M, Bax A (1998) Characterization of magnetically oriented phospholipid micelles for measurement of dipolar couplings in macromolecules. J Biomol NMR 12:361–372

Ozanne DM, Brady ME, Cook S, Gaughan L, Neal DE, Robson CN (2000) Androgen receptor nuclear translocation is facilitated by the f-actin cross-linking protein filamin. Mol Endocrinol 14:1618–1626

Pal Sharma C, Ezzell RM, Arnaout MA (1995) Direct interaction of filamin (ABP-280) with the β2-integrin subunit CD18. J Immunol 154:3461–3470

Pal Sharma C, Goldmann WH (2004) Phosphorylation of actin-binding protein (ABP-280, filamin) by tyrosine kinase $p56^{lck}$ modulates actin filament cross-linking. Cell Biol Int 28:935–941

Palmer AG (2004) NMR characterization of the dynamics of biomacromolecules. Chem Rev 104:3623–3640

Palmer AG, Kroenke CD, Loria JP (2001) Nuclear magnetic resonance methods for quantifying microsecond-to-millisecond motions in biological macromolecules. Methods Enzymol 339:204

Palmer AG, Massi F (2006) Characterization of the dynamics of biomacromolecules using rotating-frame spin relaxation NMR spectroscopy. Chem Rev 106:1700–1719

Paranavitane V, Coadwell WJ, Eguinoa A, Hawkins PT, Stephens L (2003) J Biol Chem 278:1328–1335

Paranavitane V, Stephens LR, Hawkins PT (2007) Structural determinants of LL5β subcellular localisation and association with filamin C. Cell Signal 19:817–824

Parrini E, Ramazzotti A, Dobyns WB, Mei D, Moro F, Veggiotti P *et al.* (2006) Periventricular heterotopia: phenotypic heterogeneity and correlation with Filamin A mutations. Brain 129:1892–1906

Patrosso MC, Repetto M, Villa A, Milanesi L, Frattini A, Faranda S *et al.* (1994) The exon-intron organization of the human X-linked gene (FLN1) encoding actin-binding protein 280. Genomics 21:71–76

Peng JW (2001) Cross-correlated ^{19}F relaxation measurements for the study of fluorinated ligand-receptor interactions. J Magn Reson 153:32–47

Peng JW, Moore J, Abdul-Manan N (2004) NMR experiments for lead generation in drug discovery. Prog Nucl Magn Reson Spectrosc 44:225–256

Pentikäinen U, Ylänne J (2009) The regulation mechanism for the auto-inhibition of binding of human filamin A to integrin. J Mol Biol 393:644–57

Permi P, Annila A (2004) Coherence transfer in proteins. Prog Nucl Magn Reson Spectrosc 44:97–137

Permi P, Rosevear PR, Annila A (2000) A set of HNCO-based experiments for measurement of residual dipolar couplings in ^{15}N, ^{13}C, (^{2}H)-labeled proteins. J Biomol NMR 17:43–54

Pervushin K, Riek R, Wider G, Wüthrich K (1997) Attenuated T_2 relaxation by mutual cancellation of dipole-dipole coupling and chemical shift anisotropy indicates an avenue to NMR structures of very large biological macromolecules in solution. Proc Natl Acad Sci U S A 94:12366–12371

Petoukhov MV, Svergun DI (2007) Analysis of X-ray and neutron scattering from biomacromolecular solutions. Curr Opin Struct Biol 17:562–571

Petrecca K, Miller DM, Shrier A (2000) Localization and enhanced current density of the Kv4.2 potassium channel by interaction with the actin-binding protein filamin. J Neurosci 20:8736–8744

Pfaff M, Liu S, Erle DJ, Ginsberg MH (1998) Integrin β cytoplasmic domains differentially bind to cytoskeletal proteins. J Biol Chem 273:6104–6109

Pi M, Spurney RF, Tu Q, Hinson T, Quarles LD (2002) Calcium-sensing receptor activation of Rho involves filamin and Rho-guanine nucleotide exchange factor. Endocrinology 143:3830–3838

Pickford AR, Campbell ID (2004) NMR studies of modular protein structures and their interactions. Chem Rev 104:3557–3566

Pilop C, Aregger F, Gorman RC, Brunisholz R, Gerrits B, Schaffner T *et al.* (2009) Proteomic analysis in aortic media of patients with marfan syndrome reveals increased activity of calpain 2 in aortic aneurysms. Circulation 120:983–991

Pinotsis N, Abrusci P, Djinović-Carugo K, Wilmanns M (2009) Terminal assembly of sarcomeric filaments by intermolecular β-sheet formation. Trends Biochem Sci 34:33–39

Pinotsis N, Lange S, Perriard J-C, Svergun DI, Wilmanns M (2008) Molecular basis of the C-terminal tail-to-tail assembly of the sarcomeric filament protein myomesin. EMBO J 27:253–264

Pintacuda G, John M, Su XC, Otting G (2007) NMR structure determination of protein-ligand complexes by lanthanide labeling. Acc Chem Res 40:206–212

Playford MP, Lyons PD, Sastry SK, Schaller MD (2006) Identification of a filamin docking site on PTP-PEST. J Biol Chem 281:34104–34112

Pons J-L, Malliavin TE, Delsuc MA (1996) Gifa V. 4: A complete package for NMR data set processing. J Biomol NMR 8:445–452

Popowicz GM, Müller R, Noegel AA, Schleicher M, Huber R, Holak TA (2004) Molecular structure of the rod domain of Dictyostelium filamin. J Mol Biol 342:1637–1646

Popowicz GM, Schleicher M, Noegel AA, Holak TA (2006) Filamins: promiscuous organizers of the cytoskeleton. Trends Biochem Sci 31:411–419

Post CB (2003) Exchange-transferred NOE spectroscopy and bound ligand structure determination. Curr Opin Struct Biol 13:581–588

Prandolini MJ, Denysenkov VP, Gafurov M, Endeward B, Prisner TF (2009) High-field dynamic nuclear polarization in aqueous solutions. J Am Chem Soc 131:6090–6092

Prestegard JH, Bougault CM, Kishore AI (2004) Residual dipolar couplings in structure determination of biomolecules. Chem Rev 104:3519–3540

Pudas R, Kiema T-R, Butler PJG, Stewart M, Ylänne J (2005) Structural basis for vertebrate filamin dimerization. Structure 13:111–119

Raynaud F, Jond-Necand C, Marcilhac A, Fürst D, Benyamin Y (2006) Calpain 1-γ filamin interaction in muscle cells: A possible in situ regulation by PKC-α. Int J Biochem Cell Biol 38:404–413

Reif B, Hennig M, Griesinger C (1997) Direct measurement of angles between bond vectors in high-resolution NMR. Science 276:1230–1233

Ridley AJ (2006) Rho GTPases and actin dynamics in membrane protrusions and vesicle trafficking. Trends Cell Biol 16:522–529

Ridley AJ, Schwartz MA, Burridge K, Firtel RA, Ginsberg MH, Borisy G, Parsons JT, Horwitz AR (2003) Cell migration: Integrating signals from front to back. Science 302:1704–1709

Riek R, Fiaux J, Bertelsen EB, Horwich AL, Wüthrich K (2002) Solution NMR techniques for large molecular and supramolecular structures. J Am Chem Soc 124:12144–12153

Riek R, Wider G, Pervushin K, Wüthrich K (1999) Polarization transfer by cross-correlated relaxation in solution NMR with very large molecules. Proc Natl Acad Sci U S A 96:4918–4923

Robertson SP (2004) Molecular pathology of filamin A: diverse phenotypes, many functions. Clin Dysmorphol 13:123–131

Robertson SP (2005) Filamin A: phenotypic diversity. Curr Opin Genet Dev 15:301–307

Robertson SP (2007) Otopalatodigital syndrome spectrum disorders: otopalatodigital syndrome types 1 and 2, frontometaphyseal dysplasia and Melnick-Needles syndrome. Eur J Hum Genet 15:3–9

Robertson SP, Jenkins ZA, Morgan T, Adès L, Aftimos S, Boute O *et al.* (2006). Frontometaphyseal dysplasia: Mutations in FLNA and phenotypic diversity. Am J Med Genet A 140A:1726–1736

Robertson SP, Twigg SRF, Sutherland-Smith AJ, Biancalana V, Gorlin RJ, Horn D *et al.* (2003) Localized mutations in the gene encoding the cytoskeletal protein filamin A cause diverse malformations in humans. Nature Genet 33:487–491

Ruskamo S, Ylänne J (2009) Structure of the human filamin A actin-binding domain. Acta Crystallogr D D65:1217–1221

Ryabow Y, Fushman D (2007) Structural assembly of multidomain proteins and protein complexes guided by the overall rotational diffusion tensor. J Am Chem Soc 129:7894–7902

Sadowski MI, Jones DT (2009) The sequence-structure relationship and protein function prediction. Curr Opin Struct Biol 19:357–362

Sakai T, Tochio H, Tenno T, Ito Y, Kokubo T, Hiroaki H, Shirakawa M (2006) In-cell NMR spectroscopy of proteins inside Xenopus laevis oocytes. J Biomol NMR 36:179–188

Sakakibara D, Sasaki A, Ikeya T, Hamatsu J, Hanashima T, Mishima M *et al.* (2009) Protein structure determination in living cells by in-cell NMR spectroscopy. Nature 458:102–105

Sampson LJ, Leyland ML, Dart C (2003) Direct interaction between the actin-binding protein filamin-A and the inwardly rectifying potassium channel, Kir2.1. J Biol Chem 278:41988–41997

Sanders CR, Sönnichsen F (2006) Solution NMR of membrane proteins: practice and challenges. Magn Reson Chem 44:S24–S40

Sasaki A, Masuda Y, Ohta Y, Ikeda K, Watanabe K (2001) Filamin associates with smads and regulates transforming growth factor-β signaling. J Biol Chem 276:17871–17877

Sass H-J, Musco G, Stahl SJ, Wingfield PT, Grzesiek S (2000) Solution NMR of proteins within polyacrylamide gels: Diffusional properties and residual alignment by mechanical stress or embedding of oriented purple membranes. J Biomol NMR 18:303–309

Sato M, Nagano T (2005) Involvement of filamin A and filamin A-interacting protein (FILIP) in controlling the start and cell shape of radially migrating cortical neurons. Anat Sci Int 80:19–29

Sattler M, Schleucher J, Griesinger C (1999) Heteronuclear multidimensional NMR experiments for the structure determination of proteins in solution employing pulsed field gradients. Prog Nucl Magn Reson Spectrosc 34:93–158

Saupe A, Englert G (1963) High-resolution nuclear magnetic resonance spectra of orientated molecules. Phys Rev Lett 11:462–464

Sawyer GM, Clark AR, Robertson SP, Sutherland-Smith AJ (2009) Disease-associated substitutions in the filamin B actin binding domain confer enhanced actin binding affinity in the absence of major structural disturbance: Insights from the crystal structures of filamin B actin binding domains. J Mol Biol 390:1030–1047

Schanda P (2009) Fast-pulsing longitudinal relaxation optimized techniques: Enriching the toolbox of fast biomolecular NMR spectroscopy. Prog Nucl Magn Reson Spectrosc 55:238–265

Schubert M, Labudde D, Oschkinat H, Schmieder P (2002) A software tool for the prediction of Xaa-Pro peptide bond conformations in proteins based on ^{13}C chemical shift statistics. J Biomol NMR 24:149–154

Schwaiger I, Kardinal A, Schleicher M, Noegel AA, Rief M (2004) A mechanical unfolding intermediate in an actin-crosslinking protein. Nat Struct Mol Biol 11:81–85

Schwaiger I, Schleicher M, Noegel AA, Rief M (2005) The folding pathway of a fast-folding immunoglobulin domain revealed by single-molecule mechanical experiments. EMBO Rep 6:46–51

Schwieters CD, Kuszewski JJ (2006) Using Xplor-NIH for NMR molecular structure determination. Prog Nucl Magn Reson Spectrosc 48:47–62

Scott MGH, Pierotti V, Storez H, Lindberg E, Thuret A, Muntaner O *et al.* (2006) Cooperative regulation of extracellular signal-regulated kinase activation and cell shape change by filamin A and β-arrestins. Mol Cell Biol 26:3432–3445

Seck T, Baron R, Horne WC (2003) Binding of filamin to the C-terminal tail of the calcitonin receptor controls recycling. J Biol Chem 278:10408–10416

Seo M-D, Seok S-H, Im H, Kwon A-R, Lee SJ, Kim H-R *et al.* (2009) Crystal structure of the dimerization domain of human filamin A. Proteins 75:258–263

Shadiack AM, Nitkin RM (1991) Agrin induces α-actinin, filamin, and vinculin to co-localize with AChR clusters on cultured chick myotubes. J Neurobiol 22:617–628

Sharif-Naeini R, Folgering JHA, Bichet D, Duprat F, Lauritzen I, Arhatte M *et al.* (2009) Polycystin-1 and -2 dosage regulates pressure sensing. Cell 139:587–596

Shatunov A, Olivé M, Odgerel Z, Stadelmann-Nessler C, Irlbacher K, van Landeghem F *et al.* (2009) In-frame deletion in the seventh immunoglobulin-like repeat of filamin C in a family with myofibrillar myopathy. Eur J Hum Genet 17:656–663

Sheen VL, Dixon PH, Fox JF, Hong SE, Kinton L, Sisodiya SM *et al.* (2001) Mutations in the X-linked filamin 1 gene cause periventricular nodular heterotopia in males as well as in females. Hum Mol Genet 10:1775–1783

Sheen VL, Feng Y, Graham D, Takafuta T, Shapiro SS, Walsh CA (2002) Filamin A and filamin B are co-expressed within neurons during periods of neuronal migration and can physically interact. Hum Mol Genet 11:2845–2854

Sheen VL, Jansen A, Chen MH, Parrini E, Morgan T, Ravenscroft R *et al.* (2005) Filamin A mutations cause periventricular heterotopia with Ehlers-Danlos syndrome. Neurology 64:254–262

Shen D-W, Liang X-J, Gawinowicz MA, Gottesman MM (2004) Identification of cytoskeletal [^{14}C]carboplatin-binding proteins reveals reduced expression and disorganization of actin and filamin in cisplatin-resistant cell lines. Mol Pharmacol 66:789–793

Shen Y, Delaglio F, Cornilescu G, Bax A (2009) TALOS+: a hybrid method for predicting protein backbone torsion angles from NMR chemical shifts. J Biomol NMR 44:213–223

Shifrin Y, Arora PD, Ohta Y, Calderwood DA, McCulloch CA (2009) The role of FilGAP-filamin A interactions in mechanoprotection. Mol Biol Cell 20:1269–1279

Shimba N, Takahashi H, Sakakura M, Fujii I, Shimada I (1998) Determination of protonation and deprotonation and tautomeric states of histidine residues in large proteins using nitrogen-carbon J couplings in imidazole ring. J Am Chem Soc 120:10988–10989

Shin J, Lee W, Lee W (2008) Structural proteomics by NMR spectroscopy. Expert Rev Proteomics 5:589–601

Shizuta Y, Shizuta H, Gallo M, Davies P, Pastan I (1976) Purification and properties of filamin, an actin binding protein from chicken gizzard. J Biol Chem 251:6562–6567

Shuker SB, Hajduk PJ, Meadows RP, Fesik SW (1996) Discovering high-affinity ligands for proteins: SAR by NMR. Science 274:1531–1534

Sippl MJ (2009) Fold space unlimited. Curr Opin Struct Biol 19:312–320

Sjekloća L, Pudas R, Sjöblom B, Konarev P, Carugo O, Rybin V *et al.* (2007) Crystal structure of human filamin C domain 23 and small angle scattering model for filamin C 23–24 dimer. J Mol Biol 368:1011–1023

Skinner AL, Laurence JS (2008) High-field solution NMR spectroscopy as a tool for assessing protein interactions with small molecule ligands. J Pharm Sci 97:4670–4695

Skrynnikov NR (2004) Orienting molecular fragments and molecules with residual dipolar couplings. C R Physique 5:359–375

Small JV, Fürst DO, De Mey J (1986) Localization of filamin in smooth muscle. J Cell Biol 102:210–220

Solé G, Coupry I, Rooryck C, Guérineau E, Martins F, Devés S *et al.* (2009) Bilateral periventricular nodular heterotopia in France: frequency of mutations in FLNA, phenotypic heterogeneity and spectrum of mutations. J Neurol Neurosurg Psychiatry 80:1394–1398

Spirin AS, Swartz JR (Ed.) (2008) Cell-free protein synthesis: Methods and protocols. Wiley-VCH, Weinheim

Spronk CAEM, Linge JP, Hilbers CW, Vuister GW (2002) Improving the quality of protein structures derived by NMR spectroscopy. J Biomol NMR 22:281–289

Srere PA (1987) Complexes of sequential metabolic enzymes. Ann Rev Biochem 56:89–124

Stahlhut M, van Deurs B (2000) Identification of filamin as a novel ligand for caveolin-1: Evidence for the organization of caveolin-1-associated membrane domains by the actin cytoskeleton. Mol Biol Cell 11:325–337

Standing KG (2003) Peptide and protein de novo sequencing by mass spectrometry. Curr Opin Struct Biol 13:595–601

Staunton D, Schlinkert R, Zanetti G, Colebrook SA, Campbell ID (2006) Cell-free expression and selective isotope labelling in protein NMR. Magn Reson Chem 44:S2–S9

Stefanova M, Meinecke P, Gal A, Bolz H (2005) A novel 9 bp deletion in the filamin A gene causes an otopalatodigital-spectrum disorder with a variable, intermediate phenotype. Am J Med Genet A 134A:386–390

Stockman BJ, Dalvit C (2002) NMR screening techniques in drug discovery and drug design. Prog Nucl Magn Reson Spectrosc 41:187–231

Stossel TP, Condeelis J, Cooley L, Hartwig JH, Noegel A, Schleicher M, Shapiro SS (2001) Filamins as integrators of cell mechanics and signalling. Nat Rev Mol Cell Biol 2:138–145

Su X-C, Otting G (2009) Paramagnetic labelling of proteins and oligonucleotides for NMR. J Biomol NMR, in press

Sudmeier JL, Bradshaw M, Coffman Haddad KE, Day RM, Thalhauser CJ, Bullock PA, Bachovchin WW (2003) Identification of histidine tautomers in proteins by 2D $^{1}H/^{13}C^{\delta 2}$ one-bond correlated NMR. J Am Chem Soc 125:8430–8431

Sverdlov M, Shinin V, Place AT, Castellon M, Minshall RD (2009) Filamin A regulates caveolae internalization and trafficking in endothelial cells. Mol Biol Cell 20:4531–40

Szeverenyi I, Cassidy AJ, Chung CW, Lee BTK, Common JEA, Ogg SC *et al.* (2008) The human intermediate filament database: Comprehensive information on a gene family involved in many human diseases. Hum Mutat 29:351–360

Tadokoro S, Shattil SJ, Eto K, Tai V, Liddington RC, de Pereda JM, Ginsberg MH, Calderwood DA (2003) Talin binding to integrin β tails: A final common step in integrin activation. Science 302:103–106

Takada F, van der Woude DL, Tong H-Q, Thompson TG, Watkins SC, Kunkel LM, Beggs AH (2001). Myozenin: An α-actinin- and γ-filamin-binding protein of skeletal muscle Z lines. Proc Natl Acad Sci U S A 98:1595–1600

Takafuta T, Saeki M, Fujimoto T-T, Fujimura K, Shapiro SS (2003) A new member of the LIM protein family binds to bilamin B and localizes at stress fibers. J Biol Chem 278:12175–12181

Takafuta T, Wu G, Murphy GF, Shapiro SS (1998) Human β-filamin is a new protein that interacts with the cytoplasmic tail of glycoprotein Ibα. J Biol Chem 273:17531–17538

Takala H, Nurminen E, Nurmi SM, Aatonen M, Strandin T, Takatalo M *et al.* (2008) β2 integrin phosphorylation on Thr758 acts as a molecular switch to regulate 14-3-3 and filamin binding. Blood 112:1853–1862

Takeuchi K, Wagner G (2006) NMR studies of protein interactions. Curr Opin Struct Biol 16:109–117

Tavano R, Contento RL, Jimenez Baranda S, Soligo M, Tuosto L, Manes S, Viola A (2006) CD28 interaction with filamin-A controls lipid raft accumulation at the T-cell immunological synapse. Nat Cell Biol 8:1270–1276

Thelin WR, Chen Y, Gentzsch M, Kreda SM, Sallee JL, Scarlett CO *et al.* (2007) Direct interaction with filamins modulates the stability and plasma membrane expression of CFTR. J Clin Invest117:364–374

Thompson TG, Chan Y-M, Hack AA, Brosius M, Rajala M, Lidov HGW *et al.* (2000). Filamin 2 (FLN2): A muscle-specific sarcoglycan interacting protein. J Cell Biol 148:115–126

Tigges U, Koch B, Wissing J, Jockusch BM, Ziegler WH (2003) The F-actin cross-linking and focal adhesion protein filamin A is a ligand and in vivo substrate for protein kinase Cα. J Biol Chem 278:23561–23569

Tolman JR, Flanagan JM, Kennedy MA, Prestegard JH (1995) Nuclear magnetic dipole interactions in field-oriented proteins: Information for structure determination in solution. Proc Natl Acad Sci U S A 92:9279–9283

Tolman JR, Ruan K (2006) NMR residual dipolar couplings as probes of biomolecular dynamics. Chem Rev 106:1720–1736

Torrado M, Senatorov VV, Trivedi R, Fariss RN, Tomarev SI (2004) Pdlim2, a novel PDZ-LIM domain protein, interacts with α-actinins and filamin A. Invest Ophthalmol Vis Sci 45:3955–3963

Tousignant A, Pelletier JN (2004) Protein motions promote catalysis. Chem Biol 11:1037–1042

Travis MA, van der Flier A, Kammerer RA, Mould AP, Sonnenberg A, Humphries MJ (2004) Interaction of filamin A with the integrin β7 cytoplasmic domain: Role of alternative splicing and phosphorylation. FEBS Lett 569:185–190

Trifonov EN, Frenkel ZM (2009) Evolution of protein modularity. Curr Opin Struct Biol 19:335–340

Tseng Y, An KM, Esue O, Wirtz D (2004) The bimodal role of filamin in controlling the architecture and mechanics of F-actin networks. J Biol Chem 279:1819–1826

Tsuneda SS, Torres FR, Montenegro MA, Guerreiro MM, Cendes F, Lopes-Cendes I (2008) A new missense mutation found in the FLNA gene in a family with bilateral periventricular nodular heterotopia (BPNH) alters the splicing process. J Mol Neurosci 35:195–200

Tu Y, Wu S, Shi X, Chen K, Wu C (2003) Migfilin and Mig-2 link focal adhesions to filamin and the actin cytoskeleton and function in cell shape modulation. Cell 113:37–47

Tugarinov V, Kay LE (2003a) Ile, Leu, and Val methyl assignments of the 723-residue malate synthase G using a new labeling strategy and novel NMR methods. J Am Chem Soc 125:13868–13878

Tugarinov V, Kay LE (2003b) Quantitative NMR studies of high molecular weight proteins: Application to domain orientation and ligand binding in the 723 residue enzyme malate synthase G. J Mol Biol 327:1121–1133

Tugarinov V, Choy W-Y, Orekhov VY, Kay LE (2005) Solution NMR-derived global fold of a monomeric 82-kDa enzyme. Proc Natl Acad Sci U S A 102:622–627

Tugarinov V, Muhandiram R, Ayed A, Kay LE (2002) Four-dimensional NMR spectroscopy of a 723-residue protein: Chemical shift assignments and secondary structure of malate synthase G. J Am Chem Soc 124:10025–10035

Tycko R, Blanco FJ, Ishii Y (2000) Alignment of biopolymers in strained gels: A new way to create detectable dipole-dipole couplings in high-resolution biomolecular NMR. J Am Chem Soc 122:9340–9341

Ueda K, Ohta Y, Hosoya H (2003) The carboxy-terminal pleckstrin homology domain of ROCK interacts with filamin-A. Biochem Biophys Res Commun 301:886–890

Unger S, Mainberger A, Spitz C, Bähr A, Zeschnigk C, Zabel B, Superti-Furga A, Morris-Rosendahl DJ (2007) Filamin A mutation is one cause of FG syndrome. Am J Med Genet A 143A:1876–1879

Uribe R, Jay D (2009) A review of actin binding proteins: new perspectives. Mol Biol Rep 36121–125

Vadlamudi RK, Li F, Adam L, Nguyen D, Ohta Y, Stossel TP, Kumar R (2002) Filamin is essential in actin cytoskeletal assembly mediatedby p21-activated kinase 1. Nat Cell Biol 4:681–690

van der Flier A, Sonnenberg A (2001a) Function and interactions of integrins. Cell Tissue Res 305:285–298

van der Flier A, Sonnenberg A (2001b) Structural and functional aspects of ¢lamins. Biochim Biophys Acta Mol Cell Res 1538:99–117

van der Flier A, Kuikman I, Kramer D, Geerts D, Kreft M, Takafuta T, Shapiro SS, Sonnenberg A (2002) Different splice variants of filamin-B affect myogenesis, subcellular distribution, and determine binding to integrin β subunits. J Cell Biol 156:361–376

van der Ven PFM, Ehler E, Vakeel P, Eulitz S, Schenk JA, Milting H, Micheel B, Fürst DO (2006) Unusual splicing events result in distinct Xin isoforms that associate differentially with filamin c and Mena/VASP. Exp Cell Res 312:2154–2167

van der Ven PFM, Wiesner S, Salmikangas P, Auerbach D, Himmel M, Kempa S *et al.* (2000). Indications for a novel muscular dystrophy pathway: γ-filamin, the muscle-specific filamin isoform, interacts with myotilin. J Cell Biol 151:235–247

Vanhoorelbeke K, Ulrichts H, Van de Walle G, Fontayne A, Deckmyn H (2007) Inhibition of platelet glycoprotein Ib and its antithrombotic potential. Curr Pharm Design 13:2684–2697

Vaynberg J, Qin J (2006) Weak protein-protein interactions as probed by NMR spectroscopy. Trends Biotechnol 24:22–27

Venselaar H, Joosten RP, Vroling B, Baakman CAB, Hekkelman ML, Krieger E, Vriend G (2009) Homology modelling and spectroscopy, a never-ending love story. Eur Biophys J, in press

Vogel C, Bashton M, Kerrison ND, Chothia C, Teichmann SA (2004a) Structure, function and evolution of multidomain proteins. Curr Opin Struct Biol 14:208–216

Vogel C, Berzuini C, Bashton M, Gough J, Teichmann SA (2004b) Supra-domains: Evolutionary units larger than single protein domains. J Mol Biol 336:809–823

Vorgerd M, van der Ven PFM, Bruchertseifer V, Löwe T, Kley RA, Schröder R *et al.* (2005) A mutation in the dimerization domain of filamin C causes a novel type of autosomal dominant myofibrillar myopathy. Am J Hum Genet 77:297–304

Wallach D, Davies PJA, Pastan I (1978a) Cyclic AMP-dependent phosphorylation of filamin in mammalian smooth muscle. J Biol Chem 253:4739–4745

Wallach D, Davies PJA, Pastan I (1978b) Purification of mammalian filamin. J Biol Chem 253:3328–3335

Wang H-Y, Burns LH (2009) Naloxone's pentapeptide binding site on filamin A blocks Mu opioid receptor-Gs coupling and CREB activation of acute morphine. PLoS ONE 4:e4282

Wang H-Y, Frankfurt M, Burns LH (2008) High-affinity naloxone binding to filamin A prevents Mu opioid receptor-Gs coupling underlying opioid tolerance and dependence. PLoS ONE 3:e1554

Wang K (1977) Filamin, a new high-molecular-weight protein found in smooth muscle and nonmuscle cells. Purification and properties of chicken gizzard filamin. Biochemistry 16:1857–1865

Wang K, Ash JF, Singer SJ (1975) Filamin, a new high-molecular-weight protein found in smooth muscle and non-muscle cells. Proc Natl Acad Sci U S A 72:4483–4486

Wang K, Singer SJ (1977) Interaction of filamin with F-actin in solution. Proc Natl Acad Sci U S A 74:2021–2025

Wang L, Xie J, Schultz PG (2006) Expanding the genetic code. Annu Rev Biophys Biomolec Struct 35:225–249

Wang Y, Kreisberg JI, Bedolla RG, Mikhailova M, deVere White RW, Ghosh PM (2007) A 90 kDa fragment of filamin A promotes Casodex-induced growth inhibition in Casodex-resistant androgen receptor positive C4-2 prostate cancer cells. Oncogene 26:6061–6070

Washington RW, Knecht DA (2008) Actin binding domains direct actin-binding proteins to different cytoskeletal locations. BMC Cell Biol 9:10.

Waterhouse AM, Procter JB, Martin DMA, Clamp M, Barton GJ (2009) Jalview version 2-A multiple sequence alignment editor and analysis workbench. Bioinformatics 25:1189–1191

Watts SW, Priestley JRC, Thompson JM (2009) Serotonylation of vascular proteins important to contraction. PLoS ONE 4:e5682

Webb AG (2006) Advances in probe design for protein NMR. Annu Rep NMR Spectrosc 58:1–50

Weissman KJ, Müller R (2008) Protein-protein interactions in multienzyme megasynthetases. ChemBioChem 9:826–848

Wiesmann C, Muller YA, de Vos AM (2000) Ligand-binding sites in Ig-like domains of receptor tyrosine kinases. J Mol Med 78:247–260

Wiesner S, Legate KR, Fässler R (2005) Integrin-actin interactions. Cell Mol Life Sci 62:1081–1099

Williams AF, Barclay NA (1988) The immunoglobulin superfamily – Domains for cell surface recognition. Ann Rev Immunol 6:381–405

Williamson D, Pikovski I, Cranmer SL, Mangin P, Mistry N, Domagala T *et al.* (2002) Interaction between platelet glycoprotein Ibα and filamin-1 is essential for glycoprotein Ib/IX receptor anchorage at high shear. J Biol Chem 277:2151–2159

Williamson MP, Havel TF, Wüthrich K (1985) Solution conformation of proteinase inhibitor IIA from bull seminal plasma by ^{1}H nuclear magnetic resonance and distance geometry. J Mol Biol 182:295–315

Winder SJ (2003) Structural insights into actin-binding, branching, and bundling proteins. Curr Opin Cell Biol 15:14–22

Winder SJ, Ayscough KR (2005) Actin-binding proteins. J Cell Sci 118:651–654

Witze ES, Old WM, Resing KA, Ahn NG (2007) Mapping protein post-translational modifications with mass spectrometry. Nat Methods 4:798–806

Wollacott AM, Zanghellini A, Murphy P, Baker D (2007) Prediction of structures of multidomain proteins from structures of the individual domains. Protein Sci 16:165–175

Woo MS, Ohta Y, Rabinovitz I, Stossel TP, Blenis J (2004) Ribosomal S6 kinase (RSK) regulates phosphorylation of filamin A on an important regulatory site. Mol Cell Biol 24:3025–3035

Wright PE, Dyson HJ (2009) Linking folding and binding. Curr Opin Struct Biol 19:31–38

Xia B, Tsui V, Case DA, Dyson HJ, Wright PE (2002) Comparison of protein solution structures refined by molecular dynamics simulation in vacuum, with a generalized Born model, and with explicit water. J Biomol NMR 22:317–331

Xie Z, Xu W, Davie EW, Chung DW (1998) Molecular cloning of human ABPL, an actin-binding protein homologue. Biochem Biophys Res Commun 251:914–919

Xu W, Xie Z, Chung DW, Davie EW (1998) A novel human actin-binding protein homologue that binds to platelet glycoprotein Ibα. Blood 92:1268–1276

Yamazaki M, Furuike S, Ito T (2002) Mechanical response of single filamin A (ABP-280) molecules and its role in the actin cytoskeleton. J Muscle Res Cell Motil 23:525–534

Yang D, Kay LE (1999) TROSY triple-resonance four-dimensional NMR spectroscopy of a 46 ns tumbling protein. J Am Chem Soc 121:2571–2575

Yang D, Venters RA, Mueller GA, Choy WY, Kay LE (1999) TROSY-based HNCO pulse sequences for the measurement of ^{1}HN-^{15}N, ^{15}N-^{13}CO, ^{1}HN-^{13}CO, ^{13}CO-^{13}C$^{\alpha}$ and ^{1}HN-^{13}C$^{\alpha}$ dipolar couplings in ^{15}N, ^{13}C, ^{2}H-labeled proteins. J Biomol NMR 14:333–343

Yoshida K, Suzuki Y, Honda E, Amemiya K, Nakatani T, Ebina M *et al.* (2002) Leucine-rich repeat region of decorin binds to filamin-A. Biochimie 84:303–308

Yoshida N, Ogata T, Tanabe K, Li S, Nakazato M, Kohu K *et al.* (2005) Filamin A-bound PEBP2β/CBFβ Is retained in the cytoplasm and prevented from functioning as a partner of the Runx1 transcription factor. Mol Cell Biol 25:1003–1012

Yu N, Erb L, Shivaji R, Weisman GA, Seye CI (2008) Binding of the P2Y2 nucleotide receptor to filamin A regulates migration of vascular smooth muscle cells. Circ Res 102:581–588

Yuan Y, Shen Z (2001) Interaction with BRCA2 suggests a role for filamin-1 (hsFLNa) in DNA damage response. J Biol Chem 276:48318–48324

Zenker M, Nährlich L, Sticht H, Reis A, Horn D (2006) Genotype-epigenotype-phenotype correlations in females with frontometaphyseal dysplasia. Am J Med Genet A 140A:1069–1073

Zenker M, Rauch A, Winterpacht A, Tagariello A, Kraus C, Rupprecht T, Sticht H, Reis A (2004) A dual phenotype of periventricular nodular heterotopia and frontometaphyseal dysplasia in one patient caused by a single FLNA mutation leading to two functionally different aberrant transcripts. Am J Hum Genet 74:731–737

Zerbe O (Ed.) (2003) BioNMR in drug research. Wiley-VCH, Weinheim

Zhang D, Herring JA, Swaney SS, McClendon TB, Gao X, Browne RH *et al.* (2006) Mutations responsible for Larsen syndrome cluster in the FLNB protein. J Med Genet 43:e24

Zhang M, Liu J, Cheng A, DeYoung SM, Saltiel AR (2007) Identification of CAP as a costameric protein that interacts with filamin C. Mol Biol Cell 18:4731–4740

Zhang W, Han SW, McKeel DW, Goate A, Wu JY (1998) Interaction of presenilins with the filamin family of actin-binding proteins. J Neurosci 18:914–922

Zheng L, Baek H-J, Karsenty G, Justice MJ (2007) Filamin B represses chondrocyte hypertrophy in a Runx2/Smad3-dependent manner. J Cell Biol 178:121–128

Zhou X, Borén J, Akyürek LM (2007a) Filamins in cardiovascular development. Trends Cardiovasc Med 17:222–229

Zhou X, Tian F, Sandzén J, Cao R, Flaberg E, Szekely L *et al.* (2007b) Filamin B deficiency in mice results in skeletal malformations and impaired microvascular development. Proc Natl Acad Sci U S A 104:3919–3924

Zhu G, Xia Y, Nicholson LK, Sze KH (2000) Protein dynamics measurements by TROSY-based NMR experiments. J Magn Reson 143:423–426

Zhu G, Yao X (2008) TROSY-based NMR experiments for NMR studies of large biomolecules. Prog Nucl Magn Reson Spectrosc 52:49–68

Zou P, Pinotsis N, Lange S, Song Y-H, Popov A, Mavridis I *et al.* (2006) Palindromic assembly of the giant muscle protein titin in the sarcomeric Z-disk. Nature 439:229–233

Zuiderweg ERP (2002) Mapping protein-protein interactions in solution by NMR spectroscopy. Biochemistry 41:1–7